Plasma treatments on lignin for improved compatibility in lignin-polypropylene compounds

MASTER THESIS IN MATERIALS ENGINEERING AND NANOTECHNOLOGY – INGEGNERIA DEI MATERIALI E DELLE NANOTECNOLOGIE

AUTHOR: SOFIA GRAZIELLA REGOLI

ADVISOR: GIANMARCO ENRICO GRIFFINI

CO-ADVISORS: RUGGERO BARNI, EMANUELA BELLINETTO, OUSSAMA BOUMEZGANE

ACADEMIC YEAR: 2020-2021

1. Introduction

Climate change and plastic pollution are pushing governments and companies to redesign the production processes of polymers and to find more sustainable solutions. A highly attractive innovation that would reduce resource depletion, greenhouse gases emissions and plastic pollution is the incorporation of lignin in polymeric products. Lignin is a side-product from the paper industry constitutes up to 33% of plants and trees biomass, which makes it a biodegradable renewable resource with great availability [1]. The formation of lignin results from the reaction of three different cinnamyl alcohol monomers (also called *monolignols*): *para*-coumaryl alcohol (H-type), coniferyl alcohol (G-type), and sinapyl alcohol (S-type) [1]. The relative amount of the three monolignols in plants is different depending on the species, which makes it difficult to have a universal description of the material. In general, studies revealed that there are two main structures of lignin, shown in Figure 1.1.

Lignin has proven to be a valid candidate as component in plastic products for high-value applications, providing satisfying mechanical properties [2]. However, compatibility between lignin and polymers is usually hindered by the low chemical reactivity of lignin with other polymeric species. This issue is further increased when considering highly hydrophobic polymers, such as polyolefins, because compatibility problems also arise from the presence of polar hydroxyl groups in lignin's chemical structure.
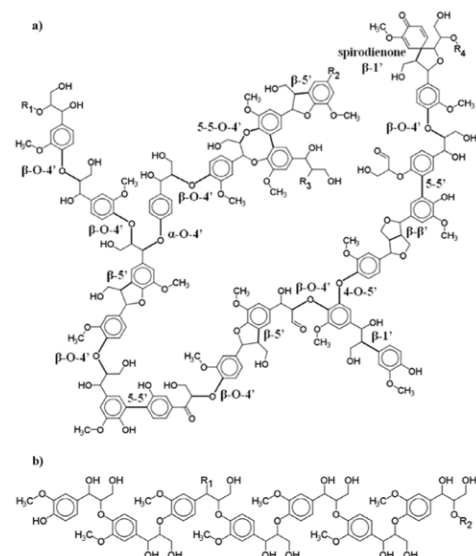

Figure 1.1 The model structure of spruce lignin. (a) Type 1 lignin and (b) type 2 lignin [1].

Several types of techniques exist for the surface treatment of polymers that can be applied to lignin to reduce its hydrophilicity. Among all of them, plasma treatments are particularly attractive for being simple and environmentally friendly processes, since they are solvent-free. Nonetheless, plasma treatments on lignin have not been greatly investigated yet, because instruments specifically designed to treat powdery materials must be used [3]. During plasma treatments, the surface of polymers interacts with energetic particles and photons through free-radical chemistry mechanisms bringing, among other effects, to chemical surface modification. The free radicals formed on the polymer's surface, after interaction with the plasma, can easily react with gases or solutions they are exposed to; this is usually performed to increase the hydrophilicity of plastics through oxidation by exposing them to air after treatment in air plasma or Argon plasma [4]. Instead, to increase the hydrophobicity of the treated material, like in the case of this thesis work, a functionalizing gas with the desired chemical characteristics can be added as plasma gas.

The aim of this thesis work is to perform plasma treatments on lignin with a Gliding Arc Tornado device (GAT) to reduce the hydroxyl groups concentration and/or to graft new active sites on the lignin particles surface. The treatment was carried out using either compressed air or Argon as gas source for the plasma, while other functionalizing gases were added in the process when they were needed for the specific experiment. The functionalizing gases employed (separately) were Hexane and Hexamethyldisiloxane (HMDSO).

2. Experimental methods

After performing the plasma treatment with the GAT device, characterization of plasma-treated lignin was performed to assess whether chemical changes occurred in the material. Characterization techniques were first used to investigate variations in the hydrophilic behaviour of lignin. These methods were Fourier-transformed infrared (FT-IR) spectroscopy, differential scanning calorimetry (DSC), and solubility tests. Later, to quantitatively evaluate changes in the hydroxyl (-OH) and carboxylic (-COOH) groups concentrations, nuclear magnetic resonance (^{31}P-NMR) was employed.

The results of the characterization were used to select the treatments that showed satisfying results in terms of hydroxyl groups reduction to blend them with polypropylene (PP). The four samples selected after ^{31}P-NMR spectroscopy and pristine lignin have been blended with polypropylene with three different lignin contents with a twin-screw extruder: 5%, 10% and 20%. The goal was to evaluate both the effects of the treatments and of the biopolymer content on the properties of the compounds. After the blends were produced, they have been processed through injection moulding for the realization of the specimens for the tensile tests. Characterization of the blends have then been performed to evaluate how the different plasma treatments and the lignin content affected compatibility between the two polymers through mechanical, rheological and thermal analysis. The lignin used in this thesis work was Protobind 1000, supplied by Tanovis AG (Alpnach, Switzerand).

3. Results and discussion

3.1. GAT device

The plasma treatment on lignin was performed through the GAT device, an instrument that allows the addiction of both the lignin powder and the functionalizing gas (separately) and that ensures the control of the electrical characteristics of the discharges, avoiding short-circuit.

When generating a plasma at high pressure, i.e. greater than 1 atm, two main discharge regimes can be observed: the dark *Townsend regime* and the bright *arc regime* [5]. The first one occurs at low values of imposed current, while the second one at high values. By continuously increasing the value of imposed current, the transition from the Townsend to the arc regime happens. The formation of a stable arc discharge is not instantaneous, and before that happens it is possible to detect a secondary discharge regime called the *spark regime*, which consists in an intermitting discharge. The spark and the arc regimes are the ones that have been employed for the plasma-treatments on lignin in this thesis work. The GAT is a particular configuration of gliding arc where the gas flux is used to create a vortex-tornado regime to improve the self-cooling of the system and to increase the residence time of the gas in the plasma region. The main components of the GAT device are shown in Figure 3.1.
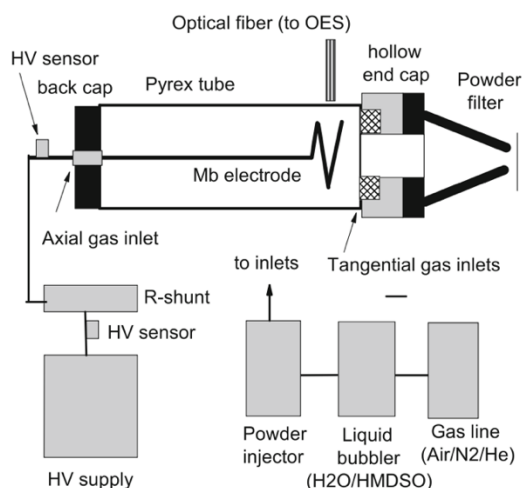
Figure 3.1 Representation of the GAT device [6].

In the GAT setup, one of the two electrodes necessary for the formation of the plasma coincides with the hollow end cap of the chamber, while the other one is a spiral Molybdenum electrode. The spiral geometry is responsible of creating the vortex flow typical of this instrument. The high voltage DC generator allows the control of the electrical parameters of the circuit by keeping the current fixed at the imposed desired level.

For the aim of this thesis work, lignin was subjected to eight different plasma treatments. The varying parameters were: the discharge regime, the gas source for the plasma and the functionalizing gas. The details of the treatments are shown in Table 3.1.

Table 3.1 Plasma treatments performed on lignin.

Treatment	Regime	Gas source	Funct. gas
S.-air-0	Spark	Compr. air	None
A.-air-0	Arc		
S.-Ar-0	Spark	Argon	None
A.-Ar-0	Arc		
S.-Ar-HEX	Spark	Argon	Hexane
A.-Ar-HEX	Arc		
S.-Ar-HMDSO	Spark	Argon	HMDSO
A.-Ar-HMDSO	Arc		

A characterization of the electrical parameters of the instrument was needed to detect the values of imposed current at which the spark or the arc regime could be observed. To do so, a high voltage probe and a current probe connected to an

oscilloscope were used. First, the influence of the distance between the electrodes, the gas pressure, and the nature of the plasma gases (gas source and functionalizing gas) on the position of the spark-to-arc transition (I_{th}) was studied. It was observed that the electrodes distance does not significatively alter the value of imposed current at which the transition is observed, while when increasing the gas pressure I_{th} linearly increases as well. Instead, by keeping fixed the other experimental parameters, the addition of a functionalizing gas can shift the transition from 275 mA to 500 mA. Considering the results of the electrical characterization, the parameters selected to perform the treatments in the spark and arc regimes are the listed in Table 3.2.

Table 3.2 Experimental parameters used to perform the plasma treatments in spark and in arc regime.

Parameter	Spark regime	Arc Regime
Imposed DC current (mA)	200	750
Distance between the electrodes (mm)	18	
Pressure (atm)	3 for Argon, 2 for compressed air	

The decision to choose a specific value of imposed DC current to perform the plasma treatments in the spark or arc regime, independently on the nature of the plasma gases, was the easiest one from an operational point of view. Indeed, the focus of this thesis work was mostly on studying the effects of a treatment performed with an intermitting (spark) or a stable (arc) discharge. To do so, values of imposed current sufficiently far from the spark-to-arc transition that were observed with or without functionalizing gases were chosen. Also, different values of pressure were employed depending on the gas source used. With compressed air a pressure of 2 atm was enough to carry the lignin powders along the circuit, while with Argon 3 atm of pressure were needed.

3.2. Characterization of the plasma-treated powders

FT-IR spectroscopy was used to detect changes from the IR spectrum of pristine lignin. It is possible to identify two different regions in lignin's

spectrum: the -OH region at wavenumbers between 3600 cm^{-1} and 2400 cm^{-1}, and the fingerprint region in the range 1800-1000 cm^{-1}. The -OH region is the relevant one to evaluate the variation in the hydrophilicity of the powder (Figure 3.2).
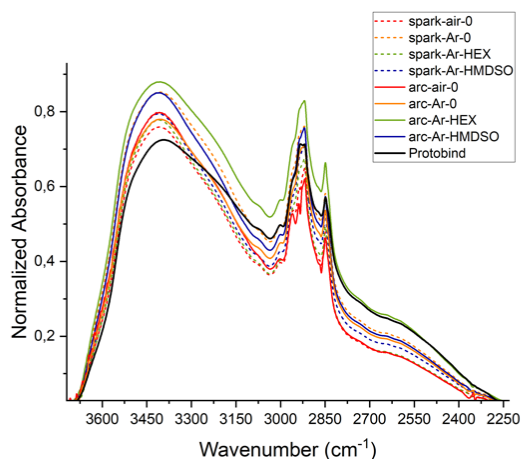

Figure 3.2 FT-IR spectra (-OH region) of pristine and plasma-treated lignin.

Nonetheless, no significant differences can be detected between pristine lignin and the plasma-treated powders. Similar results were provided by solubility tests performed in methylethylketone, toluene, ethyl acetate, and cyclohexane, where no shift from a weakly-hydrophilic to a hydrophobic behaviour was observed.

Results from the DSC measurements on the plasma-treated powders are shown in Table 3.3.

Table 3.3 Glass transition temperatures of the plasma-treated powders.

Gas source - Functionalizing gas	Tg (°C) - Spark regime	Tg (°C) - Arc regime
Air - /	133	148
Argon - /	138	138
Argon - Hexane	147	138
Argon - HMDSO	140	137

The glass transition temperature (T$_g$) of pristine lignin is 132°C, which is lower than all the values presented in the table. It is likely that the plasma treatment induced repolymerization of lignin within itself in all the samples, increasing its molecular weight and shifting the transition to higher temperatures. Differences between the lignins treated in the arc and the spark regime can

also be observed, except for the treatment in Argon without functionalizing gases. The high energy provided to lignin by the continuous arc discharge probably favoured the reaction between the biopolymer and the reactive gases in the chambers. In case of compressed air, this brought to enhanced oxidation and therefore stronger interactions among the polymer's chains, with consequent increase in the T$_g$. Instead, the reaction between lignin and n-hexane or HMDSO brought to the deposition of non-polar functional groups at the place of hydroxyl polar groups, resulting in lower intermolecular interactions and lower T$_g$.

Eventually, ^{31}P-NMR was used to quantify the variations in the hydroxyl and carboxylic groups concentrations. Comparison of the results of plasma-treated and pristine lignin is shown in Figure 3.3.
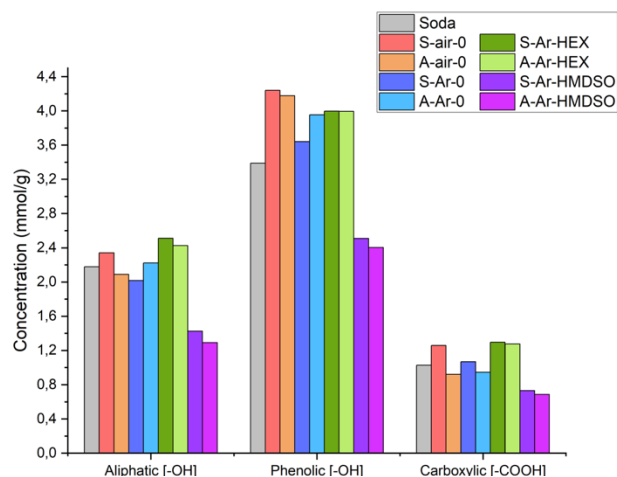

Figure 3.3 Results of ^{31}P-NMR spectroscopy on pristine and plasma-treated lignin.

Only the couple of treatments performed in HMDSO effectively reduced the total -OH and the -COOH concentration, lowering them to approximately 65% and 72% respectively. Surprisingly, treatments with n-hexane brought to the highest increase in the hydrophilicity of the powders, probably due to fast ageing of the samples. Slight decreases in the aliphatic hydroxyl and carboxylic groups concentrations are observed also in the samples Arc-Air-0 and Spark-Ar-0. Since these types of treatments are expected to oxidize the polymers, it might have happened that unreacted active sites took the place of polar groups of lignin and that they were still present at the time of the measurement. Stability of the treatments over time was also studied with ^{31}P-NMR. Specifically, it was observed that after 14

days from the treatment the hydroxyl and carboxylic groups concentrations experience an increase, bringing them to values even higher than the ones of pristine lignin.

The results from ^{31}P-NMR were determining for selecting the treatments to proceed with for the blending to evaluate their effect on the properties of lignin-polypropylene compounds. The goal was to investigate differences between a couple of treatments performed with a functionalizing gas (Spark-Ar-HMDSO and Arc-Ar-HMDSO) and a couple with only the gas source (Spark-Ar-0 and Arc-Ar-0). The ones with the overall lowest concentration of polar functional groups have been selected for the blending with a twin-screw extruder.

3.3. Characterization of the lignin-polypropylene compounds

The mechanical and chemical properties of the blends, as well as their thermal stability, were studied by tensile tests, rheological tests, differential scanning calorimetry, and thermogravimetric analysis.

Rheology tests showed that at low lignin contents (5% and 10%) the presence of the biopolymer does not affect the behaviour of pure polypropylene, bringing to similar relaxation times, indistinctively on the type of treatment performed on lignin. With 20% lignin content, a decrease in the relaxation time of approximately 25% is experienced in all the samples. This is probably related to low compatibility between lignin and polypropylene, bringing to the formations of voids that facilitate the flow of chains over the others, lowering the relaxation time.

Thermogravimetric analysis was performed only on the samples with lignin content equal to 10%, in order to study the effect of the different plasma treatments on the thermal stability of polypropylene. It was observed that the samples containing pristine lignin (PP+SODA) and plasma-treated lignin in the spark regime (PP+Spark-Ar-0, PP+Spark-Ar-HMDSO) acted as thermal stabilizers on polypropylene, increasing the temperature of maximum degradation by ~5% (Figure 3.4). The residual mass detected at the end of the measurement was also higher in the case of the blends, compared to pure polypropylene.
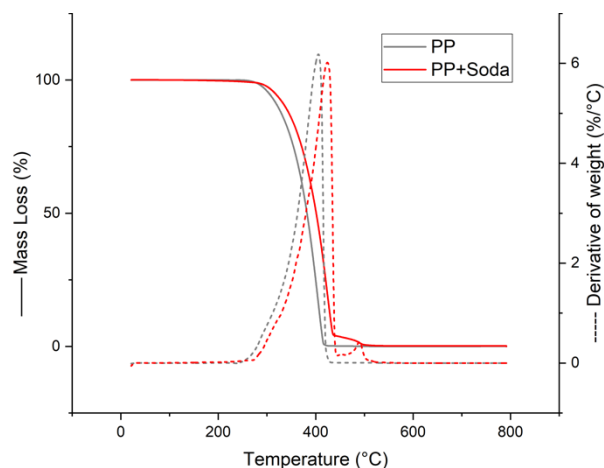

Figure 3.4 Results of the thermogravimetric analysis on pure polypropylene and on polypropylene blended with 10% of soda lignin

Variations in polypropylene's normalized fusion enthalpy and melting temperature when it is blended with 10% or 20% of lignin was also investigated through DSC. The melting temperature seems not to be affected either by the type of lignin in the compound or by its amount, bringing to only variations of ± 3°C on the melting temperature of pure PP. The normalized fusion enthalpy, instead, reasonably decreases in the samples with 20% of lignin content, being the fraction of crystallized material lower. In blends with 10% lignin content only small variations are observed, which is surprising since also in this case there is reduction in the crystalline fraction. It might have happened that lignin acted as nucleating site for the formation of the new phase (liquid), balancing therefore the effect of the reduction in the fraction of crystalline material.

Tensile tests were the most important ones for this thesis work, since they characterized the mechanical properties of the blends, which are closely connected to the aim of the project. An increase in the elastic modulus compared to the one of pure PP is observed in all the samples, except for Arc-Ar-HMDSO, which is reasonably explained by the increase in stiffness provided by lignin. However, a decrease in the ultimate strength compared to pure polypropylene is observed in all the blend indistinctively, testifying compatibility problems between PP and the biopolymer. Positive results were instead provided when comparing the elongation at break (ε_B) of PP+Soda blends with the ones containing plasma-treated lignin (Figure 3.5).
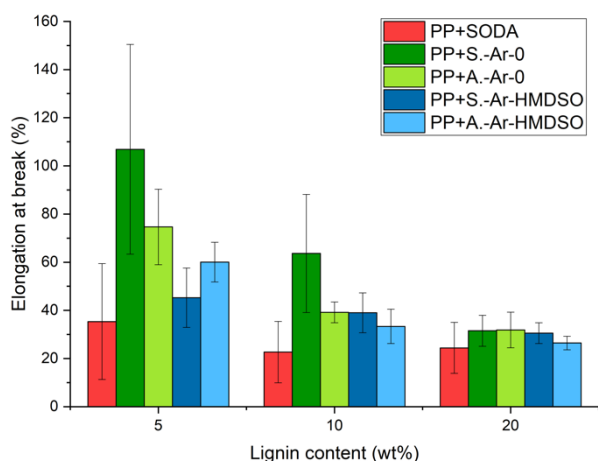
5

Figure 3.5 Elongation at break of polypropylene-lignin blends.

Especially for 5% and 10% lignin content, an increase in the ε_B of blends containing plasma-treated lignin is observed, compared to the ones with pristine lignin. With the sample PP+Spark-Ar-0 (5) the elongation at break increased even by approximately 300% from the one of PP+Soda (5). At 20% lignin content, the effect of the plasma treatment on the biopolymer seem to vanish.

It must be underlined than all the compounds show a ε_B that is much lower than the one of pure polypropylene, equal to 830%.

4. Conclusions

^{31}P-NMR was used to evaluate variations in the hydrophilicity of the lignin powders, assessing satisfying results for the plasma-treatments performed with HMDSO. However, tensile tests showed that the decrease in the polar groups concentration alone is not enough to achieve an improvement in the mechanical properties of the lignin-polypropylene compounds. Indeed, since the samples treated in Argon showed better results for the elongation at break, it might be that grafting of new active sites on the surface of lignin particles acted more efficiently on mechanical performances than the replacement of -OH groups with non-polar ones.

Bibliography

[1]   D. Kun and B. Pukánszky, "Polymer/lignin blends: Interactions, properties, applications," *Eur. Polym. J.*, vol. 93, pp. 618–641, 2017, doi: 10.1016/j.eurpolymj.2017.04.035.

[2]   D. Kai, M. J. Tan, P. L. Chee, Y. K. Chua, Y. L. Yap, and X. J. Loh, "Towards lignin-based functional materials in a sustainable world," *Green Chem.*, vol. 18, no. 5, pp. 1175–1200, 2016, doi: 10.1039/c5gc02616d.

[3]   T. Atz Dick, J. Couve, O. Gimello, A. Mas, and J. J. Robin, "Chemical modification and plasma-induced grafting of pyrolitic lignin. Evaluation of the reinforcing effect on lignin/poly(L-lactide) composites," *Polymer (Guildf).*, vol. 118, pp. 280–296, 2017, doi: 10.1016/j.polymer.2017.04.036.

[4]   B. Keun, T. Lee, J. M. Goddard, and J. H. Hotchkiss, "Plasma Modification of Polyolefin Surfaces," *Packag. Technol. Sci.*, vol. 22, no. 3, 2008, pp. 139–150, 2009, doi: 10.1002/pts.829

[5]   C. F. Gallo, "Coronas and Gas Discharges in Electrophotography: a Review," *IEEE Trans. Ind. Appl.*, vol. IA-11, no. 6, pp. 739–748, 1975.

[6]   R. Barni *et al.*, "Characterization of the electrical and optical properties of a gliding arc tornado device," *Eur. Phys. J. D*, vol. 75, no. 5, pp. 1–6, 2021, doi: 10.1140/epjd/s10053-021-00121-8.

Plasma treatments on lignin for improved compatibility in lignin-polypropylene compounds

MASTER THESIS IN
MATERIALS ENGINEERING AND NANOTECHNOLOGY

Author: **Sofia Graziella Regoli**

Student ID:	943586
Advisor:	Gianmarco Enrico Griffini
Co-advisors:	Ruggero Barni, Emanuela Bellinetto, Oussama Boumezgane
Academic Year:	2020-21

Abstract

Climate change and plastic pollution are pushing governments and companies to redesign polymers production processes to make them more sustainable and environmentally friendly. The idea of using lignin as an added-value resource in polymeric materials is gaining interest over the years because it would mitigate the problems of resources depletion, greenhouse gases emissions, and dispersion of plastic waste in the environment. Lignin constitutes up to 33% of lignocellulosic biomass in plants and trees and it is a side-product of the paper industry. The annual production of lignin ranges from 500 to 3600 millions of tons and nowadays only 2% of it is used in polymeric materials production. The remaining amount is mostly used as renewable resource-derived fuel. The incorporation of lignin in plastics would meet the sustainability requirements of today's environmental agreements, being lignin a renewable and biodegradable resource. Several scientific studies have already shown that lignin is a valid candidate as component in plastic products, since it is able to provide good mechanical properties for bulk applications. However, there are some issues regarding the compatibility of lignin with highly hydrophobic polymers, such as polyolefins, due to the presence of several hydroxyl groups in its chemical structure. This thesis project aims at modifying the surface chemistry of lignin particles to make them more compatible with polyolefins, in order to achieve satisfying miscibility in a polypropylene-lignin blend. Specifically, plasma treatments have been performed on lignin to reduce the hydroxyl groups concentration and/or to graft new active sites on the lignin particles surface. Functionalizing gases, i.e. n-hexane and hexamethyldisiloxane, were also employed during some of the plasma treatments. Plasma treatments are particularly attractive because they are solvent-free, unlike alternative chemical methods for lignin functionalization. The results of the plasma treatments on lignin powders were investigated through Fourier-transformed infrared spectroscopy, solubility tests, differential scanning calorimetry and nuclear magnetic resonance spectroscopy. The mechanical and chemical properties of the blend, as well as its thermal stability, were studied by tensile tests, rheological tests, differential scanning calorimetry, and thermogravimetric analysis.

Key-words: lignin, polyolefins, circular economy, plasma treatment, polypropylene-lignin blend, lignin functionalization.

Estratto in lingua italiana

Il cambiamento climatico e l'inquinamento da plastica stanno spingendo governi e imprese a modificare i processi di produzione dei materiali polimerici per renderli più sostenibili e per ridurre il loro impatto ambientale. L'idea di utilizzare la lignina come componente in miscele polimeriche col fine di ridurre il problema dell'esaurimento delle risorse, le emissioni di gas serra e la dispersione dei rifiuti di plastica nell'ambiente sta acquistando sempre più interesse nel corso degli anni. La lignina costituisce fino al 33% della biomassa lignocellulosica di piante ed alberi ed è un prodotto di scarto dell'industria della carta. La produzione annuale di lignina oscilla tra i 500 e i 3600 milioni di tonnellate, e attualmente soltanto il 2% è utilizzato nella produzione di materiali polimerici, mentre la restante parte è utilizzata invece come carburante derivante da risorse rinnovabili. L'incorporazione della lignina in materiali polimerici è in linea con i requisiti di sostenibilità presenti negli accordi ambientali odierni, essendo una risorsa rinnovabile e biodegradabile. Diversi studi hanno messo in evidenza che la lignina può essere un valido candidato come componente nei materiali polimerici, essendo in grado di conferire buone proprietà meccaniche. Tuttavia, esistono diversi problemi legati alla sua compatibilità con polimeri altamente idrofobici, quali le poliolefine, a causa della presenza di numerosi gruppi idrossilici nella sua struttura chimica. Questo progetto di tesi ha lo scopo di modificare la chimica di superficie delle particelle di lignina in modo da renderle più compatibili con le poliolefine e, di conseguenza, di facilitare la formazione di miscele polipropilene-lignina. In particolare, la lignina è stata sottoposta a trattamenti al plasma al fine di ridurne la concentrazione di gruppi idrossilici e di introdurre nuovi siti reattivi sulla superficie delle particelle di lignina. Gas funzionalizzanti, quali n-esano ed esametildisilossano, sono stati inoltre talvolta utilizzati durante questi processi. I trattamenti al plasma sono particolarmente attraenti per la funzionalizzazione della lignina in quanto non coinvolgono l'utilizzo di solventi, a differenza dei metodi chimici alternativi a questo processo. Gli effetti dei trattamenti al plasma sulle polveri di lignina sono stati indagati con spettroscopia FT-IR, test di solubilità, calorimetria a scansione differenziale e spettroscopia di risonanza magnetica nucleare. Le proprietà chimiche e meccaniche della miscela e la sua stabilità termica sono state studiate tramite prove a trazione, test reologici, calorimetria a scansione differenziale e analisi termogravimetriche.

Parole chiave: lignina, poliolefine, trattamento al plasma, economia circolare, miscela polipropilene-lignina, funzionalizzazione della lignina

Contents

1. Introduction

1.1 Environmental issue with focus on plastic pollution

1.1.1 Global warming and governments' actions to arrest the environmental crisis

The target of this project thesis is deeply connected to the environmental problems that are affecting life on our planet, especially to the problem of plastic pollution and increasing greenhouse gases emissions. This work aims to redesign plastic production to obtain a more sustainable product which at the same time can provide satisfying mechanical performances for bulk applications. The basic idea is to produce a blended material made of lignin and polypropylene. Lignin is a sub-product of paper production that constitutes until 33% of tree trunks. Implementing this substance in a polymeric matrix would make the final material partly derived from a renewable source, partly biodegradable and less impacting in terms of greenhouse gases emissions. Moreover, using lignin as filler lies in an optic of circular economy. However, being lignin a weakly-hydrophilic material that does not blend properly with highly non-polar polymers such as polyolefins, it needs to be treated to enhance the compatibility among the two materials. In this project, lignin is meant to be subjected to a physical treatment, which is the plasma functionalization technique, to lower the hydrophilicity of its particles. Through plasma-treatment functionalization with properly selected chemicals, lignin is expected to become more hydrophobic and compatibility with polyolefins should increase. Plasma-treatment of lignin is a highly attractive method because it is solvent-free, unlike chemical functionalization techniques, which makes the process even "greener". The effectiveness of the treatment and its influence on the properties of the compound have been verified during the experimental part of the thesis and the results are discussed in the following sections.

The need of finding more sustainable alternatives to nowadays technologies and materials is driven by global warming and all the environmental consequences that derive from that. Indeed, the threat of climate change on human, wild and natural life is increasing yearly. The last 6 years were recorded as the warmest in history, and the

trend of the last 150 years suggests that in the future temperatures will keep increasing (Figure 1.1) [1]. According to the report published on the 9th of August 2021 made by the Intergovernmental Panel on Climate Change (IPCC), which is the UN body for assessing the science related to climate change, some almost-irreversible climate change effects are already in motion. It is not impossible to stop them, but immediate, rapid, and large-scale initiatives must be taken to have effective results. Particularly, strong and sustained reductions of carbon dioxide emissions (CO_2) and other minor greenhouse gases (methane (CH_4) and nitrogen oxides (NO_x)) would limit the catastrophic changes the report is referring to [2].
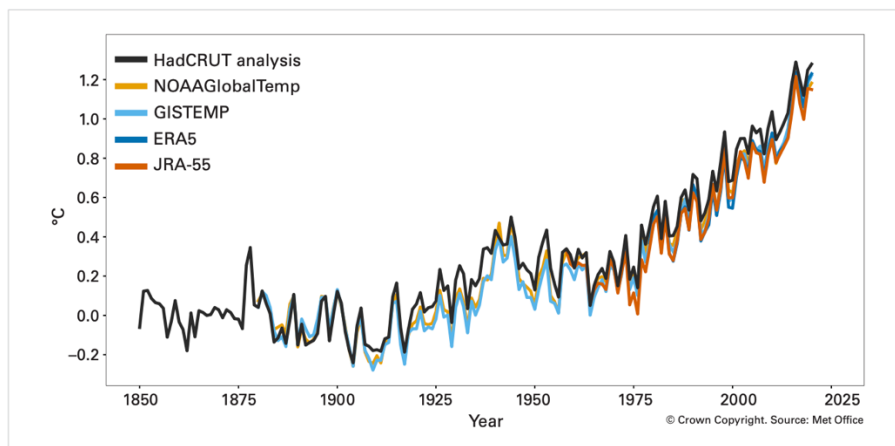

Figure 1.1 Global annual mean temperature difference from pre-industrial conditions (1850–1900) for five global temperature data sets [1].

The average planet's temperature has increased by 1.1°C since the 1880s. However, when talking about average temperature, it must be considered that the calculation is mediated all over the globe, which means that already nowadays there are some areas in the world that experience frequent unsustainable heat waves [3]. This usually happens in the poorest regions of our planet, where it is also financially difficult to implement climate change adaptation solutions (Figure 1.2) [1], [3].
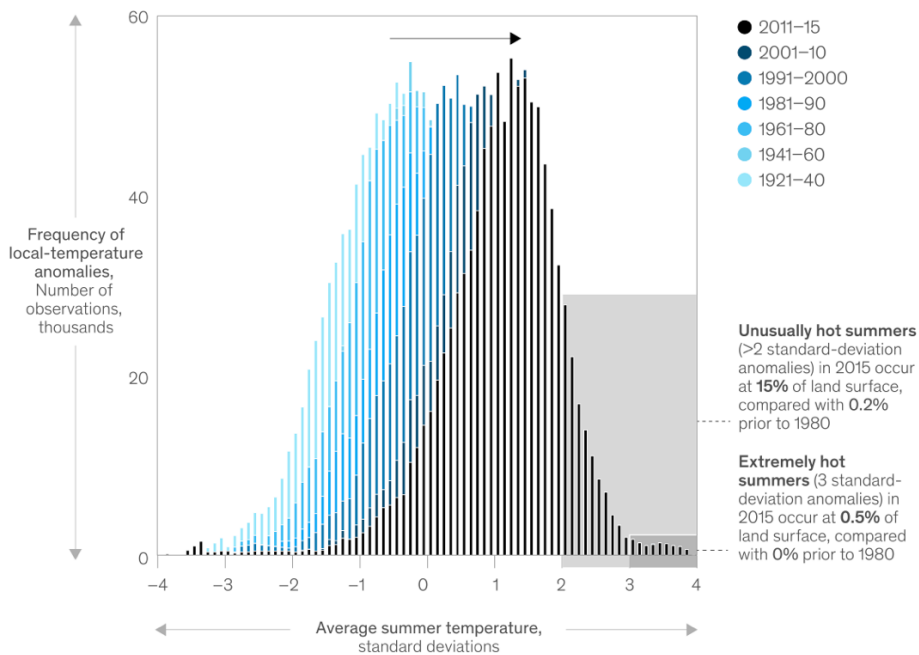
Figure 1.2 Northern hemisphere summer temperature shifts [3].

The number of yearly natural disasters is as well increasing as consequence of climate change. Just in 2005, the most catastrophic year in history, 442 incidents caused 90000 deaths all over the world. Warmer temperatures increase the risk of droughts as well as the intensity of storms and create wetter monsoon. Since 1960 the number of natural disasters increased by ten times (Figure 1.3) [1].
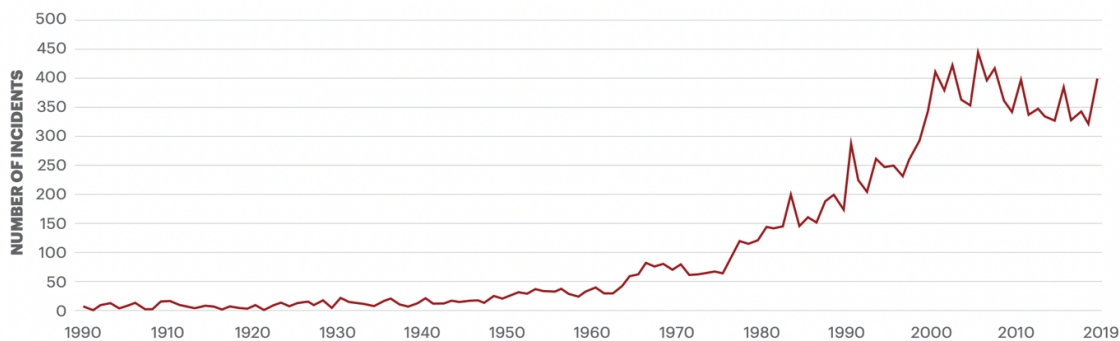

Figure 1.3 Number of natural disasters from 1900 to 2019 [1].

Climate change not only affects life and health conditions of people, but it also brings economic and social consequences. Considering as example the food industry, it is easy to imagine how dramatic the world situation would be if the 5 main food-providing areas, responsible of almost 60% of the world's food production, would be ruined by extreme climate conditions and natural catastrophes [3]. People living in

those areas and working in agriculture would remain unemployed and probably homeless if the environmental situation is so hard to cause migration. Other than that, the whole world's food request might not be satisfied.

Governments and companies acknowledged the environmental problem and decided to take part in initiatives with the goal of attenuating, or ideally stopping, the situation from getting worse. This happened in 2015, when the Paris Agreement was signed by 191 Parties (190 countries plus the European Union) [4]. It is a legally binding treaty that focuses on fighting the climate change. The aim of the agreement is to keep global warming below 2°C, ideally 1.5°C, in comparison with pre-industrial levels. The Global Green Growth Institute (GGGI) studied the relationship between economic growth, social well-being, and increasing emissions and predicted how these might interact and evolve during time [5]. The GGGI studies the development of these factors in two different scenarios: one considers the "Business as usual" (BAU) conditions that result with an average increase in global temperatures of 3-4°C, the other one supposes a scenario in which the goal of keeping global warming below 1,5-2°C is reached (Figure 1.4 and Figure 1.5) [5]. Considering that economists do not trust in a continuous and endless economic and social growth with BAU, the risk of collapse of economic sectors, especially for developing countries, is real.
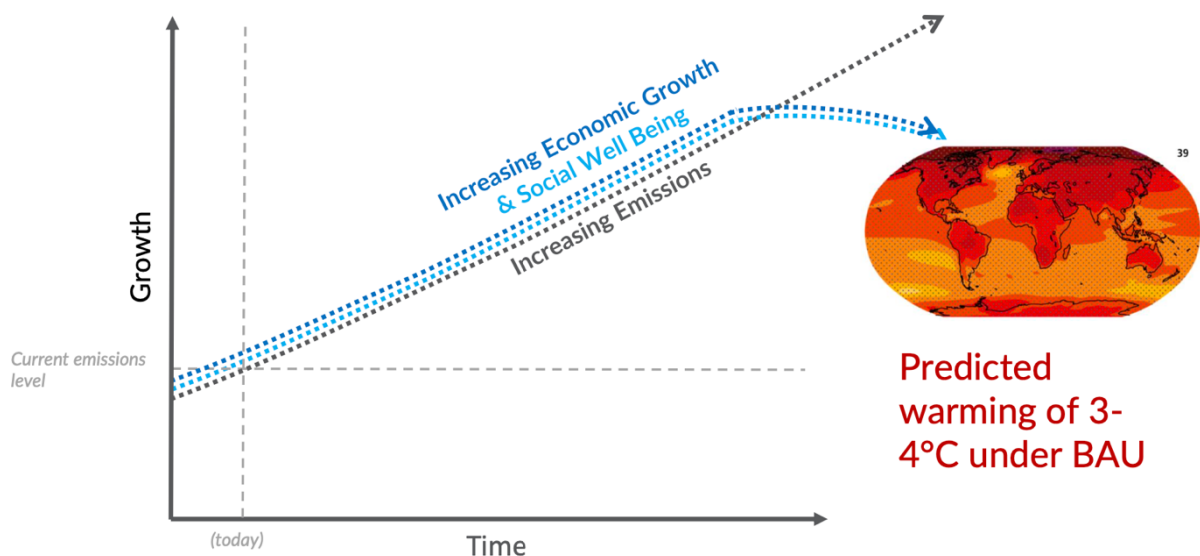

Figure 1.4 Economic growth and social development with BAU conditions considering economists' predictions [5].
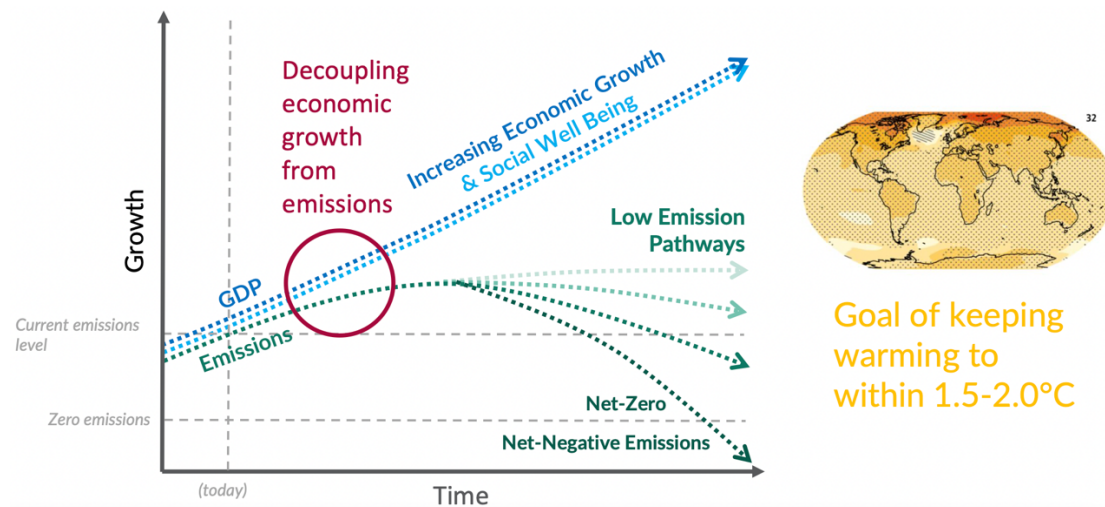
Figure 1.5 Economic growth and social development while reducing or slowing emissions [5].

These predictions should work as a motivation for people, stakeholders, and countries to change their lifestyles and policies to more sustainable ones.

According to the Paris Agreement, countries must develop executive plans of increasingly ambitious climate actions that must be reviewed every 5 years from 2025 until 2100. The *Nationally Determined Contributions (NDCs)* is the name given to these action plans. In these documents parties communicate the measures they will take to lower their greenhouse gases emissions to meet the requirements of the Agreement. In addition, in the NDCs it must also be stated how countries will act in order to build resilience to adapt to the future increase in temperatures [4]. Up to now, more than 110 parties over 191 have submitted the next national action plan. Unfortunately, there is the need of increasing the commitment and the ambition in terms of emissions reduction: considering the measures declared by the countries in the NDCs, only a 12% emission reduction will be reached in 2030, which is much lower than the required 45% to meet the goal of a maximum temperature rise of 1,5-2°C (Figure 1.6) [6].

● 12%

Reduction in greenhouse gas emissions by 2030 as defined in new/updated NDCs

● 45%

Emissions reductions needed by 2030 to keep warming to no more than 1.5 degrees Celsius
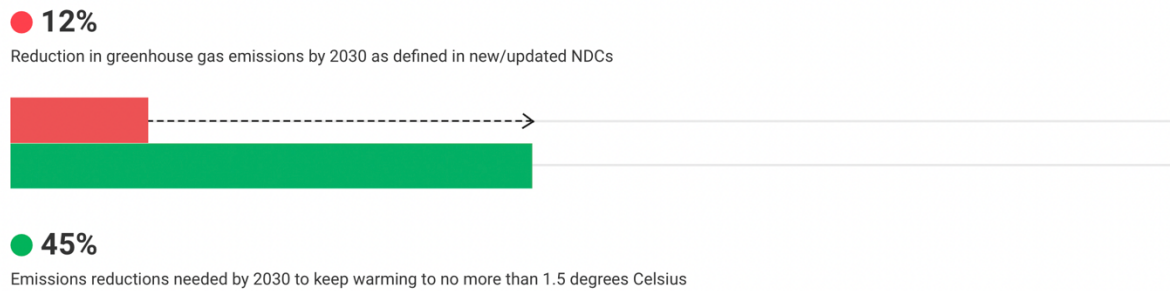
Figure 1.6 Reduction in greenhouse gases emissions by 2030 as defined in the new NDCs vs. emissions reduction needed to reach the goal defined by the Paris Agreement [6].

Moreover, according to the Paris Agreement, the signing parties must provide financing to developing countries to support them in mitigating climate change and in adapting to climate impacts [4].

To achieve the goal of limiting global warming and to satisfy all the requirements of the Agreement, also the so called *long-term low greenhouse gas emission development strategies* (LT-LEDS) have been defined [5]. Differently from NDCs, the LT-LEDSs are not mandatory [4]. They must align and support existing development plans and budgets of parties and they provide guidelines and policies to follow to achieve the goals. This social and economic transformation is only possible if the process is inclusive and all stakeholders and countries participate to the development [5].

In 2015, in addition and separately to the Paris Agreement, also the UN Sustainable Development Goals (SDGs) were defined. Here the target is to bring signing countries (all the United Nations) to engage a more sustainable behaviour not only in terms of environmental sustainability, but also social and economic [7]. By deciding to pursue them, governments are stating that they are promoting prosperity while protecting the planet, which should bring to a scenario like the one presented in Figure 1.5. The SDGs consist of 17 different goals that must be pursued before 2030 (Figure 1.7) [7].

Figure 1.7 UN Sustainable Development Goals (SDGs) [7].

During the last SDG Summit in 2019 world leaders called for a *Decade of Action* with the aim of intensifying the sustainable policies and plans to achieve the 2030 goals. In particular, at the core of 2020-2030 actions there are initiatives to tackle growing poverty, empower women and girls, and address the climate emergency [7].

1.1.2 Plastic pollution is affecting life in the oceans and on earth

On the 9th of September 2021 the General Assembly for the SDG decided to convene a Conference in Lisbon at the end of June 2022 to focus on the implementation of the SDG n°14 which protects life under water: *"Conserve and sustainably use the oceans, seas and marine resources for sustainable development"* [8]. Global warming can indeed affect the marine environment in many ways. Being the rise in temperature driven by an increase in the CO_2 concentration, oceans are affected as well since carbon dioxide diffuses in the water to reach a chemical equilibrium. A higher concentration of CO_2 in the oceans brings to acidification of the water, which affects organisms and ecosystems [1]. Moreover, as the pH of the ocean rises, it becomes more difficult for the water to absorb CO_2 from atmosphere and therefore its moderating effect on climate change is hindered.

Another important consequence of global warming on the ocean is the increase in the world's average temperature on the sea level. In the last 30 years the mean rate of sea-

level rise reached 3.3 ± 0.3 mm per year [1]. Oceans nurture 80% of life on the planet, they are responsible of producing 50% of the oxygen in the atmosphere, and they absorb 25% of the carbon dioxide present in the air [8]. If the Ocean equilibrium is tackled, consequences would highly affect the life on earth.

However, acidification of the water it is not the main phenomenon affecting life in the oceans. Indeed, plastic pollution is severely threatening the marine ecosystem. To increase the awareness about the growing concern for the marine ecosystem, the *World Oceans Day* was announced in 2018 and fixed on the 8th of June [9]. People need to recognise the value of this resource and to contribute on limiting the dispersion of plastic waste in the oceans. As reported by the UN Environment, one million plastic drinking bottles are purchased every minute, while up to 5 trillion single-use plastic bags are used worldwide every year. According to nowadays trends, half of the plastic produced yearly is meant to be single-use, and this, combined with an ineffective plastic waste management, brings to having around 8 billion kilograms of plastics entering the marine environment every year [9]. Once plastic is in the oceans, it takes hundreds of years to degrade and during this extremely long-lasting process it generates microplastics (< 5 mm) that might contain toxic organic pollutants which easily enter in the food chain [10][11]. This phenomenon has consequences on the health of marine species that eat them, but also on human health.

As stated by the International Union for Conservation of Nature and Natural Resources (IUCN) more than a third of the plastic currently polluting our ocean consists in microplastics [12]. These millimetric plastics are not only present in oceans, but also on the land, in the air and in tap water. Approximately 35% of the total amount of microplastic enter the environment from the abrasion of synthetic textiles during laundry, while 28% is generated from the abrasion of tyres while driving. Other minor sources of microplastic are the weathering and abrasion of road markings by vehicles, the weathering, application and maintenance of marine coatings, the loss during use of personal care products, and the manufacturing, transport and recycling of plastic pellets [12]. Tyre abrasion is considered responsible of 5-7% of the particulate present in air pollution, and it was assessed responsible of causing 3 million deaths in 2012 by the World Health Organization (WHO) [12].

Humans also ingest and drink microplastics, other than breathing them. Fishes commonly happen to eat microplastics, and since the 20% of the world's intake of proteins comes from fish there is a high probability that these materials enter the human food chain. The effects of plastic ingestion are still under study, but considering the presence of toxic additives in plastic (e.g. phthalate plasticizers, polybrominated biphenyls (BPBs)), their ingestion could cause cancer or endocrine disruption [12]. Moreover, it was tested that microplastic are found in a great variety of samples of tap

water all over the globe. The highest percentage of samples positive to the presence of microplastics was found in the USA (94%), while Europe was found to be the country with the lowest but still considerable amount (72%) [12].

A study was made to quantitatively assess the impact of hypothetical measures to reduce plastic pollutions. Referring to Figure 1.8 it is possible to compare the predictions of plastic emissions in the aquatic ecosystem in three different scenarios: BAU, therefore considering current plastic usage and management trends over the years; an ambitious scenario following the global commitments to reduce plastic emissions; target scenario of < 8 million metric tons (Mt) dispersed in the environment, which is the estimated global dispersion in 2010 to the oceans. This amount is a frequently cited statistic in global policy discussions as an unacceptable amount of plastic emissions to the marine ecosystem alone (a subset of the aquatic ecosystems considered here). The study also made specific considerations (graphs B) depending on the level of socioeconomic status of a country, as defined by the World Bank (high income (HI), upper-middle income (UMI), lower-middle income (LMI), and low income (LI)) [13].
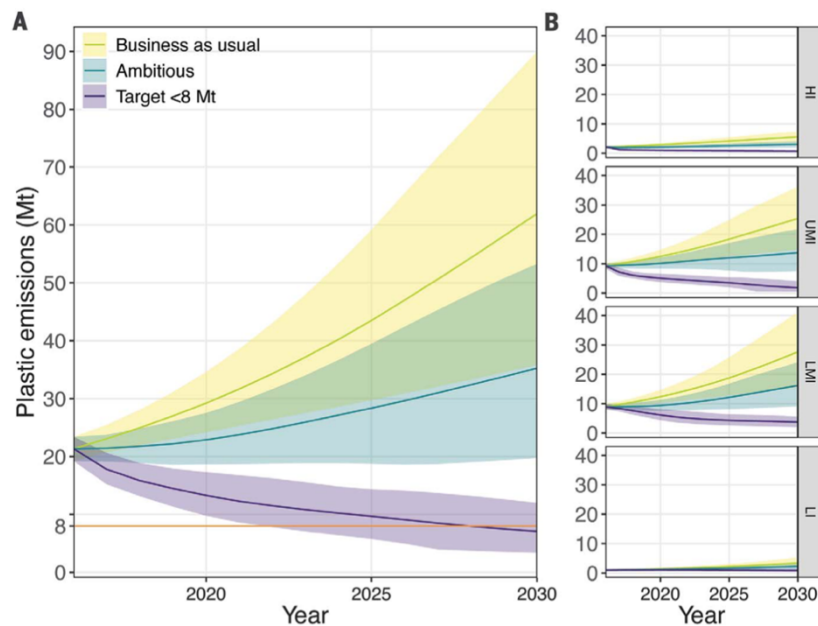

Figure 1.8 Annual global plastic emissions into aquatic ecosystems. Data include major rivers, lakes, and the oceans in million metric tons (Mt) from 2016 to 2030 (A) and for each income status (B) as defined by the World Bank showing the BAU (yellow), ambitious (blue), and target <8 Mt (purple) scenarios. Shaded areas represent 80% credible intervals indicating the uncertainty in plastic waste generation and the scenario implementation into the future [13].

The prevision following the ambitious target still brings to a plastic emission between 20 and 53 Mt/year by 2030, remaining at or exceeding 2016 levels despite incredible reduction efforts by the global community. This study shows that a better waste management alone is not capable of contrasting the increasing plastic waste generation and other measures must be taken to effectively reduce the problem of plastic pollution. It is important to realise that plastic pollution does not start when the material is released in the environment, but it has its roots in the raw materials selection and in the design of production processes. There are many environmental problems related to plastic production, from the resource's depletion to carbon dioxide emissions, improper waste management, and recycling management. Therefore, a life-cycle approach is necessary to evaluate every step which needs modification to satisfy the environmental requirements [10].

The plastic pollution crisis is mostly driven by improper recycling combined with a massive use of single-use plastics. Individual should redesign their habits trying to increase the life of plastics they use while governments and companies should act on improving waste management and on redesigning polymeric products to make them more safe and sustainable [10].

1.1.3   Redesign of plastic production to tackle plastic-related environmental problems

The most desirable ways of reducing plastic pollution are deeply connected to individuals behaviour, who are encouraged to reduce the employment of single-used plastic and to find ways to increase the lifetime of plastic objects (Figure 1.9) [14]. Relying on consumers behaviour, however, should be strongly accompanied by actions from all economic producers, policy-makers, and businesses [10].
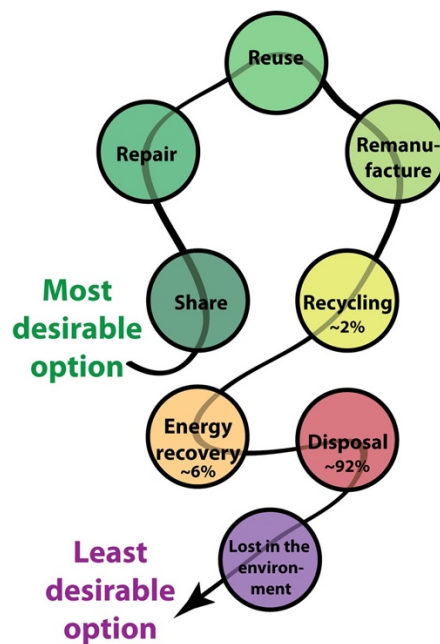
Figure 1.9 Waste management hierarchy [14].

The concept of directly involving worldwide producers in lowering the environmental impact of plastics is in line with Goal 12 of the SDG "Responsible consumption and production". Within this context, a redesign of plastic products is necessary to achieve a transformation towards a more sustainable production [10]. Remanufacture is indeed at the highest positions in the waste management hierarchy shown in Figure 1.9.

Plastic is a necessary material in human life and therefore it is not beneficial to hope in a world without it. It is a very versatile material in terms of production and applications because it is easy to process and it has many advantageous property such as transparency, light-weight, it is hygienic and, most importantly from an industrial point of view, it is cost effective [15]. Since it is not possible or desirable to delete plastic from our planet, alternative solutions must be found to make the material more sustainable.

Polyolefins, the class of materials considered in this thesis work, highly impact the environment both for their typical manufacturing process and for their disposal. Even though only 4% of petroleum resources are used for plastic production, manufacturing sectors are motivated to redesign their production processes because of the high impact that this transformation would have on the environment, having commodity plastics a huge market share [15].

There are two main ways that industries follow to reduce the environmental impact of plastic: recycling of used products or selection of alternative raw materials [12], [15].

The second is the one this project is focusing on. Since more than 10 years ago bioplastic started to become more attractive than polyolefins for plastic production due to fossil fuel saving, lower toxicity, and biodegradability (in some cases) deriving from their implementation. To produce biopolymers renewable resources are needed, and this brings to lower (or null) raw materials depletion and decreased CO_2 emissions [15]. However, polymers entirely produced from natural resources are not highly performant in terms of mechanical properties and they are therefore mostly used for packaging applications.

One way to produce a plastic material that is more sustainable than a complete petroleum-derived one, while keeping satisfying thermo-mechanical characteristics, is to produce a blend consisting of both a polymer from renewable sources and one from fossil fuel. This is the idea that lies behind the concept of this thesis work: mixing lignin with polyolefins would lower the environmental impact of the material due to the reduction in emissions and to the implementation of a renewable and biodegradable resource that re-enters the production chain in an optic of circular economy. Moreover, the obtained material would have improved mechanical characteristics compared to other biopolymers.

1.2   Lignin

1.2.1   Structure, properties, and applications of lignin

Lignocellulosic biomass is nowadays the most promising alternative to satisfy the need of replacing petroleum resources as raw materials for polymers production. It contains partially reduced multi-carbon molecules that can therefore act as macro-monomers [16],[17]. Lignocellulosic biomass is plants' dried matter, and it is composed of cellulose, hemicellulose, and lignin. Most of the mass of these three biopolymers is found in the macro- and micro-fibrils of the walls of plant cells (Figure 1.10) [18]. In this section of the thesis the attention will be focused on lignin because of its high potential value in future industry applications and its inherence to this work.
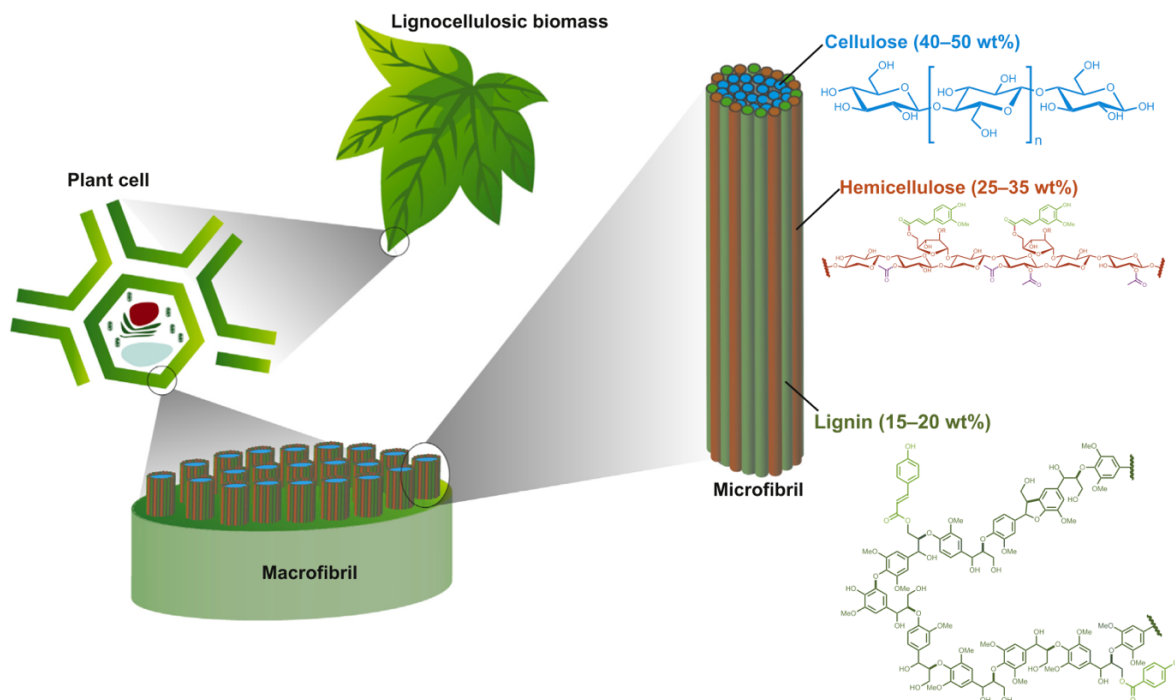
Figure 1.10 Overview of the structure of lignocellulosic biomass [18].

Lignin is the second most abundant natural biomass on Earth, just after cellulose, and it accounts for between 17% and 33% of the mass of trees and plants, depending on the species [19]. It is synthesised by plants and trees during the photosynthesis through an enzyme-mediated dehydrogenation polymerization process, also called lignification. The formation of lignin results from the reaction of three different cinnamyl alcohol monomers (also called *monolignols*): *para*-coumaryl alcohol (H-type), coniferyl alcohol (G-type), and sinapyl alcohol (S-type) (Figure 1.11). The relative amount of the three monolignols in plants is different depending on the species [16]. For instance, the H/G/S ratio is 0–5/95–100/0 in softwood, 0–8/25–50/46–75 in hardwood and 5–33/33–80/20–54 in grasses [19]. Consequently, the lignin isolated from different types of trees, plants or grass will have a different chemical structure which makes it extremely difficult to have a universal description and characterization of the material. Model structures of lignin have been proposed in literature, and studies revealed that there are two main structures (Figure 1.12): *type 1* which forms 48 wt% of softwood lignin and *type 2* that correspond to the 40 wt%. Type 1 lignin is located in a complex which is directly connected to cellulose fibrils through hydrogen-bonds, while type 2 can be found in a different complex that is located around the cellulose fibrils embedded in type 1 lignin [19].
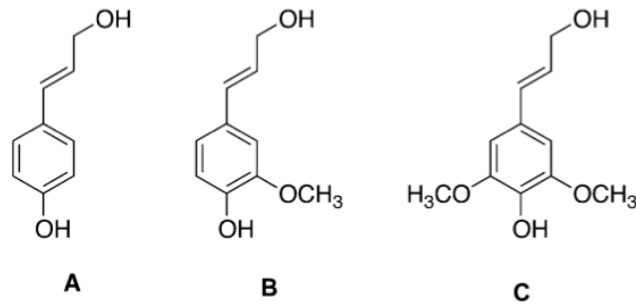
Figure 1.11 Three standard monolignol monomers. A = p-coumaryl alcohol; B = coniferyl alcohol; C = sinapyl alcohol [16].
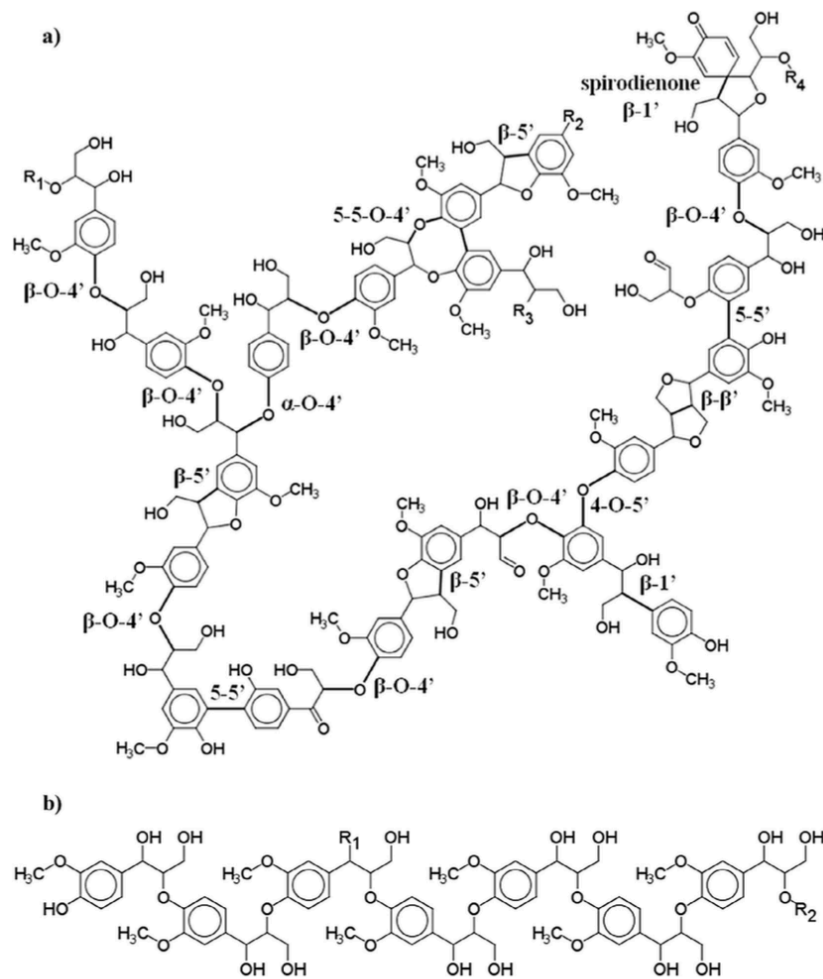

Figure 1.12 The model structure of spruce lignin. (a) Type 1 lignin and (b) type 2 lignin [19].

In plants and trees lignin is responsible both for structural integrity of cell walls and for the stiffness of the entire plant. Thanks to the hydrophobic nature of lignin, it also

regulates transport of water and other nutrients. Moreover, lignin can provide protection against biological stresses by inhibiting enzymatic degradation of other components and it can act as anti-bacterial against microorganisms [16],[17].

From the industrial point of view lignin is a side-product of the paper industry, and it has been generally considered a low-value resource. Indeed, it has mainly been used as a source of renewable energy by the pulp and paper industry. However, lignin's energy content is not high enough to satisfy the energy demand, and it would be therefore more interesting to employ it in other applications that could recognise it as a high-value resource [18]. Other common low-value applications for lignin are concrete additives, dust control, pesticides, stabilizing agents, dyestuff dispersants and surfactants or binders for animal feed [17],[20].

The interest about lignin derives from the possibility of using it as component in plastic materials. It could both contribute to the production of a more sustainable type of plastic and to solve the problem of depletion of resources. Indeed, the annual production of lignin ranges from 500 to 3600 millions of tons and nowadays only 2% of the total lignin produced from the paper industry during the extraction of cellulose is used in polymers production [20]. Because of its great availability, lignin is an inexpensive resource and its incorporation in any value added application would bring a considerable economic gain [18]. It also has many attractive properties for high-value applications; it has a high carbon content, high thermal stability, antioxidant activity, and favourable stiffness [17]. Additionally, it is biodegradable since a certain type of wood-rotten fungi is able to efficiently depolymerize it and mineralize it [20].

Extraction of lignin can be performed from its botanical source and from pulping chemical processes as well. More details about extraction processes will be discussed in the following section.

1.2.2 Lignin extraction processes

The paper industry is the main large-scale producer of lignin, which isolates the biopolymer from cellulose during the purification process of cellulose [18]. Extraction of lignin can involve either physical or chemical methods, and both kind of processes can be referred to as *pulping*. Nowadays the chemical methods are the most applied ones; they involve chemicals that degrade the cross-linked or highly branched structure of lignin, with cellulose remaining intact. After this step lignin becomes soluble in the reaction medium and cellulose fibres can be easily separated through filtration [19].

Lignin can be isolated through four main industrial chemical processes, which can be divided in two categories whether the extracted product contains sulphur or not. The

two methods whose products contain sulphur are the *sulphite process* and the *kraft process*, while the other two are the *soda process* and the *organosolv process* [16]. The lignins isolated with these methods are called *technical lignins*, and their structural characteristics are different according to the extraction process they were isolated with. These differences not only involve the sulphur content, but the resulting products have different purity, different molecular weight an structure of the obtained fragments [17],[16]. More details about the four extraction processes are presented as follows [19].

Soda process: the soda process is the first chemical pulping method patented. It is mostly employed to isolate lignin from plants with low content of lignin, such as wheat straw, sugar cane, flax, and bagasse. To extract lignin, wood chips are cooked in an alkaline aqueous medium containing sodium hydroxide (NaOH). The phenolic hydroxyl groups of lignin are deprotonated by NaOH, and this starts a consecutive reaction that results in the cleavage of some of the most frequent bonds in the repeating units of lignin. The lignin obtained through this method has a quite high level of purity [16],[19]. In this thesis work the employed lignin was extracted through the soda process.

Kraft process: the kraft process can be considered a development of the soda process and it is nowadays the most often used pulping method. In addition to NaOH, also sodium sulphite is added to the cooking liquor to extract lignin to further accelerate the degradation process of lignin. Unfortunately, most of kraft lignin is burnt as source of energy during cellulose production and it is rarely used in materials production [19].

Sulphite process: lignin extracted through the sulphite process is the main source of commercially available lignin (equal to 1.0 million tons in 2014). It employs a heated solution containing sulphite or bisulphite salts of sodium, ammonium, magnesium, or calcium. The concentration and proportion of the sulphite, bisulphite and sulphur dioxide present in the cooking medium depends on the chosen counterion, and therefore pH, of the mix. This choice determines the degradation process of lignin. There are four main variations of the sulphite process, which are performed at different pH ranges. The most used chemical methods are carried out at acid pH, and they are called the *acid bisulphite* and the *bisulphite processes*. Due to the residual sulphur-containing functional groups at the end of the extraction process, this type of technical lignin has a larger molecular weight compared to the one of kraft lignin. Moreover, the resulting lignosulphonate is water soluble in the solution as well as hemicellulose. Therefore, an additional step to achieve complete isolation of lignin is required. [19],[16].

Organosolv process: this extraction process of lignin is widely spread at the laboratory level. It is based on the isolation of lignin by using polar organic solvents like

methanol, ethanol, formic acid, and acetic acid. Since many different types of solvents can be employed, the polarity, structure, and properties of the resulting organosolv lignin will depend on the solvent selected for the extraction. Among all the various organosolv processes, the Alcell® one is the most used and cited in literature. In this case, the aqueous medium is a solution containing 40-60 wt% of ethanol. The recovery of the solvents has not been optimized yet, which makes the organosolv method a relatively high cost process and not very environmentally friendly [16],[19].

1.2.3 Blending lignin with polymers

As mentioned in the previous sections, lignin is attracting interest as alternative resource to produce new polymeric materials since it would be energetically and environmentally friendly [16]. Being lignin the responsible element for structural support in plants, a reasonable intuition would be to use it as reinforcing-agent in a polymeric matrix. Polymer-lignin composites have actually become very popular for being high performance composites [17]. It is although difficult to develop miscible lignin-polymer combinations since there is a poor interfacial binding among lignin and polymer particles, which results in particle aggregation and phase separation of the matrix, especially if it is highly non-polar [17]. This problem is connected to the high chemical reactivity of lignin, which tends to undergo uncontrolled condensation and repolymerization with itself, highly hindering its incorporation into polymers [18]. Through these internal reactions lignin forms a great number of C-C bonds, with the consequence of increasing the branching degree of the polymer and therefore its molecular weight. When lignin undergoes repolymerization, it also changes its space distribution with the result of increasing the number of inter- and intra-molecular interactions (such as hydrogen bonds, CH-π bonds, π-π bonds) that lower lignin solubility and miscibility in a wide range of polymers and solvents. The formation of new C-C bonds occurs on the aromatic rings or from the disappearance of hydroxyl groups, which both are the most reactive sites of lignin [18]. Different solutions to overcome the compatibility problem of lignin with plastics have been explored. Plasticization or chemical modification of lignin can be performed to improve its dispersion in plastics, or interfacial adhesion can be increased by the addition of plasticizers. Moreover, lignin can be used as reactive component in many different types of resins and polymers [19].

When discussing about mixing of polymers with lignin, it is important to specify whether it is a blend or a composite. A blend is "a mixture of at least two polymers interacting through interdiffusion", while a composite is a mixture where "a polymer and the filler interact through adsorption at the desired interface" [19]. It is difficult to practically distinguish if lignin is acting as a filler or as a blending component due to

its branching degree and molecular weight. Lignin particles need to be small enough to create a homogenous mixture with the other polymer to result in a blend. Nonetheless, since the lignin resulting from pulping processes is often slightly degraded and its molecular weight is therefore decreased, it is very likely that mixing it with plastics will result in a blend [19]. There are many literature examples of lignin blends with polyolefins (e.g. polyethylene, polypropylene), aromatic polymers (e.g. polystyrene, polyethylene terephthalate), H-bonds containing polymers (e.g. polyethylene oxide, polyvinyl pyrrolidone, polyvinyl chloride). Depending on the class of polymers that lignin wants to be mixed with, different issues might appear depending on the chemical compatibility between the two species. Among all of them, the most promising results were delivered by combinations that involved slightly polar polymers, therefore those that have chemical characteristics similar to the ones of lignin [18], [19]. Miscibility of the blends can be evaluated through a combination of characterization techniques, and the most common are DSC measurements, FTIR spectroscopy and microscopy. However, it is very difficult to obtain unambiguous results, and in the literature there are a lot of conflicting opinions on the topic because of this issue [19].

Concerning polyolefins, P. Alexya et al. studied how the presence of lignin in lignin-polyethylene and lignin-polypropylene blends affected processing stability, mechanical properties, and light degradation of the pure polyolefins. They showed that lignin acts as process and light stabilizers in both types of compounds, especially when it is blended with polypropylene. However, mechanical properties of the two polyolefins were worsened by the presence of lignin, with decreasing tensile strength when increasing the lignin content [21].

Chemical modification of lignin is the most employed way of increasing its compatibility with polymers. The goal of these treatments is to increase the number of non-covalent interactions between lignin and the polymer, improving the blending process [18]. Functionalization processes of lignin, also referred to as *grafting processes*, are all based on the high reactivity of the aromatic rings and the hydroxyl groups along the chain. Examples of possible functionalization reactions are shown in Figure 1.13.
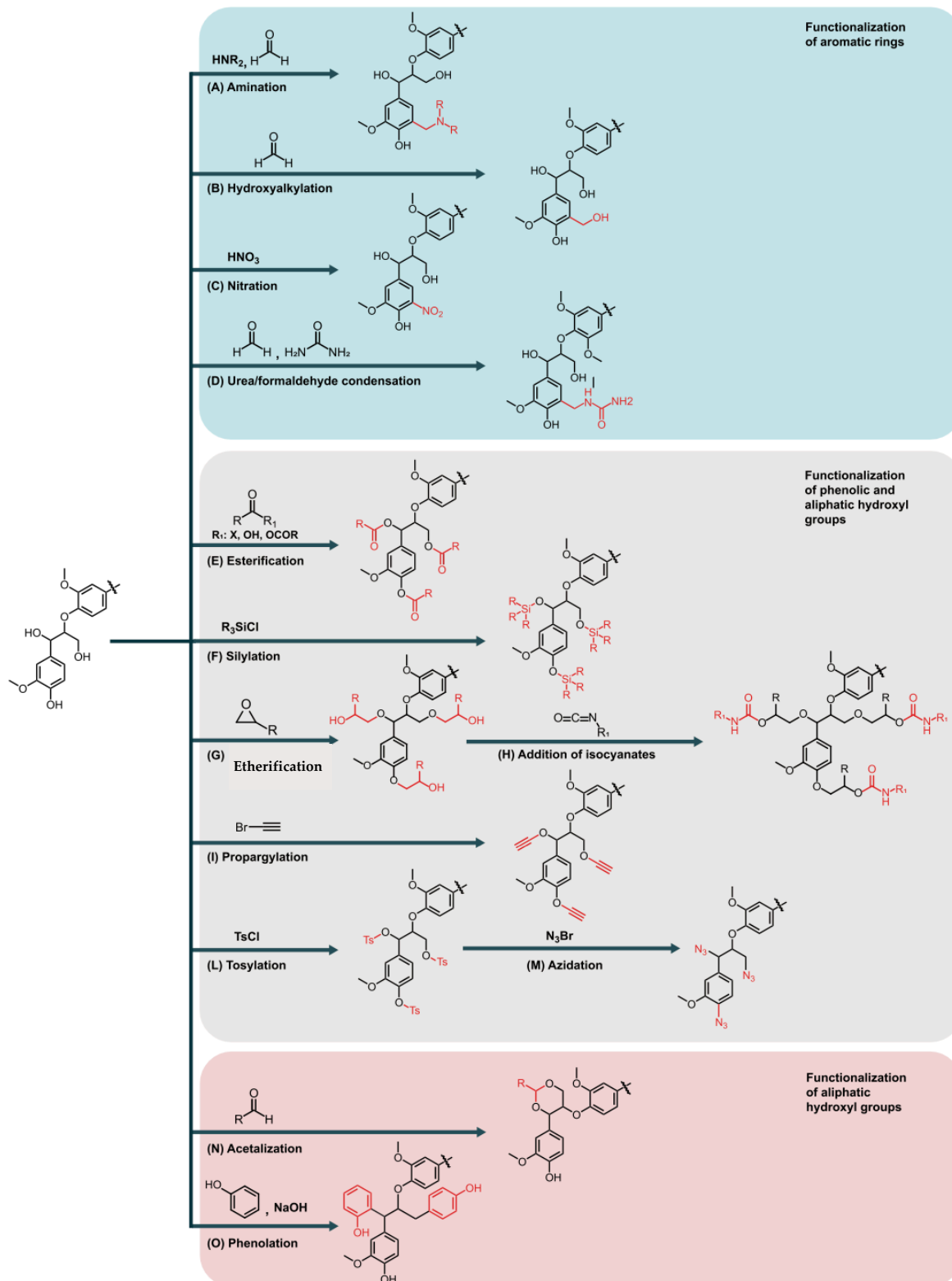
Figure 1.13 Examples of chemical modifications of lignin's backbone [18].

The aim of this thesis work is to surface-modify lignin particles through plasma treatment, through reaction between hydroxyl functional groups of lignin and species present in the plasma reaction chamber. The treatment was carried out using either compressed air or Argon as gas source for the plasma, while other functionalizing gases were added in the process when they were needed for the specific experiment. The functionalizing gases employed (separately) were hexane and hexamethyldisiloxane (HMDSO). The plasma treatment performed on lignin's powder with the gliding arc tornado (GAT) setup employed in this project can be compared to a plasma enhanced chemical vapour deposition (PECVD) process localized on the surface of the particles. Usually, PECVD results in homogeneous deposited layer, which is although very unlikely to happen with lignin due to low treatment times and to the irregular geometry of the particles. To hypothesize the results of plasma functionalization of lignin using hexane and HMDSO, it is possible to refer to previous works where deposition of these chemicals was performed on bulk polymers. According to Thomas R. Gengenbach et al., n-hexane plasma can be used to obtain polyolefins on a substrate from n-hexane polymerization itself [22]. Instead, by using HMDSO as species to be deposited, layers with chemical structure $SiO_xC_yH_z$ can be obtained [23].

1.3   Plasma treatments on polymers

1.3.1   Theoretical introduction to plasma physics

A plasma can be defined as a collection of *charged*, *moving* particles that *mutually interact* through Coulombian forces [24]. An ionized gas is a species that meets all these requirements: it is composed by positive ions (ionized gas molecules or atoms) and free electrons that oscillate at the plasma frequency and interact among each other through electrical forces. The transition from gas to plasma can occur by increasing its temperature to thousands of Kelvin degrees [24]. To understand the mechanism behind the formation of a plasma we must make some statistical considerations.

A gas at temperatures different from 0 K is a set of free and moving particles. They move following a random path and when they happen to get so close that repulsive forces are felt by the particles, they experience a *collision*. During this interaction, particles exchange energy and momentum. Because of all these random collisions happening in the gas, the system of particles can be described through the Maxwell-Boltzmann (MB) statistics. The distribution of velocities of molecules and atoms can therefore be expressed by a bell-shaped curve, whose hight and width depend on the temperature of the system (Figure 1.14) [24].
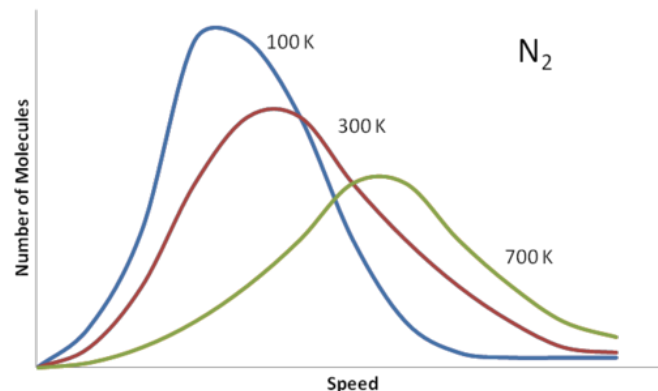
Figure 1.14 Maxwell-Boltzmann distribution for a gas at three different temperatures (100 K, 300 K, 700 K) [24].

The Maxwell-Boltzmann equation for 1 mole of gas is the following:

$$f(v) = \frac{1}{n} \cdot \frac{dn}{dv} = A \cdot \left(\frac{m}{2RT}\right)^{3/2} \cdot v^2 \cdot e^{-\frac{mv^2}{2RT}} \tag{1.1}$$

Where n is the number density of particles per unit volume, A is a constant, m is the molecular mass of the gas, R is the gas constant, T is the system temperature, v is the velocity of the particle. From Figure 1.14 it can be noticed that when the curve is flatter, the fraction of molecules with high velocity becomes more significant. This happens at high temperatures, when the kinetic energy of particles is higher.

The formation process of a plasma is based on the energy exchanged during collisions. Electrons in gas atoms and molecules are bonded to their nucleus with a binding energy that is higher than the average energy that can be reached by gaseous particles at high temperature. However, considering that the system is characterized by a distribution of velocities, there is a fraction of more energetic particles that becomes more relevant at high temperatures. Therefore, by increasing the temperature of a gas it becomes more probable to generate ions and free electrons after collisions.

In a laboratory, the ionization process is enhanced by applying an electromagnetic field (i.e. a potential difference) that accelerates the charged particles (ions and electrons) to increase their kinetic energy and stimulate further ionizations through collisions of molecules with these species. A common and basic setup to generate a plasma is composed of two plane parallel electrodes immersed in a chamber where the gas source to be ionized is present (Figure 1.15) [25].
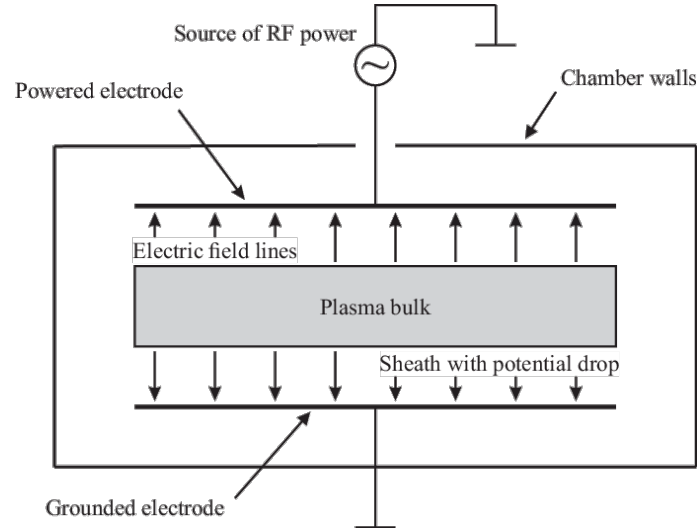
Figure 1.15 Basic setup for plasma generation composed of two plane parallel electrodes [25].

When a gas is subjected to an increasing potential difference, it behaves as insulator until the breaking potential is reached and the dielectric break occurs. Then, free electrons are generated, and the gas is crossed by a current flow. At this point a sufficiently high number of free electrons has been generated so that they can sustain the flow of a noticeable electric current. It is produced by the motion of the electrons which are moving with their drift velocities in the external electric field. Moving electrons collide inelastically with gas molecules and, if enough energy is transferred from the electrons, ionization occurs according to the following equation:

$$e^- + A \rightarrow A^+ + 2e^- \tag{1.2}$$

where A is the gas species.

The value of the breaking potential (V_r) of a gas is not unique but mostly dependent on its pressure (p) and the distance (d) between the electrodes. The relationship among these parameters is described by the Paschen's law [24], [26]:

$$V_r = \frac{k \cdot pd}{ln(pd + k')} \tag{1.3}$$

where k and k' are constants. A minimum of the breaking potential value can be reached for a specific combination of the product pd. Examples of Paschen's curves of different gases are shown in Figure 1.16 [26].
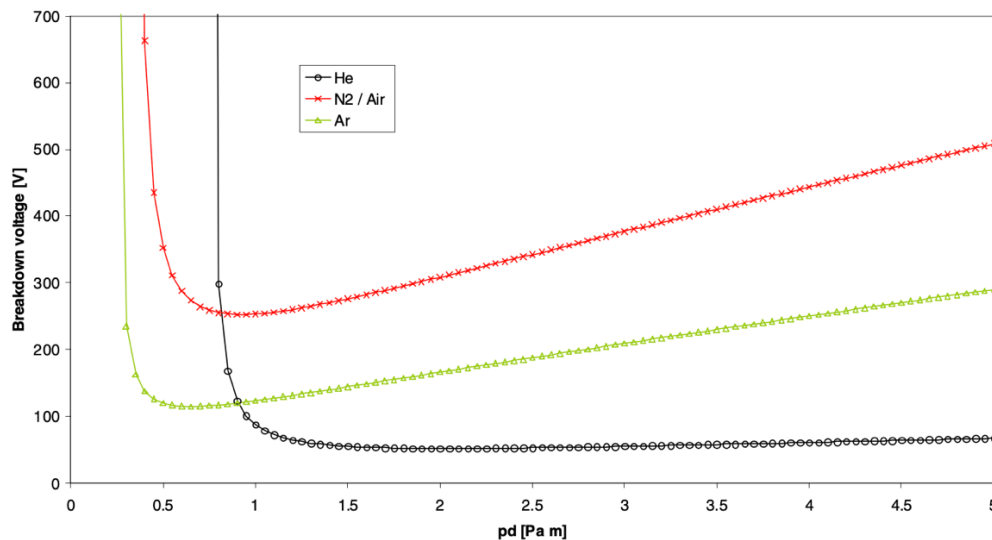
Figure 1.16 Paschen's curves for several commonly used gases (helium, nitrogen, and argon) [26].

1.3.2 Regimes of a plasma discharge

There are different types of gas discharges in terms of electrical characteristic and self-sustaining capacity of the discharge itself, and their manifestation depends on a wide variety of parameters. The most important variables are: the nature of the gas, the magnitude of the applied voltage and the electrical characteristics of the circuit and the power supply, the electrode materials and the geometry of the setup and the electrodes [27]. The nature of the gas mostly affects the Paschen's curve, and therefore the value of the breaking voltage, since its trend depends on the ionization energy of the gas and the cross section of its molecules or atoms [24]. By fixing the setup and the circuit-related parameters it is possible to study the trend of the voltage-current relationship and the different discharge regimes.

Considering the simple setup of Figure 1.15 connected to a current-limited DC power supply, for low values of pressure the current-voltage trend shown in Figure 1.17 can be obtained [27]. There are three main discharge regimes that can be detected: the Townsend discharge, the glow discharge and the arc discharge [24], [27], [28].
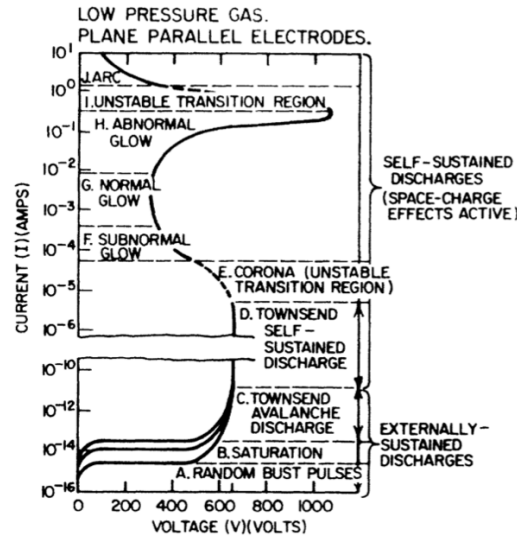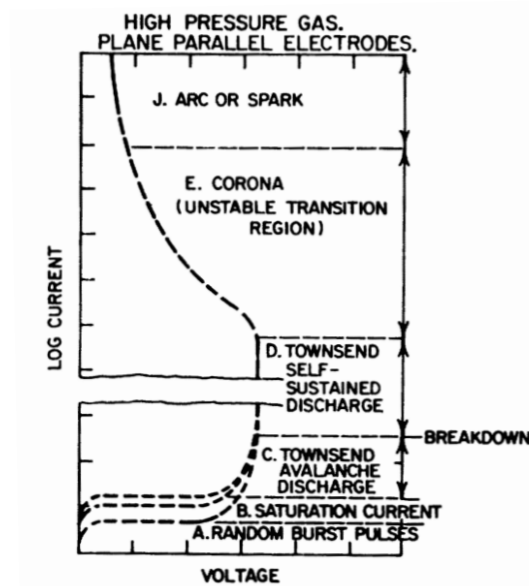
Figure 1.17 Typical current-voltage relation in a low-pressure gas between plane-parallel electrodes with current-limited DC voltage. This curve is for Neon at 1 Torr pressure with disk electrodes of 2 cm diameter and 50 cm separation [27].

The *Townsend discharge* occurs with low values of current and voltage, when the ionization process of the gas is only due to random collision processes described by the MB distribution. At sufficiently high voltage, the dielectric break of the gas occurs and the energy acquired by the electrons is high enough to ionize the gas by collision giving rise to the *Townsend avalanche discharge*, which is the first stage of this regime [27], [28]. At this point the discharge is still *externally sustained*, and the current can be described by:

$$i \cong \frac{i_0 e^{\alpha d}}{1 - \gamma e^{\alpha d}} \tag{1.4}$$

Where i_0 is the saturation current, α is the ionization coefficient, d is the distance between the electrodes, and γ is the "Townsend's second ionization coefficient", which is the efficiency of production of secondary electrons [27]. When the number of secondary electrons is high enough to make the denominator of the above equation null, the *self-sustained breakdown* occurs.

After the transition, with furtherly increasing the current it is possible to reach the *glow discharge* region. This regime is characterized by many dark and light regions in the chamber and lower voltages.

For even higher values of current, after another unstable transition, the *arc discharge* is initiated, which is characterized by high values of current and low voltage. With these circumstances the electrodes have become sufficiently hot to emit a significant number

of electrons through thermionic emission which contribute to further sustaining the discharge. The gas too is substantially heated.

The just described current-voltage profile is valid, as previously mentioned, for low-pressure gases. For values of pressure higher than 1 atm, such as in the case of the experiments performed for this thesis work, the current-voltage curve is compressed compared to the one in Figure 1.17 and only the *Townsend discharge regime* and the *arc discharge regime* are detected (Figure 1.18) [27].

Figure 1.18 Schematic current-voltage relation in a high-pressure gas between plane-parallel electrodes with a current-limited voltage [27].

Before reaching the arc regime equilibrium, however, the discharge can become unstable and intermittent. This phenomenon observed during the transition from the Townsend to the arc regime is called the *spark regime*. During the spark regime, whenever the threshold value of voltage is achieved and the discharge initiated, after a few milliseconds the discharge turns itself off and the electric current goes to zero (Figure 1.19). This trend is repeated with an approximately constant frequency [29].
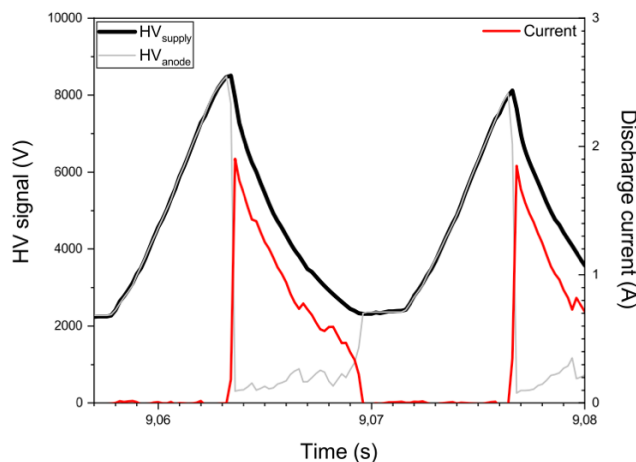
Figure 1.19 Evolution of the High Voltage (HV) signal and the calculated discharge current over time [29].

1.3.3   Plasma functionalization of polymers

During the last decades plastic has taken the place of other classes of materials due to its physical and chemical characteristics and relatively low cost. Even though plastics' bulk properties are mostly satisfying, their surface properties are responsible for technical problems during manufacturing operations. Plastics' surfaces have in many cases a very low surface tension, which results in poor adhesion with deposited layers and therefore poor printability, bonding and coating properties [30],[31]. Surface modification of polymers is often performed to improve the adhesion of thin metal films; specific examples of polymer-metal combinations are silver-polyester (for ion selective electrodes), copper-polyimide (microelectronics), copper or nickel or chromium with acrylonitrile-butadiene-styrene (ABS) or polyphenylene oxide (PPO) (for automotive parts). Pre-treatments of polyolefins is widely used in the food industry before the deposition o aluminium for food packaging. Polymer-polymer adhesion is also widely studied for coatings applications [31].

Several methods to modify the surface properties of plastics have been used over the years: mechanical treatments (roughening of the material to increase its real surface value), wet-chemical treatments with strong acids or basis, treatments with photons, UV, ozone, laser, ion and electron beam irradiation, exposure to flames, corona discharges, and glow discharge plasmas [30],[32]. However, the great majority of these methods have drawbacks especially from the environmental point of view. Wet-chemical treatments, for instance, need etching and disposal of hazardous materials which has both safety and environmental issues. Moreover, wet-chemical treatments, as well as exposure to flames, have problems of uniformity and reproducibility [32].

Plasma treatments are the ones that attract most of the attention among plastic surface treatments, because of being environmentally friendly, versatile, uniform and reproducible methods [30]. Also, they can be performed at ambient pressure using ambient air. This could have drawbacks if the desired effect is not limited to simple oxidation of the surface, but this issue can be easily avoided by adding a functionalizing gas in the reaction chamber [32].

During plasma treatments the surface of polymers interact with energetic particles and photons through free-radical chemistry mechanisms. Four main effects derive from this exchange in energy: *surface cleaning* (organic contamination removal), *etching* (removal of weak boundary layer and increase of the surface area), *crosslinking or branching of near-surface molecules* (strengthening of the surface layer), *chemical modification of the surface* (during or post-treatment through exposure to a reactive chemical) [32]. All these effects are present at some degree when performing plasma treatments, but depending on the operating parameters, gas and substrate materials, and reactor design, some can be favoured over others.

Over the past years, chemical surface modification is the effect among the four that is gaining more interest since it allows a tailored modification of the material's surface without the environmental problems of a wet-chemical functionalization. The reactive free radicals formed on the polymer's surface after interaction with the plasma can easily react with gases or solutions they are exposed to; this is usually performed to increase the hydrophilicity of plastics through oxidation by exposing them to air. Air plasma is considered to be the most effective one in increasing surface energy of polymers, with Argon plasma still providing satisfying results [30]. However, it is important to state that additional processes may occur after the surface has been chemically treated. There could be loss of surface functionalization through reaction or reorientation of surface groups towards the bulk that could both bring to loss of wettability. Because of these phenomena, stability and duration of plasma treatments could be a concern. Nevertheless, there are still evidences of plasma treatments stable for long times if the modified polymer is stored in a controlled environment or coated immediately after the treatment is performed [31].

Plasma treatments have been commonly performed on the surface of bulk materials, but similar considerations to the ones just presented are applicable to powders and dispersions as well [31]. However, not many experiments are reported in the literature about plasma functionalization of powders, since instrumental setups specifically designed for powdery materials must be used [33]. There are few works regarding plasma functionalization of lignin. Most of them have the goal of adding slightly polar functional groups on the particles' surface to improve adhesion with the polymer lignin wants to be blended with. T. Atz Dick et al., for instance, subjected lignin to

atmospheric plasma treatment and subsequently they immersed it in a toluene solution containing L-lactide (L-La). The goal was to obtain grafted L-La lignin (Figure 1.20) to improve the blending properties of the powder in a PLLA matrix. PLA-grafting of lignin was proven to be effective, with an increase of C=O functionalities, but the mechanical properties of the composite material were unfortunately not tested [33].
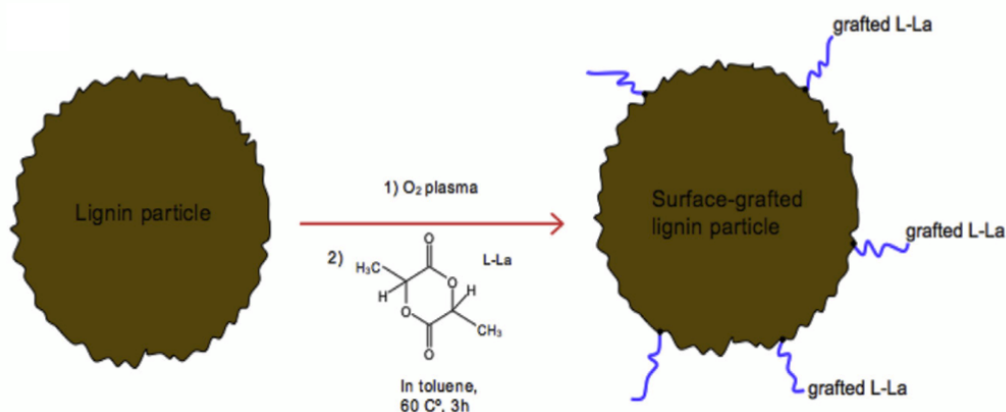

Figure 1.20 Schematic way of the chemical modification of lignin via surface-grafting of particles induced by plasma treatment [33].

In another work made by G. Toriz et al., kraft lignin was plasma-treated in vacuum in the presence of two different functionalizing gases, separately: silicon tetrachloride (SiCl4) and acryloyl chloride (CH2=CH-COCl). With the first treatment they were able to reach implantation of silicon on the material, while with the second one they achieved copolymerization of acryloyl chloride on lignin. In this study as well, characterization of the resulting materials have not been performed [34].

In this thesis work the goal is to reduce the concentration of hydroxyl groups from the surface of lignin particles and substitute them with more hydrophobic functional groups to decrease the polarity of the particles. In order to achieve this, the functionalizing chemical was inserted in the gas circuit of the setup. The functionalizing vapour and lignin were allowed to interact for limited time in the plasma chamber where they underwent formation of free-radicals and subsequent react. Both properties of the treated powders and the blends were tested and analysed.

2. Materials and methods

2.1 Materials

In this section all the materials and chemicals involved in the experiments will be presented. They will be divided in 3 subsections: materials for blending, materials for plasma treatment, chemicals for the characterization of the materials.

2.1.1 Materials for the blending

2.1.1.1 Soda lignin

The chosen soda lignin is Protobind 1000, supplied by Tanovis AG (Alpnach, Switzerand) and it is originated from a non-woody (wheat straw/Sarkanda-grass) process. It appears in the form of polymeric brown granules of different size (Figure 2.1).

Figure 2.1 Soda lignin powder.

The polypropylene used to form the blending was provided by LATI Industria Termoplastici S.p.A.. It has a melt flow index of 2,5 g/min and a density of 0,90 g/cm³. Common values for polypropylene's melting temperature and glass transition temperature are respectively 165°C and -10°C. The pellets provided by the company were previously reduced in powder to better fit the geometry of the extruder used in the blending process.

2.1.2   Materials for the plasma treatment

2.1.2.1   Plasma gases

The gases to be ionized to produce the plasma are Argon and compressed air (approximate composition: 78 % nitrogen, il 21 % oxygen, 1 % argon. Water vapour may also be present between 0,1 % and 4 %). They have been used separately to perform different treatments on lignin.

2.1.2.2   Functionalizing gases

When performing the plasma treatment on lignin, 2 different functionalizing gases have been used: n-hexane (Honeywell, Chromasolv™ for HPLC, ≥ 97,0%) and hexamethyldisyloxane (Fluka, ≥ 98,5%).

Hexane is an organic hydrocarbon that is widely used as a cheap, volatile non-polar solvent. It is a colourless liquid that acts as main constituent in gasoline. Its structure is shown in Figure 2.2.
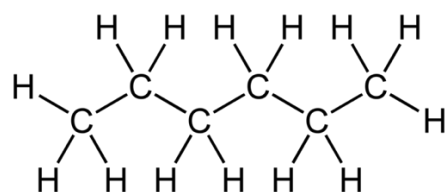
Figure 2.2 Hexane's chemical structure.

Hexamethyldisiloxane is an organosilicon compound that appears as a colourless liquid. It is mainly used as non-polar solvent or as reagent in organic synthesis. Its structure is shown in Figure 2.3.
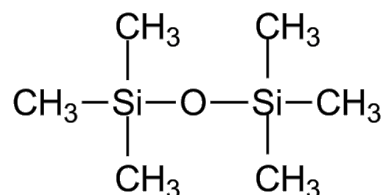
Figure 2.3 Hexamethyldisiloxane's chemical structure.

2.1.3 Chemicals for the characterization of the material

2.1.3.1 Solubility tests – methylethylketone, toluene, ethyl acetate, cyclohexane

The Methylethylketone (Figure 2.4) that was used as solvent in the solubility experiments was provided by Sigma-Aldrich and it has a purity of ≥ 99%. Methylethylketone is most known as Butanone, and it appears as a colourless and volatile liquid with a pungent odour. It is mainly employed as a solvent, as reactant to produce other chemicals, and for production of wax from petroleum. Butanone has a density of 0,805 g/cm³ and it can be considered a polar/water-miscible solvent.
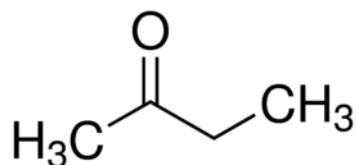
Figure 2.4 Methylethylketone's chemical structure.

Toluene (Figure 2.5) is an aromatic hydrocarbon composed of a benzene ring linked to one methyl group. The one used in the experiment of this thesis work has a purity of ≥ 99,5% and it was provided by Sigma-Aldrich. Toluene is commonly used a solvent or as a chemical intermediate in various industrial applications. It appears as a clear colourless liquid with a characteristic aromatic odour. Its density is equal to 0,867 g/cm³ and it acts as a non-polar/water-immiscible solvent.
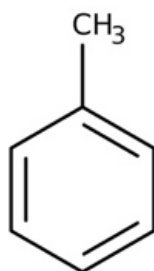
Figure 2.5 Toluene's chemical structure.

Ethyl acetate (Figure 2.6) was provided by Sigma-Aldrich, and its purity is $\geq$ 99,5%. It appears as a clear colourless liquid with a fruity odour. Ethyl acetate is the acetate ester formed between acetic acid and ethanol. Its density is equal to 0,902 g/cm³ and it is a polar/water-miscible aprotic solvent.
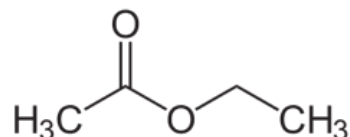
Figure 2.6 Ethyl acetate's chemical structure.

Cyclohexane (Figure 2.7) is an alicyclic hydrocarbon comprising a ring of six carbon atoms. The chemical was provided by Sigma-Aldrich, and it has a purity of $\geq$ 99%. Cyclohexane is mainly used as a raw material in the manufacture of nylon. It has a role as a non-polar/water-immiscible solvent and its density is 0,779 g/cm³.
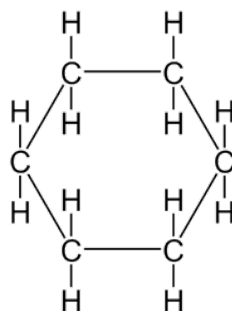
Figure 2.7 Cyclohexane's chemical structure.

2.2   Experimental methods

2.2.1 Gliding Arc Tornado (GAT) device

This section will focus on describing the experimental setup, the operational strategy followed to perform the plasma treatment on lignin, and the methods employed for the characterization of the electrical parameters of the instrument.

2.2.1.1   Experimental setup

The GAT is a particular configuration of gliding arc where the gas flux is used to create a vortex-tornado regime to improve the self-cooling of the system and to increase the residence time of the gas in the plasma region. Specifically, the gliding arc itself consists in the arc discharge regime at atmospheric pressure, during which the arc is kept sliding along the electrodes. The arc is generally pushed by the gas flow, such as in the GAT device where a tornado flow is employed.

The GAT device allows the addiction of both the lignin powder and the functionalizing gas (separately) and that ensures the control of the electrical characteristics of the discharges, avoiding short-circuit. Thanks to this instrumental setup it is possible to add powders to the circuit that are brought in the plasma-chamber by the gas flow of Argon or compressed air. A functionalizing gas can also be added to the flow through an additional inlet. The plasma treatments on lignin were performed with two different discharge regimes, which are the spark one and the arc one. The two regimes differ for the value of imposed current, which is higher in the case of the arc discharge, and for the nature of the discharge. Indeed, In the arc regime the current flow is constant, while in the spark one it is intermittent, and each pulse is repeated with an approximately constant frequency. Detailed characteristics of the two regimes will be discussed in the following sections.

The main components of the device will be described in this paragraph. A schematic representation of the setup is also shown in Figure 2.8.
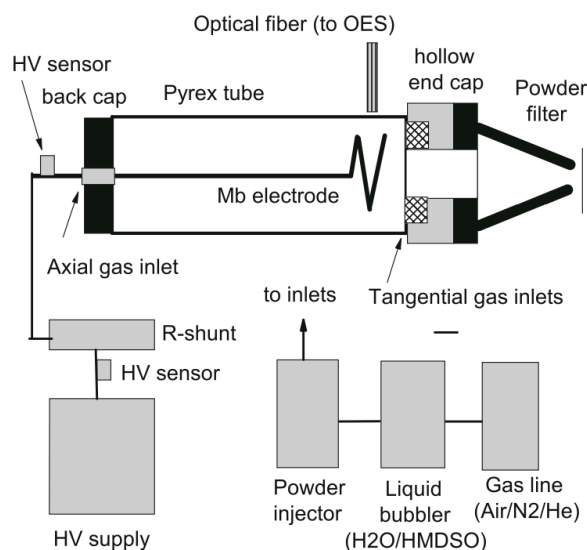
Figure 2.8 Schematic representation of the experimental setup to perform the plasma treatment on lignin [29].

GAT chamber: it is the place where the discharge is generated. The GAT chamber consists of a Pyrex tube (39 mm inner diameter, 2.5 mm thick, 200 mm long), closed at one side by a Teflon cylinder cap, through which the electrode wire enters. On the other side, the tube is partially closed by a hollow stainless-steel disk (25 mm hole diameter, 8 mm thick). Gas inlet and sealing are provided by a couple of Teflon hollow disks surrounding the Pyrex tube. The chamber has an effective height of 55 mm and a volume of about 60 cm³ that was obtained by filling the tube with a Teflon cylinder to reach the desired extension. Gas is injected tangentially by two opposite channels

with square cross section (3×3 mm^2) excavated in one of the Teflon disks. A reverse flow vortex is produced in the chamber spiralling downward along the Pyrex inner surface until it reaches the back cap, and a jet is formed along the axis exiting from the front disk central hole [29]. A picture of the GAT chamber is presented in Figure 2.9.
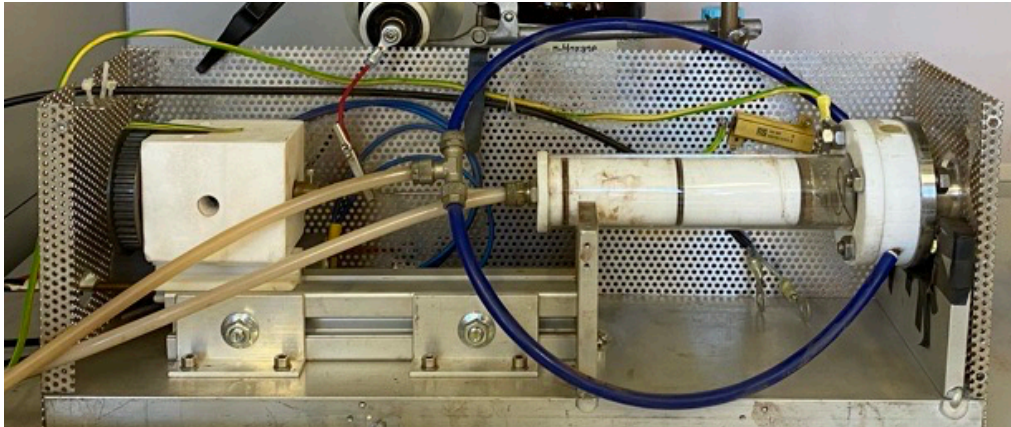

Figure 2.9 GAT chamber.

In the GAT configuration one of the two electrodes, the grounded one, coincides with the metallic head of the source (which forms part of the "hollow end cap" of Figure 2.8), while the other one is a spiral electrode made of Molybdenum (Figure 2.10). The spiral geometry of the electrode is necessary to develop the vortex flow, characteristic of this setup.
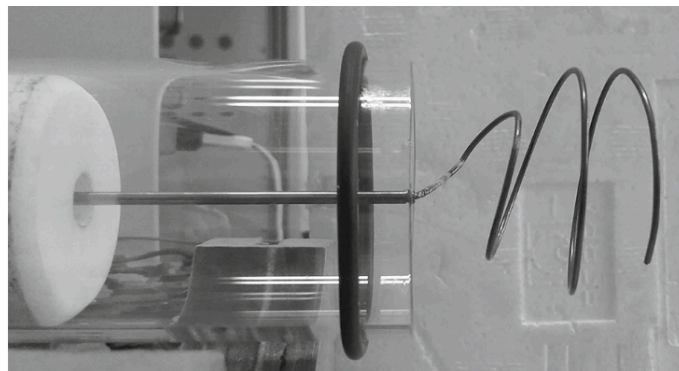
Figure 2.10 Spiral electrode for the GAT configuration [29].

High-voltage DC generator (SHV9000 by Alintel): it is necessary to provide the power needed for the initiation of the plasma. It gives the circuit a maximum power of approximately 10 kW. Specifically, it allows a maximum of 5kV and 2A simultaneously.

Set of 16 high-voltage, high-power resistances: they provide a global resistance of 4 kΩ. This implementation protects the generator when the discharge is turned off and avoids short-circuit.

Powder injector: it is the structure through which lignin is added to the circuit. The injector consists in a cylindrical Pyrex-glass container with a small circular opening on one side close to the bottom of the cylinder. The powder is added to the circuit through the opening with small horizontal tube that acts like a spoon. It consists in a small cylindrical plastic tube with a cavity on the lateral surface that can host up to 0,3 g of lignin (Figure 2.11). Therefore, the powder is cyclically added to the circuit multiple times to reach the desired amount of material. Once the cavity is full of powder, the spoon is inserted in the glass cavity, and it is turned by 180° to be emptied and to add the powder to the flow. This step needs to be done once the gas flow is activated. Indeed, the flow is directed from the bottom of the container to the top and it can therefore transport the powder with it.

Figure 2.11 Powder injector (left) and zoom on the injection channel (right).

Liquid bubbler: it consists in a cylindrical Pyrex-glass, and it is the container where the functionalizing chemical is poured. Since HMDSO and hexane are liquid at room temperature and atmospheric pressure, gaseous molecules of these species can be generated and added to the gas flow by making the fluids gurgling. This occurs when the Argon or compressed air flow passes in the container generating bubbles in the

fluid and allowing some molecules to evaporate. The flow of Argon or compressed air entering the liquid bubbler is qualitatively regulated through a rotating valve (Figure 2.12). No devices that allowed a quantitative evaluation of the gas evaporating from the bubbler were available in the laboratory, and therefore the flow of functionalizing gas was qualitatively kept constant by fixing the open position of the valve.

Figure 2.12 Rotating valve to open and regulate the gas flux of Argon or compressed air entering the liquid bubbler.

Collector for the treated powders: it is a setup consisting in a metallic drilled tube filled in with a polyester filter sheet (A4-sheet approximate dimension) rolled up on itself to collect the treated powders that exits the GAT chamber (Figure 2.13). The end of the tube is capped so that the powders do not get lost in the environment. The fabric has a maximum capacity of approximately 2 g of lignin, and after this threshold is reached, the exceeding powder remains in the previous parts of the apparatus, especially in the GAT chamber. Therefore, after 2 g of lignin have been inserted in the circuit, the experiment must be suspended to empty the filter and to clean the apparatus from residues.
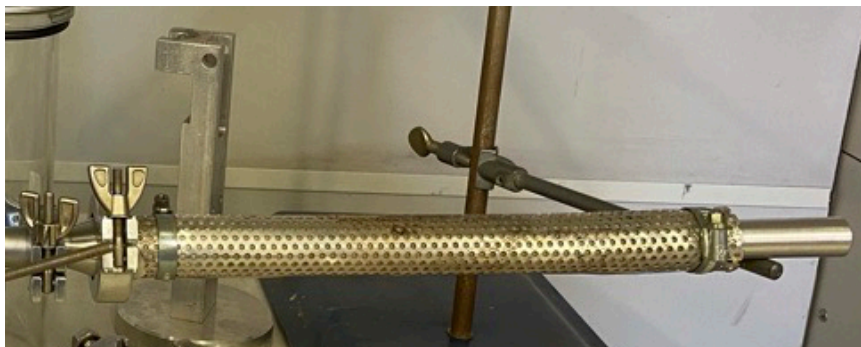
Figure 2.13 Powder collector setup.

Now that the main elements of the device have been introduced, the path that the flow of Argon or compressed air follows to bring both lignin and the functionalizing gas in the GAT chamber can be explained. The gas flow splits up at the beginning of the circuit in two different channels, one going through the powder injection cylinder and the other one going to the liquid bubbler to generate the vapour of the functionalizing gases. The two flows, after crossing these two regions, join back together and the powder and the gases are mixed. Before entering the GAT chamber the flow is again split up so that it enters the chamber in two different points (radial and tangential) creating a more favourable hydrodynamic flux for the formation of the vortex-tornado.

2.2.1.2   Operating strategy for the treatment

Before performing the treatment on lignin, the setup had to be prepared.

First, the textile filter had to be rolled up and inserted in the metallic drilled tube, which had to be plugged on one end and connected to the GAT chamber on the other one. To avoid burning or ignition of the filter due to random contact with the plasma discharge, the filter was never directly connected to the chamber. Indeed, the discharge could instantaneously exit from the chamber and touch the areas in proximity. When the treatment was performed in spark regime, the filter setup was connected to the chamber through a I tube. Instead, when the chosen regime was the arc one, an additional part had to be connected to separate the textile from the chamber. This extra precaution was needed because the arc regime generates higher temperatures (Figure 2.14). It is difficult to evaluate the temperature of the system during the treatment. Indeed, it is possible to define a temperature field where the maximum temperature is reached locally at the centre of the discharge, and it can touch even thousands of Kelvin degrees.
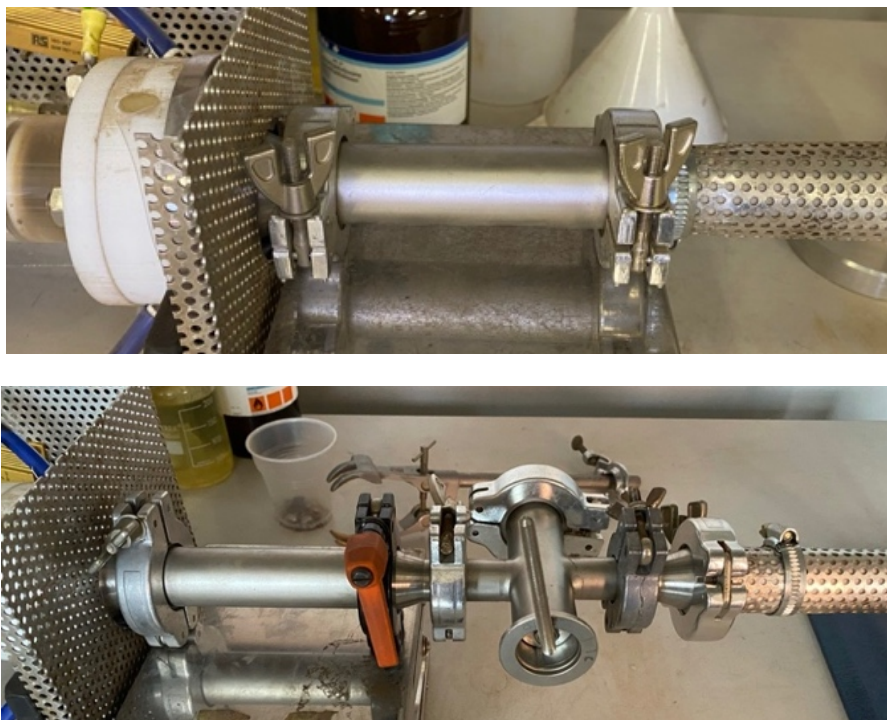
Figure 2.14 Additional setup to connect the powder collector to the GAT chamber when performing the treatment in the spark regime (up) and in the arc regime (down).

After the powder collector apparatus was prepared, the functionalizing liquid could be poured in the bubbler (if required in the treatment) and the circuit could be connected to the desired plasma gas source (compressed air or Argon) at the required pressure. Depending on the gas source used, the pressure employed was different and its value was established after the characterization of the electrical parameters, which will be discussed in section 2.2.1.3. The last step of the preparing procedure was to set the imposed current necessary for the treatment, which is the parameter that determined the discharge regime.

After all the previous steps were completed, the treatment was ready to be performed. The gas source flow could be opened, as well as the valve of the liquid bubbler, if required by the experiment, and lignin could be added to the circuit through the powder injector.

When the maximum capacity of the collecting filter was reached, the treated powders had to be extracted from it. However, not all the lignin subjected to the treatment could be transported to the filter, probably because it reached its full capacity or because lignins were too heavy to be transported by the flow to that location. Therefore, some powders settled in the GAT chamber and they had to be extracted directly from it.

Indeed, the lignin extracted from the chamber was visibly of a much coarser grain compared to the filtered one (Figure 2.15). This phenomenon makes it difficult to evaluate the treatment time of lignin. The fraction of powders that transit the GAT chamber directly reaching the filter only meets the plasma for approximately ten milliseconds, while the one that settles in the chamber can undergo even a minute of treatment. Because of the difference in the treatment time of the two sets of powders, they have been separately tested to evaluate if longer exposure to the plasma brought to different modifications to the chemistry of the lignin's particles.

Figure 2.15 Plasma-treated lignin extracted from the chamber (left) and from the filter (right).

To extract the powders from the textile they had to be scratched off with a spatula (Figure 2.16) while the ones in the chamber were simply taken with a small spoon.

Figure 2.16 Extraction of plasma-treated lignin from the filter.

For the aim of this project, eight different plasma treatments on lignin were performed to investigate the best conditions to increase the hydrophobicity of pristine lignin. The parameters that could be changed during the experiments were: discharge regime (spark or arc), plasma gas source (air or Ar), presence and type of functionalizing gas. The gases chosen as functionalizing gas are hexane (HEX) and HMDSO. The experimental conditions of the eight treatments performed on lignin are shown in Table 2.1.

Table 2.1 Conditions of the plasma treatments performed on lignin.

Treatment name	Discharge regime	Plasma gas	Functionalizing gas
Spark-air-0	Spark	Compressed air	None
Arc-air-0	Arc		
Spark-Ar-0	Spark	Argon	None
Arc-Ar-0	Arc		
Spark-Ar-HEX	Spark	Argon	Hexane
Arc-Ar-HEX	Arc		
Spark-Ar-HMDSO	Spark	Argon	HMDSO
Arc-Ar-HMDSO	Arc		

All the treatments listed above have been performed both on thermally pre-treated lignin and on not pre-treated lignin. The thermal treatment was performed in vacuum oven for 90 minutes at 120°C. The goal of the thermal treatment was to remove humidity from the powder. Influence of this treatment on the results will be analysed in section 3.2.1.1.

2.2.1.3 Characterization of the electrical parameters of the instrument

Before performing the treatments on the powders, the characterization of the electrical parameters of the instrument had to be performed. Indeed, it was necessary to determine the values of imposed current at which the transition from spark to arc regime occurred. The discharge characterization was carried out by studying the transition when varying four main parameters:

- Nature of the plasma gas (gas source and functionalizing gas when present)
- Pressure of the gas source
- Distance between the electrodes
- Imposed current

The analysis was carried out with by using an oscilloscope to detect the trend of both voltage and current during time. To do so, a high voltage probe and a current probe connected to the oscilloscope were used. The oscilloscope used in this thesis work is the IDS 1074B from RS-PRO.

The first step of the study was to detect the value of imposed current (I_{th}) at which the spark-to-arc transition occurred, while keeping the other parameters fixed. Later on, it was investigated how the different parameters affect the position of the transition. Specifically, the shift in I_{th} was studied when varying the distance between the electrodes, the gas pressure, and the presence of a functionalizing gas. The measurements were carried out separately, while the non-investigated parameters were kept fixed, with exception of the imposed current which had to be modified to detect the new value of I_{th}.

2.2.2 Blend and specimen preparation

The polymer blend composed of both plasma-treated lignin and PP was prepared by using a twin-screw extruder.

Extrusion is a very commonly employed mixing technology in the case of thermoplastic polymers blending. The machine used in this thesis work was the Process 11 parallel corotating twin-screw extruder by Thermo Fisher scientific (Figure 2.17). Each of the screw has a diameter of 11 mm and the typical output of the extruder can range from 20 g/h up to 2.5 kg/h. For this thesis work, approximately 60 g for each

specific blend have been extruded. The overall setup also included an automatic feeder and a cooling system.

Figure 2.17 Process 11 parallel corotating twin-screw extruder by Thermo Fisher scientific

The function of the two corotating screws was to achieve the melting and a good dispersive mixing of the material. During the process the material melts gradually following a predefined temperature profile, shown in Table 2.2. The melting process is favoured both by the mechanical energy provided by the rotating screws and the several heaters placed along the barrel where the screws are contained. In the final section of the barrel the molten compound is forced into a die with a circular cross section. The extruded filament solidifies once it exits the die, and it is then cut in approximately 3 cm-long pieces so that they could be collected in small bags. The extrusion process was run at a fixed feeding rate in the hopper controlled by a dedicated screw rotating at 20 rpm, while the extrusion screws were set at 75 rpm.

Table 2.2 Temperature profile to achieve proper melting of PP during the extrusion process.

Zone	Zone 2	Zone 3	Zone 4	Zone 5	Zone 6	Zone 7	Zone 8	Die
Temperature (°C)	170	170	180	185	185	180	170	170

Once the blend was produced, it had to be grinded with dry ice to achieve a finer grain. The obtained powder had a proper granulometry to be processed to produce the dog-bone shaped specimen needed to perform the mechanical tests on the blend. The specimen preparation was processed by injection moulding by an external company (Rambaldi&CO I.T. Srl). Before shipping the material, it had to be thermally treated overnight at 80°C to remove moisture. The injection moulding of the samples was performed with a Babyplast 6/12 machine with the process parameters presented in Table 2.3.

Table 2.3 Process parameters employed during injection moulding of the samples.

Parameter	Value
Injection temperature	200°C
Injection pressure	590 bar
Injection time	6 seconds
Injection velocity	55 mm/s

Due to time limitations, only four treatments among the eight performed listed in Table 2.1, were chosen to study their effect on lignin behaviour in the blend. The selected treatments are the ones listed in Table 2.4.

Table 2.4 Plasma-treatments selected for the blending.

Sample name	Discharge regime	Plasma gas	Functionalizing gas
Spark-Ar-0	Spark	Argon	-
Arc-Ar-0	Arc		
Spark-Ar-HMDSO	Spark	Argon	HMDSO
Arc-Ar-HMDSO	Arc		

The reasoning behind the selection of these specific plasma-treatments was to investigate the differences between the samples of lignin treated with and without a functionalizing species. The decision was also supported by the results of the preliminary characterization tests on the treated powders, presented in section 3.2.

For each lignin-PP combination, three blends with different lignin content were prepared. The selected percentages were 5%, 10% and 20%. Also blends obtained by combining PP and untreated lignin were extruded, to have a comparison with the performances of pristine lignin.

2.3   Characterization techniques

Several types of characterization techniques were performed on plasma-treated lignin to evaluate any changes in the surface chemistry or thermal behaviour of lignin, and on the PP-lignin blend to study its mechanical behaviour and thermal properties.

Particularly, for what concerns the characterization of plasma-treated powders, the focus was on detecting if the substitution of hydroxyl polar groups with other non-polar groups occurred, which is needed to improve the hydrophobicity of the material and, therefore, the compatibility with polyolefins. The techniques that were specifically used for the characterization were Fourier-Transformed Infrared (FT-IR) spectroscopy, solubility tests, Differential Scanning Calorimetry (DSC), and ^{31}P-Nuclear Magnetic Resonance (^{31}P-NMR). The first three methods were performed to have a first evaluation of the effects of the plasma treatment on lignin. Later, ^{31}P-NMR was used to quantitatively assess variation in the hydroxyl groups concentration that occurred after the treatment. For all the tests, results have been compared with the ones of non-plasma-treated lignin to evaluate the effect of the treatments. Before performing all the measurements on lignin powders, they were dried in a vacuum oven at 50° for one night. The purpose of this step was to remove moisture from the samples, since it might have affected the results of the tests.

The mechanical properties of the PP-lignin blends were studied through tensile tests. Rheology tests were also performed to study the viscoelastic behaviour of the blends. Moreover, Thermogravimetric Analysis (TGA) and DSC were used to evaluate the thermal stability of the samples and their melting temperatures to be compared to the ones of the original materials, respectively.

2.3.1 Fourier-Transformed Infrared Spectroscopy (FT-IR)

Fourier-Transformed Infrared Spectroscopy is a characterization technique adopted to analyse the chemical composition, i.e. the nature of functional groups and molecular structure of a sampling material, in the liquid, solid or gas state. It belongs to the group of characterization techniques concerning the vibrational spectrometry (also known as IR spectrometry). The basic principle of the instrument is based on the physical evidence that polyatomic species are characterized by a multitude of vibrational energy levels associated to the bonds that hold the molecule together (Figure 2.18).
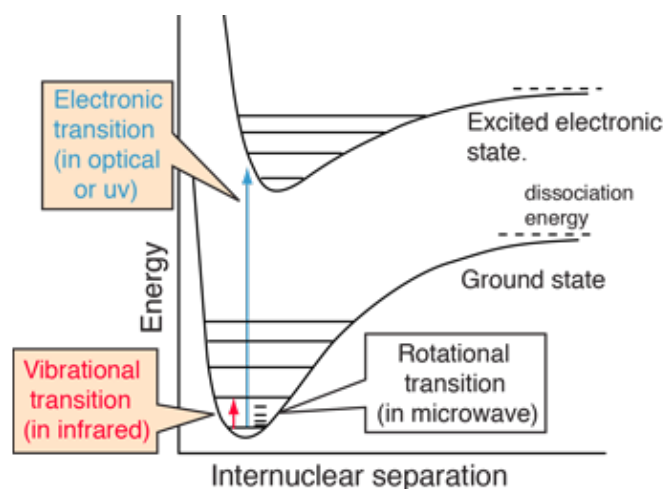
Figure 2.18 Energy states of a polyatomic species and examples of level transitions.

Molecules can experience transitions between different energy levels by absorbing or emitting quantized amount of energy, which corresponds to a specific frequency, characteristic of the specific bond, names the natural vibrational frequency. When these transitions occur in the IR range, they can be detected by the FT-IR instrument. The type of transitions that lies in this range is the vibrational transition, and therefore this characterization technique belongs to vibrational spectrometry.

To know the natural vibrational frequencies of a material with FT-IR, and therefore to get information about its functional groups, the sample to be tested is irradiated with a multitude of waves with different wavelength that cover all the IR region. When an electromagnetic field with frequency equal to the vibrational frequency of the material interacts with the sample, it gets absorbed by it and a vibrational transition occurs in the material. The waves with frequency incompatible with the vibrational transitions will cross the sample unmodified. The raw data detected by the instrument are processed by a computer through a Fourier-Transformation to make the spectrum readable. The machine that was used in this work to characterize lignin was a FT/IR 615 (Jasco Inc.) spectrometer used in absorption mode across the interval 4000-400 cm^{-1}, with a resolution of 4 cm^{-1} and 64 scans carried out per sample.

To perform the IR spectrometry on the powders, proper tablets had to be prepared with a press. To make them, lignin had to be mixed and hand-pressed with potassium bromide (KBr) or sodium chloride (NaCl) in a mortar. KBr and NaCl are fine white powders that act as filler for the formation of the tablets. They are proper materials for IR spectroscopy because, like other alkali halide, they become plastic when subjected to pressure and form a sheet that is transparent in the frame of the mid-IR region (4000-400 cm^{-1}), which is the area where we display the absorbance spectrum of the analysed

materials. After the powders have been mixed, they were then put in a press (provided by Perkin Elmer) and kept under an equivalent pressure of 8000 kg for 5 minutes.

FT-IR was used to investigate the effects of the different plasma treatments performed on lignin, both on pre-thermally treated and non-treated lignin, as well as to evaluate differences in the samples collected from the filter and from the chamber, and to study the effect of time on the treatment.

2.3.1.1   *Reference FT-IR spectra of soda lignin and of deposited films on polymers from HMDSO plasma and n-hexane plasma*

Being soda lignin an irregular polymer, the trend of its IR spectrum is not unique, and it can vary from one sample to another. However, even if intensities of the peaks are not equivalent in all the spectra, the number of peaks and their frequencies are the same, with only slight variations, for every samples of pristine lignin [35]. The position of some of the main peaks of the Protobind soda lignin employed in the experiments of this thesis work are highlighted in Figure 2.19.
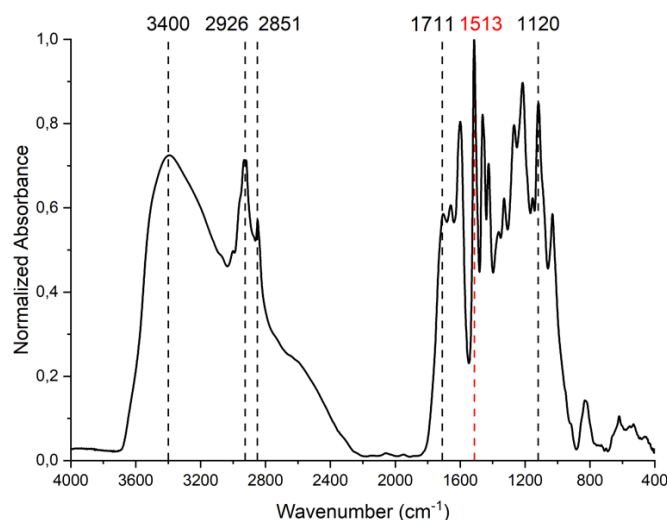
Figure 2.19 FT-IR spectrum of Protobind lignin employed in the experiments.

The broad band at 3400 cm^{-1} corresponds to the stretching vibration of hydroxyl groups, both connected to the chain or belonging to phenolic groups. At 2926 cm^{-1} and 2851 cm^{-1} there are the peaks associated to C-H stretching vibration in methoxyl (-O-CH$_3$) and methyl groups (-CH$_3$). The peaks in the region 1615-1720 cm^{-1} refers to C=O stretching in ketones, carbonyls and in ester groups. At 1120 cm^{-1} there is the C-O deformation vibration in ester bonds while at 1513 there is one of the main peaks associated to the aromatic skeletal vibration [35], [36], [37]. The data obtained during the FT-IR spectroscopy experiments of both plasma treated and untreated lignin were all normalized with respect to the peak at 1513 cm^{-1}. Since the aromatic skeleton of

lignin is not affected by the plasma treatment, this peak was chosen as reference for the normalization, to allow comparison among the several IR spectra of lignin. This strategy also allows the preparation of the tablets for the testing without the need of precise lignin-filler proportions.

Plasma treatment with HMDSO is usually performed for the deposition of PDMS films and coatings on polymers and other materials. Particularly, films deposited from HMDSO plasma are of the type -$SiO_xC_yH_z$ [23]. An example of FT-IR spectrum of deposited films from HMDSO/O_2 plasma with different dilutions is shown in Figure 2.20. In this thesis project, argon has been used instead of oxygen, but the results in the picture are still valuable to recognize the peaks relative to species deposited from HMDSO.
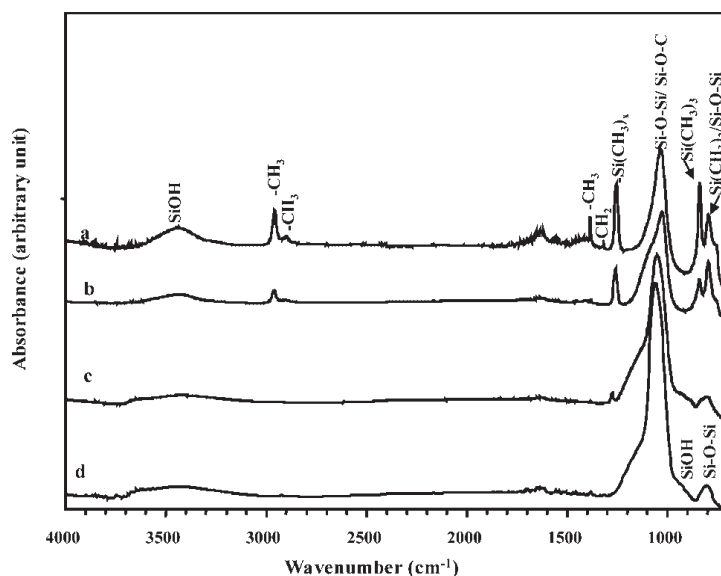
Figure 2.20 FT-IR spectra of films deposited at position A in the reactor using 50 W HMDSO/O2 plasmas with different gas ratios in the feed: a) 100:0, b) 50:50, c) 20:80, and d) 10:90) [23].

Curve *a* is not relevant for this work since it refers to a 100% HMDSO plasma which was not used. The most intense peak, especially for low concentrations of HMDSO, is the one at 1027 cm^{-1}, which refers to both Si-O-Si and Si-O-C asymmetric stretching. At 1254 cm^{-1} there is the peak of the CH_3 symmetric bending in Si(CH$_3$)$_x$. At 839 cm^{-1} and 795 cm^{-1} correspond, respectively, the rocking vibration of CH_3 in Si(CH$_3$)$_3$ and the rocking vibration of CH_3 in Si(CH$_3$)$_2$ plus the Si-O-Si bending vibration [23].

N-hexane plasma can be used to produce polyolefins coatings from n-hexane polymerization. In Figure 2.21 it is shown a reference example of an FT-IR spectrum of polymerized n-hexane, compared with the one of liquid n-hexane.
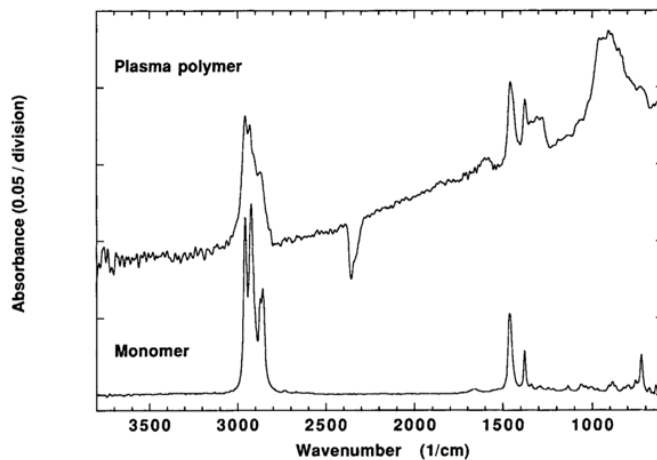
Figure 2.21 FT-IR spectra of n-hexane plasma polymer and n-hexane liquid [38].

Some new peaks appear after the polymerization, while the already present ones become broader due to the inhomogeneous chemical structure of the polymer [38]. Peaks at 2960 cm^{-1} and 2875 cm^{-1} are the most intense ones, and they refer to C-H stretching in CH$_3$ groups. At 2925 cm^{-1} and 2855 cm^{-1} there are the stretching vibrations of C-H bonds in CH$_2$ groups. C-H deformation in C(CH$_3$) and -CH$_2$- can be associated to peaks at 1465 cm^{-1} and 1380 cm^{-1}. The skeletal vibration due to a -(CH$_2$)$_n$- chain with n > 3 is linkable to the 725 cm^{-1} frequency. After the polymerization, a broad peak band appears just below 1600 cm^{-1}, representing the C=C stretching vibration. The broad features in the regions 750-960 cm^{-1} and 1270-1370 cm^{-1} can be associated to C-H bonds in unsaturated structures.

An ordered collection of the main peaks of pristine soda lignin and deposited HMDSO and n-hexane films is presented in Table 3.3 in section 3.2.1 to facilitate the reading of the spectra of plasma-treated lignin.

2.3.2 Differential Scanning Calorimetry (DSC)

Differential Scanning Calorimetry is a characterization technique used to detect temperatures and heat flows associated to thermal transitions. For this thesis work, DSC was used to evaluate variation in the transition temperatures of both the treated powders and of the lignin-PP blends.

In the case of polymers, it can be used to evaluate the glass transition temperature or the melting temperature. When a polymer is subjected to progressive cooling, T$_g$ corresponds to the temperature at which the macromolecular chains of the polymer start to be immobilized. The most common way of describing and interpreting this phenomenon is with the *free-volume theory*. Amorphous and semi-crystalline materials

have an excess free volume above the T_g that allows roto-translational motions of the chains. When cooling down the material, these motions become progressively more difficult until a critical value of temperature, the glass transition temperature, when molecules are immobilized, and the polymer reaches a vitreous-solid state. The value of temperature at which the transition occurs is affected by the polarity of the chain and cohesive interactions among them: a higher concentration of attractive forces lowers the mobility of the molecules, and when the material is cooled down the T_g is reached at higher temperature. After the plasma treatment of lignin, we hope to see a decrease in the amount of hydroxyl groups and of hydrogen bonds consequently.

To prepare the samples to be tested in the DSC, a small amount of material is weighted (5-15 mg) and put in a stainless-steel crucible hermetically closed. Then, the lignin-containing crucible is loaded into the heated chamber of the DSC together with a reference sample (an empty crucible). The instrument is set to provide a certain amount of heat per unit time to both samples in an inert atmosphere (N_2), with temperature rising at a constant time rate. When the test sample undergoes a phase transition, the two crucibles require a different amount of heat to maintain the same temperature. The difference in heat flow is detected by the thermocouples system and it is processed by the software of the machine to show an exothermic or endothermic peak in the final thermogram, plotted as a function of time and temperature. The equation used by the DSC to evaluate the heat flow (dQ/dt, with dt period of time) is the following:

$$dQ = mc_p dT \qquad (2.1)$$

Where m is the net mass of the sample, c_p is the specific heat of the tested material and dT is the change in temperature. The transition from the liquid to the glass state is a kinetic transition, not a thermodynamic one; it is defined as a second order transition, which means that after the transformation has occurred enthalpy (H) and volume remain constant, while their derivatives change. Being the specific heat defined as $c_p = \frac{\partial H}{\partial T}$ it reaches a different value after the transition. There is a temperature range where c_p linearly changes to reach its new value and this phenomenon corresponds to a change in the amount of heat required by the sample to change its temperature (Figure 2.22).
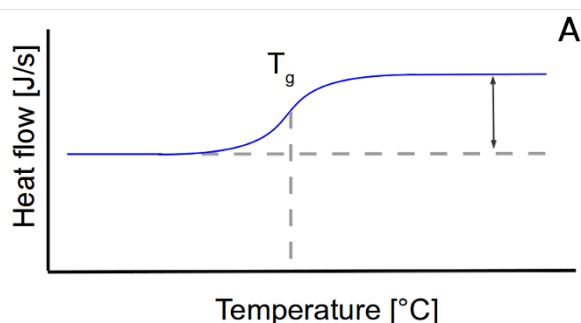
Figure 2.22 Trend of the heat flow vs. temperature curve when a glass transition is happening.

Two different thermal cycles were used to test the lignin powders or the lignin-polypropylene blends. The thermal cycle to which the samples of plasma-treated lignin powders were subjected during the tests was the same for all of them, and it is listed as follows:

$$25°C \rightarrow 200°C \qquad (1)$$

$$200°C \rightarrow 25°C \qquad (2)$$

$$25°C \rightarrow 250°C \qquad (3)$$

Heating up and cooling down of the crucibles were both performed at 20 K/min speed. Step (1) was necessary to delete the past thermal history of the samples.

Instead, the thermal cycle to which all the lignin-polypropylene compounds and pure polypropylene were subjected during the tests is the following:

$$25°C \rightarrow 200°C \qquad (1)$$

$$200°C \rightarrow -50°C \qquad (2)$$

$$-50°C \rightarrow 250°C \qquad (2)$$

Heating up and cooling down of the crucibles were both performed at 20 K/min speed. In this case as well step (1) was necessary to delete the past thermal history of the samples, specifically the previous crystallization of polypropylene. The cooling process of the first thermal cycle was run until -50°C with the goal of observing the glass transition temperature of polypropylene. Unfortunately, the transition was not detected by the instrument, and it was not possible to study how the lignin in the blends influenced the T_g of polypropylene. With the second thermal cycle, recrystallization of PP was induced in presence of lignin.

The machine used in this work for lignin characterization was a Mettler-Toledo DSC 823e.

All the eight samples of plasma-treated lignin listed in Table 2.1 were tested with this characterization method. In particular, the eight performed on thermally pre-treated lignin were considered for this measurement, since the presence of water in the sample highly affects the results. DSC was also used to investigate differences among treated lignin extracted from the GAT chamber and from the filter. For what concerns the polypropylene-lignin blends, only the compounds with 10% and 20% lignin content were tested with this technique.

2.3.3 Solubility test

Solubility tests have been performed in four solvents belonging to different chemical classes: Methylethylketone, toluene, ethyl acetate, cyclohexane. Information about these solvents is presented in Section 2.1.3.

When referring to a solid-liquid combination, solubility is defined as the maximum amount of solid (solute) that can be completely dissolved in a specific liquid (solvent) at a given temperature, and it is generally expressed in mg of solute per mL of solvent. If the solid is dissolved in the liquid without the formation of a precipitate or suspended particles, they form a homogenous mixture, i.e. a solution (Figure 2.23).
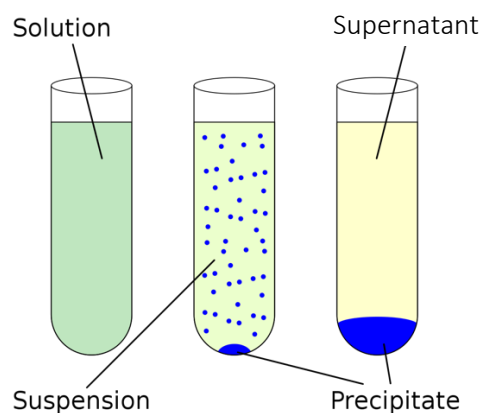
Figure 2.23 Graphic representation of the differences between a homogenous solution, a suspension, and a mixture containing an insoluble solid.

Solubility depends on many parameters, like temperature, pressure, pH, and presence of other chemical in the solutions that could either act as species that facilitate or hinder the dissolution process.

The ability of a solid to dissolve in a liquid highly depends on the physical and chemical interactions among the two. Indeed, if the solute-solvent interactions are more favourable than the solute-solute and solvent-solvent ones, it is extremely probable that they form a homogenous solution. Nonetheless, if interactions among

the two species are not favourable, the solute will precipitate from the solvent. Good solute-solvent interactions are achieved when the two materials have similar chemical characteristics in terms of polarity: polar solvents tend to dissolve hydrophilic materials, while hydrophobic solids tend to form solutions with non-polar solvents. When polymers are immersed in a compatible solvent, their dissolution occurs through chain disentanglements and solvent diffusion [39]. The solubility of polymers into solvents can be characterized by solubility parameters such as the Hildebrand parameter (δ), which is especially useful to predict the solubility of non-polar and weakly-polar polymers. According to Hildebrand's theory, the solubility parameter for these types of polymers can be defined as follows:

$$\delta = \sqrt{\frac{E}{V_m}} \qquad\qquad (2.2)$$

where E is the cohesive energy of the solute, and V_m is its molar volume, both calculated considering the contributions of atoms and functional groups, when the repeating unit of the polymer is known.

Organic materials are generally hydrophobic, and they easily dissolve in non-polar solvents such as gasoline. Lignin, however, is an organic compound with several polar hydroxyl groups in its chemical structure, which makes it more soluble in polar solvents. According to previous studies, almost complete solubility (i.e. 10 mg/mL) of non-wood soda lignin in organic solvents is reached in tetrahydrofuran (THF), pyridine and dimethyl sulfoxide (DMSO). Satisfying levels of solubility are also observed in methanol and acetone (i.e. ~ 8 mg/mL) while soda lignin is only partially soluble in ethanol and ethyl acetate (i.e. ~ 5 mg/mL) (Figure 2.24) [39]. The powder's solubility is expected to further decrease in non-polar solvents.
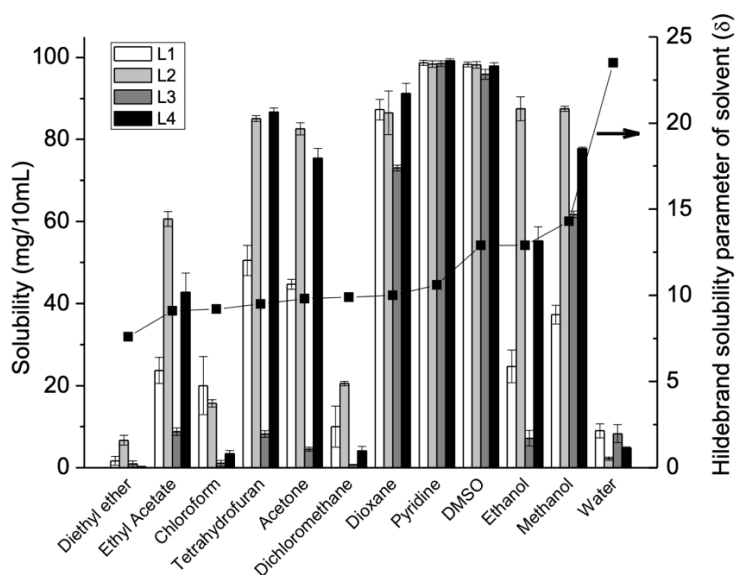
Figure 2.24 Solubility of 100 g of lignin in 10 mL of different organic solvents. The values of interest for this work are the ones for L4, which refers to Protobind lignin.

In this work, the solubility tests have been performed by making lignin-solvent mixtures with a concentration of 5 mg/mL. Once the samples were prepared in small vials, they underwent 30 minutes of ultrasonic bath treatment at room temperature. By doing this, agglomerates were supposed to break up and solubility should be optimized. The results of the tests were evaluated after 24 hours.

Solubility tests were performed on the eight plasma treated samples to detect any differences with pristine lignin in their solubility behaviour.

2.3.4 Nuclear Magnetic Resonance (NMR) Spectroscopy

NMR is a quantitative characterization technique that allows the detection of the type and the quantity of atoms present in the tested material. It is based on the measurement of the local magnetic field present around the nuclei. Indeed, every nucleus is characterized by an intrinsic magnetic field that depends on its charge and the surrounding electrical environment, i.e. the electron density. In the presence of an external magnetic field (B_o), the nucleus magnetic moment aligns in its same direction. Considering the electron as a negative charged particle moving around the nucleus, it generates a magnetic field (B_{in}) that points in the opposite direction of the imposed one, since its charge is opposite to the one of the nuclei, lowering the effective magnetic field experienced by the nucleus. To align B_{in} with B_o, energy must be provided to the electron to change its spin state, and therefore the direction of the produced magnetic

field. The amount of energy required for this transition is quantified and it is associated to a specific value of frequency, characteristic for each functional group.

For this work, ^{31}P-NMR was employed to quantitatively detect the amount of hydroxyl groups contained in the treated-lignin samples to evaluate if the plasma treatment worked effectively. To perform this type of measurement, the use of a phosphitylation reagent to allow the determination of -OH groups in the sample was needed. The employed chemical for the phosphitylation was 2-chloro-4,4,5,5-tetramethyl-1,3,2-dioxaphospholane, which can attach to -OH.

For the preparation of the sample to be tested with ^{31}P-NMR, firstly two solutions had to be prepared. The first one is the one containing the Internal Standard (IS), and it is obtained by dissolving 10 mg of Endo-N-hydroxy-5-norbornene-2,3-dicarboximide, which is the IS, in 0,5 mL of a mixture of pyridine and deuterated chloroform (CDCl$_3$) with volume-to-volume ratio (v/v) of 1,6:1. The second solution was prepared by adding 5,7 mg of chromium (III) acetylacetonate to 0,5 mL to a mixture of pyridine and deuterated chloroform with v/v of 1,6:1. At this point, the lignin sample to be tested with ^{31}P-NMR could be prepared. To do so, 40 mg of lignin were completely dissolved in 300 μL of dimethylformamide and subsequently there were added 200 μL of Pyridine, 100 μL of the IS solution, 50 μL of the second solution previously prepared, 100 μL of the phosphitylation reagent and 130 μL of CDCl$_3$.

With this characterization technique it is possible to detect and quantify different types of hydroxyl groups. They are listed, with the relative approximate ppm at which their peaks are observed, in Table 2.5. The position of the IS peak is also included.

Table 2.5 Peaks position of IS and of hydroxyl groups detected by ^{31}P-NMR.

Functional group	Peak position (ppm)
Internal Standard (IS)	153
Aliphatic -OH	150,0 - 147,0
Phenolic -OH	145,0 - 137,2
Carboxylic -OH	136,8 - 135,0

The spectra measured by the instrument can be then analysed by considering the area integral below the peaks, taking as reference the area of the IS equal to 1. Once the areas corresponding to each peak are evaluated, the different -OH concentrations are calculated through the following equation:

$$[OH] = \frac{area\ integral \cdot \text{mol IS}}{\text{g lignin sample}} \tag{2.3}$$

The technique was carried out by collecting 256 scans with a 5 seconds delay and an offset of 100 ppm. The instrument employed was a Bruker Avance 500 brand nuclear magnetic spectrometer.

2.3.5 Tensile test

Tensile test is a mechanical characterization technique to study the behaviour of a material under an elongational stress. Through this technique it is possible to build the stress-strain curve of the material, and also to obtain mechanical properties of the material, such as the Young's modulus (E), the ultimate strength (σ_u) and the elongation at break (ε_B).

The Young's modulus is defined as follows:

$$E = \lim_{\sigma \to \infty} \left(\frac{\delta\sigma}{\delta\varepsilon} \right) \tag{2.4}$$

where σ is the stress applied to the material and ε is the strain it experiences. Computational methods are therefore needed to continuously evaluate the derivative of the stress-strain curve, i.e. the above limit, to derive the value of the Young's modulus. The yield strength is defined as the value of strength at which the material's behaviour switch from elastic to plastic, and it is therefore the minimum value of stress for which the material experiences a permanent deformation. Below σ_y, the stress strain curve is linear and E is constant, while after the yield strength the Young's modulus of the material varies (Figure 2.25).
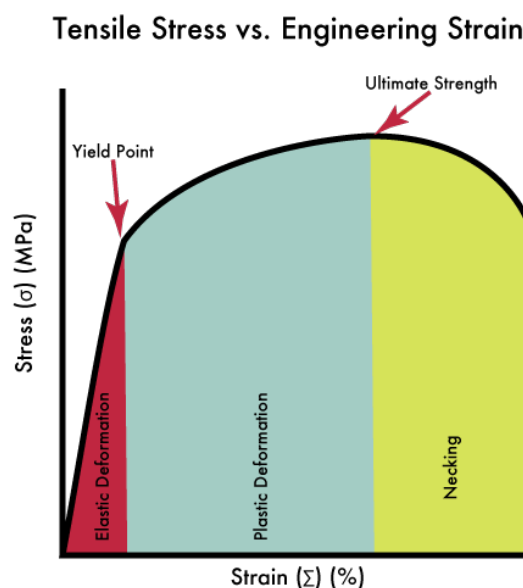
Figure 2.25 Stress-strain curve of a polymeric material.

The σ_u, as can be seen from the picture, coincides with the maximum value of stress that the material is capable of sustaining, after which it experiences necking, which consists in the localization of incredibly high stresses in a point of the material with consequent decrease of the cross-sectional area of the specimen in that point. In this work, the elongation at break was arbitrarily defined after evaluating the shape of the stress-strain curves of the blend during the tests. Indeed, after necking, the σ-ε curves were characterized by a plateau at approximately 50% of the ultimate strength of the material. After the plateau, the materials kept deforming with a constantly decreasing stress. Since the specimen, even if it was not completely broken, showed a highly damaged and reduced cross section, the value for the elongation at break of the material was chosen to be the one at which the curve transit from the plateau to a decreasing line.

To perform the measure, the dog-bone shaped specimen was first settled in the instrument. The sample was kept in a vertical position, and it was hooked by a couple of screw clamps on the two ends that pulled the material under testing during the measurement. The test was performed by applying a controlled tensile load until failure so that the ultimate tensile strength and the elongation at break could be directly measured. Specifically, the elongation was measured with strain gauges.

The instrument used in this thesis work was a dynamometer Zwick-Roell BT-FR010TH.A50 and the software used to collect and process data was TestXpert II by Zwick-Roell, which allowed the direct computation of the tangent elastic modulus of the material. Tests were carried out under displacement control at a displacement rate of 1 mm/min until a deformation of 0,8% was reached, which is the value of deformation at which the elastic modulus is evaluated. After that point, a rate of 5 mm/min is employed until the breaking of the sample.

The specimen produced by Rambaldi&CO I.T. Srl is shown in Figure 2.26 and has a rectangular gross section of 3,9x2,0 mm², with thickness around 2,0 mm.

Figure 2.26 Specimen for tensile tests.

2.3.6 Rheology test

Rheology tests are generally performed to measure the elastic recovery in polymer melts and their compounds. This characterization technique was carried out to evaluate the rheological behaviour of the lignin-polypropylene blends produced for this thesis work. Differences were evaluated between the blends containing treated and untreated lignin, also considering different lignin content. A reference sample of pure polypropylene was tested too. Specifically, rheology tests were used to evaluate the relaxation time of the samples.

Polymers are viscoelastic materials, meaning that they exhibit both elastic and viscous behaviour when they undergo a deformation, which translates in a time-dependent relationship between stress and strain. Elastic materials deform instantaneously when a load is applied and when it is removed, they instantaneously recover their original state. Viscous materials, instead, are characterized by a time-dependent strain rate and they also dissipate energy when they are subjected to a load that is then removed. When polymers are subjected to a load, its chains rearrange according to a phenomenon called creep; once the applied load is removed, they recover their original position, like elastic materials, but with energy dissipation, like viscous materials (Figure 2.27).
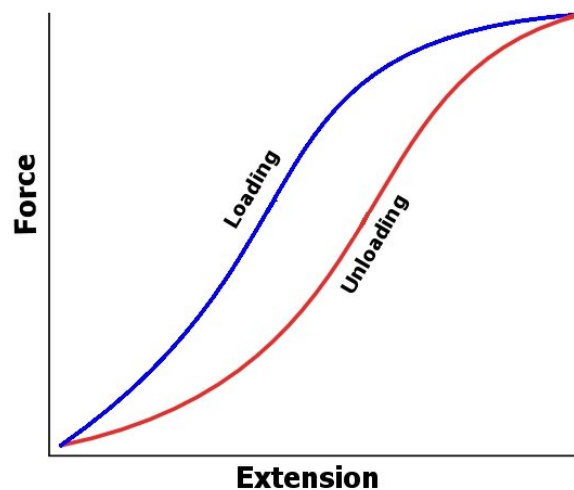
Figure 2.27 Hysteresis curve of a viscoelastic material.

The relationship between stress and strain, in polymers, is described by the shear modulus (G), defined as the ratio between the shear stress and the shear deformation. G can be divided into two components, the storage modulus (G′) and the loss modulus (G′′), which represent the elastic and the viscous components respectively. Physically, G′ represents the elastic energy stored during the deformation, while G′′ represents

the dissipated one. The ratio between the viscous and the elastic component of G is defined as damping factor (tanδ), which is an important parameter to describe the energy dissipation inside the material when deformed. It also gives a measure of the prevalence of the elastic behaviour over the viscous one, or vice versa. The equation that defines the damping factor is the following:

$$\tan(\delta) = \frac{G'}{G''} \qquad\qquad (2.5)$$

Another important parameter that characterizes viscoelastic materials is the relaxation time, which corresponds to the moment during the deformation at which the elastic behaviour overcomes the viscous one, which means that the G′ curve crosses and becomes higher than the one of G′′.

The rheometer is the instrument that performs the rheological tests, and it works by imposing a specific stress field or deformation to the analysed fluid, i.e. the melted polymer, while monitoring the resultant deformation or stress. It can be either run in steady flow or oscillatory flow, in both shear and extension. In this work, rheology measurements were performed by means of a Discovery HR-2 hybrid rheometer by TA instruments in presence of gaseous nitrogen. The geometry used to perform the experiments is a 25 mm parallel plate made of steel. The main parameters that were monitored during rheological tests are the storage modulus and the loss modulus.

Frequency sweep tests were performed in this thesis work to evaluate the relaxation time of the tested blends and polymers. Before performing the frequency sweep tests on the samples, they all had to undergo a strain sweep test aimed at knowing the linear viscoelastic range (LVR) of the material. The aim was to confirm that the deformation value employed during the rheology tests did belong to the linear viscoelastic range of the material. Both tests were performed at constant temperature of 180°C, which corresponds to the process temperatures adopted during extrusion for propylene-based materials. Results were displayed in a diagram with G′ and G′′ on the vertical axis and deformation on the horizontal one.

Strain sweep tests were performed by varying the oscillation strain percentage from 0,05% to 5,0% with fixed frequency of 1,0 Hz for the evaluation of the linear viscoelastic region. The LVR corresponds to the values of deformations where G′′ appears constant. A value for the maximum deformation to perform the frequency sweep tests was then picked from this range, preferably not too small so that the rheometer can properly operate. Specifically, a strain of 1% was chosen for this thesis work.

During the frequency sweep test, the samples were deformed while continuously increasing the oscillation frequency from 1 Hz to 100 Hz, with a maximum deformation equal to 1%. The point in the graph where the curves of G′ and G′′ overlap

is called the crossover point, which corresponds to a specific value of frequency (f_{cross}), and it is related to the relaxation time (t_{rel}) as follows:

$$t_{rel} = \frac{1}{f_{cross}} \tag{2.6}$$

2.3.7 Thermogravimetric Analysis (TGA)

Thermogravimetric analysis is a characterization technique that, through the evaluation of its mass variation while progressively increasing the temperature, it allows to study physical phenomena, such as phase transitions, absorption, adsorption and desorption, as well as chemical phenomena like thermal decomposition, thermal stability and solid-gas reactions of a material. It is a very common technique to investigate the thermal stability of polymers. Most polymers melt or degrade before 200 °C. However, there is a class of thermally stable polymers that can withstand temperatures of at least 300 °C in air and 500 °C in inert gases without structural changes or strength loss, which can be analysed by TGA. In this thesis work TGA was used to evaluate the thermal stability of blends containing plasma-treated lignin and pristine lignin.

To perform the measurement, a few milligrams of the material to be tested were placed in a platinum crucible which was then put in a furnace and gradually heated. The consequent mass loss was continuously weighted by a precision balance. The instrument could work both in inert (N_2) atmosphere or in air and the results were shown in form of a thermogram. The results of the measurement were shown as mass variation (%) and first derivative of mass variation (%), called derivative thermogravimetry (DTG), as a function of temperature.

The analyses for this thesis work were carried out in air with TGA Q500 by TA Instruments in a temperature range that goes from 25°C to 800°C with a rate of 20°C/min. Only pure polypropylene and the blends containing 10% of lignin were tested.

3. Results and discussion

3.1 Characterization of the electrical parameters of the GAT device

The characterization of the electrical parameters of the GAT device was necessary to determine the experimental parameters at which the spark or the arc regime could be observed. Indeed, the value of imposed current at which the spark-to-arc transition occurred can vary depending on the gas pressure, on the distance between the electrodes and on the nature of the plasma gas.

First, a reference value of imposed current for the spark-to-arc transition (I_{th}) had to be determined to study how changes in the other parameters would affect its position. This was done by observing the nature of the discharge, i.e. spark or arc, while keeping the other experimental parameters as shown in Table 3.1. The values of gas pressure in the GAT device shown in this work are relative to the ambient pressure, and to obtain the absolute value the two must be summed. The distance between the electrodes was set at 18 mm after a set of experiments to determine the minimum distance at which the breaking potential of the gas occurred. Considering the common shape of the Paschen's curves shown in section 1.3.1, by keeping fixed the value of pressure, this is the distance at which the breaking potential is minimum. Consequently, this point in the curve correspond to the conditions at which the energy needed for the discharge to be initiated is the lowest.

Table 3.1 Reference parameters for the spark-to-arc transition evaluation.

Parameter	Reference
Nature of the plasma gas	Argon
Gas pressure	3 atm
Distance between the electrodes	18 mm

With the above experimental conditions, the spark-to-arc transition was detected at 275 mA, where it was possible to observe a discharge that during time showed a succession of both spark and arc regime. The following experiments were performed to detect variations from the reference value of 275 mA, while separately varying other parameters.

The influence of the distance between the electrodes (d) on I_{th} was studied while keeping the gas pressure at 3 atm and using Argon as plasma gas. The results of the measurements are shown in Figure 3.1. Only 2 mm variations from the reference value of 18 mm were investigated, since smaller variations would have not brought to detectable changes. Moreover, choosing values of d more distant from the reference one would have caused the need of using higher or lower pressure to reach the breaking potential. However, none of the two options were interesting or convenient since higher pressure would have exhausted the Argon tank too quickly, while much lower pressure would have not been able to support the weight of lignin to transport it along the circuit.
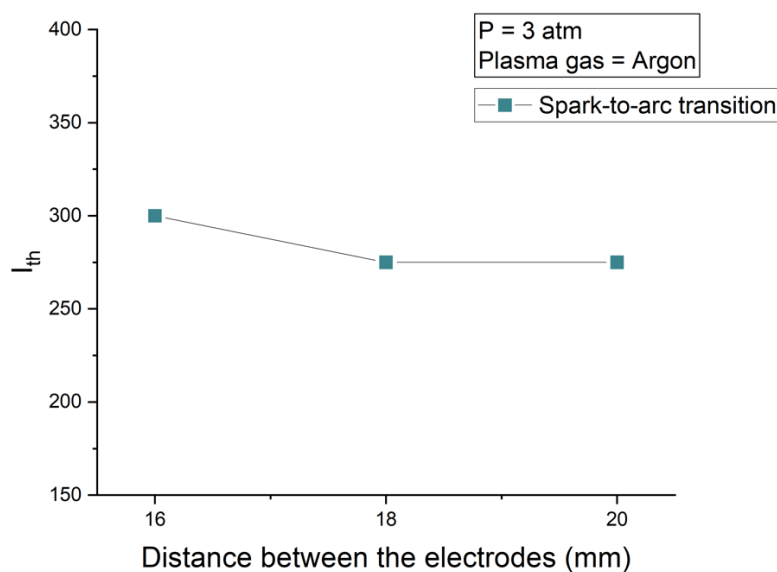
Figure 3.1 Influence of the distance between the electrodes on the position of the spark-to-arc transition.

It was observed that the spark-to-arc transition was not highly affected by the distance between the electrodes, considering only limited variations from the reference point of 18 mm.

The influence of pressure on I_{th} was also investigated. In particular, the transition was studied for pressure of Argon equal to 1 atm, 2 atm, and 4 atm while keeping the

electrodes at 18 mm of distance and using Argon as plasma gas. In Figure 3.2 it is shown how the position of the transition varied with different values of pressure.
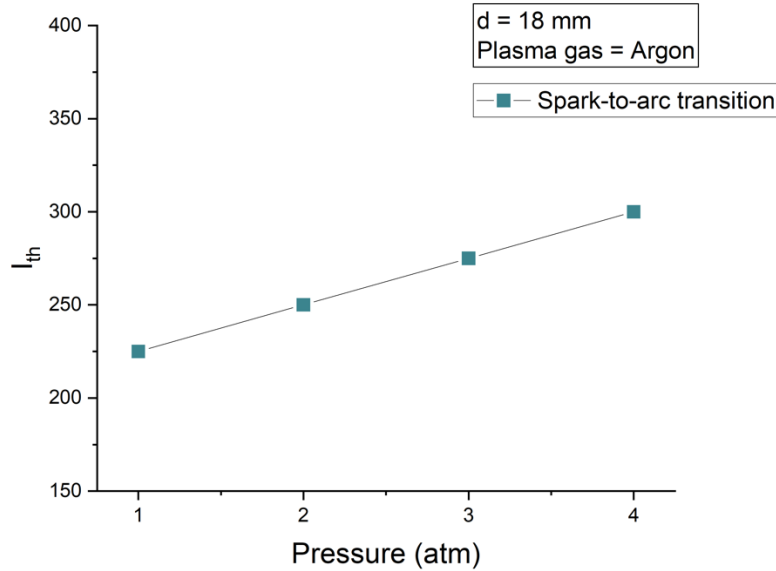
Figure 3.2 Influence of the gas pressure on the position of the spark-to-arc transition.

The trend in the I_{th}-pressure curve is linear, with higher values of I_{th} needed at higher pressure. However, the variation in the spark-to-arc transition is just moderately affected by changes in pressure.

Lastly, the effect of the addition of a functionalizing gas to the circuit, specifically n-hexane, was studied. The pressure and the distance between the electrodes were kept at their reference values, as previously shown in Table 3.1. It was observed that the addition of n-hexane as plasma gas highly affected the position of the transition between the two discharge regimes. Indeed, I_{th} was detected at 550 mA. Similar results were observed when adopting HMDSO as functionalizing gas. This evidence suggests that the presence of a functionalizing gas hinders the thermionic emission from the electrodes, which characterizes the arc discharge regime.

To perform the plasma treatments on lignin, parameters had to be carefully chosen to be sure to observe either a stable spark discharge or an arc discharge depending on the experiment needs. The set of parameters chosen are shown in Table 3.2.

Table 3.2 Experimental parameters used to perform the plasma treatments with Argon in spark regime and in arc regime.

Parameter	Spark regime	Arc Regime
Imposed DC current (mA)	200	750
Distance between the electrodes (mm)	18	

Pressure (atm)	3

The choice for the values of imposed DC current for the spark and arc regime was done so that independently on the plasma gas employed, the observed regime would have been the same. To do so, values of current sufficiently far from the I_{th} previously detected were chosen to have a stable discharge in the spark or arc regime. A detailed characterization of the discharge when using compressed air as plasma gas was not carried out. However, with the values of imposed DC current in Table 3.2, and keeping the parameters like in Table 3.1, stable spark and arc regimes are observed with compressed air as well. When compressed air was used as gas source the value of pressure was changed too. A pressure of 2 atm was enough to carry the lignin powders along the circuit, while with Argon 3 atm of pressure were needed. This is probably due to a different hydrodynamic behaviour between the two gases, which determines different carrying capabilities.

The treatments were designed to be performed either in the spark or arc regime, without changing the value of imposed current depending on the gases employed. This decision could bring to slight and non-easily detectable differences in other secondary parameters, such as impressed power and treatment time. Nonetheless, the strategy was to focus on the different effects of the treatment when using an impulse discharge (spark regime) or a continuous one (arc regime).

3.2   Characterization of the plasma-treated powders

In this section results of the characterization experiments performed to study the chemical behaviour of treated powders are presented. First, characterization methods to evaluate differences in the hydrophilicity behaviour between plasma-treated and untreated lignin were used. Later, ^{31}P-NMR was used to quantitatively assess the chemical transformations occurred on lignin particles.

3.2.1 FT-IR

By using FT-IR, the goal was to detect any consistent change in the amount of hydroxyl groups in plasma-treated lignin samples and the potential presence of new functional groups deposited from functionalizing species.

For an easier reading of the results, Table 3.3 summarizes the main peaks useful for this thesis work, which were already presented in section 2.3.1.1.

Table 3.3 Reference peaks of soda lignin, deposited films from HMDSO-plasma and from n-hexane-plasma. *only methylene groups concern n-hexane*

Band (cm^{-1})	Functional groups vibrations	Deriving species
3400 - 3000	-OH stretching from aliphatic and phenolic hydroxyl groups	Soda lignin
3000 - 2800	C-H stretching in methoxyl and methylene groups	Soda lignin, n-hexane*
2925-2855	C-H stretching in CH_2 groups	n-hexane
1615 - 1720	C=O stretching in ketones, carbonyls and in ester groups	Soda lignin
1600	C=C stretching vibration	n-hexane
1600, 1500, 1425	Aromatic skeletal vibrations	Soda lignin
1465	C-H deformation in C-(CH_3)	n-hexane
1380	C-H deformation in –(CH_2)-	n-hexane
1254	CH_3 symmetric bending in $Si(CH_3)_x$	HMDSO
1027	Si-O-Si and Si-O-C asymmetric stretching	HMDSO
1120 - 1125	C–O deformation in ester bonds	Soda lignin
1031	-OH stretching of primary alcohols	Soda lignin
839	CH3 rocking vibration in $Si(CH_3)_3$	HMDSO
835	Aromatic C–H deformation out-of-plane bending	Soda lignin
795	CH_3 rocking vibration $Si(CH_3)_2$ and Si-O-Si bending vibration	HMDSO
725	Skeletal vibration due to –(CH_2)$_n$- chains with n > 3	n-hexane

3.2.1.1 *Effects of different plasma treatments on lignin*

The effects of the eight different plasma treatments performed on lignin samples have been explored through FT-IR spectroscopy. First, to evaluate the influence of the presence of humidity in the powders on the measures, the plasma treatments have been performed both on thermally treated and on not-thermally treated lignin. Comparison of the FT-IR spectra for all plasma treatments are shown in Figure 3.3.
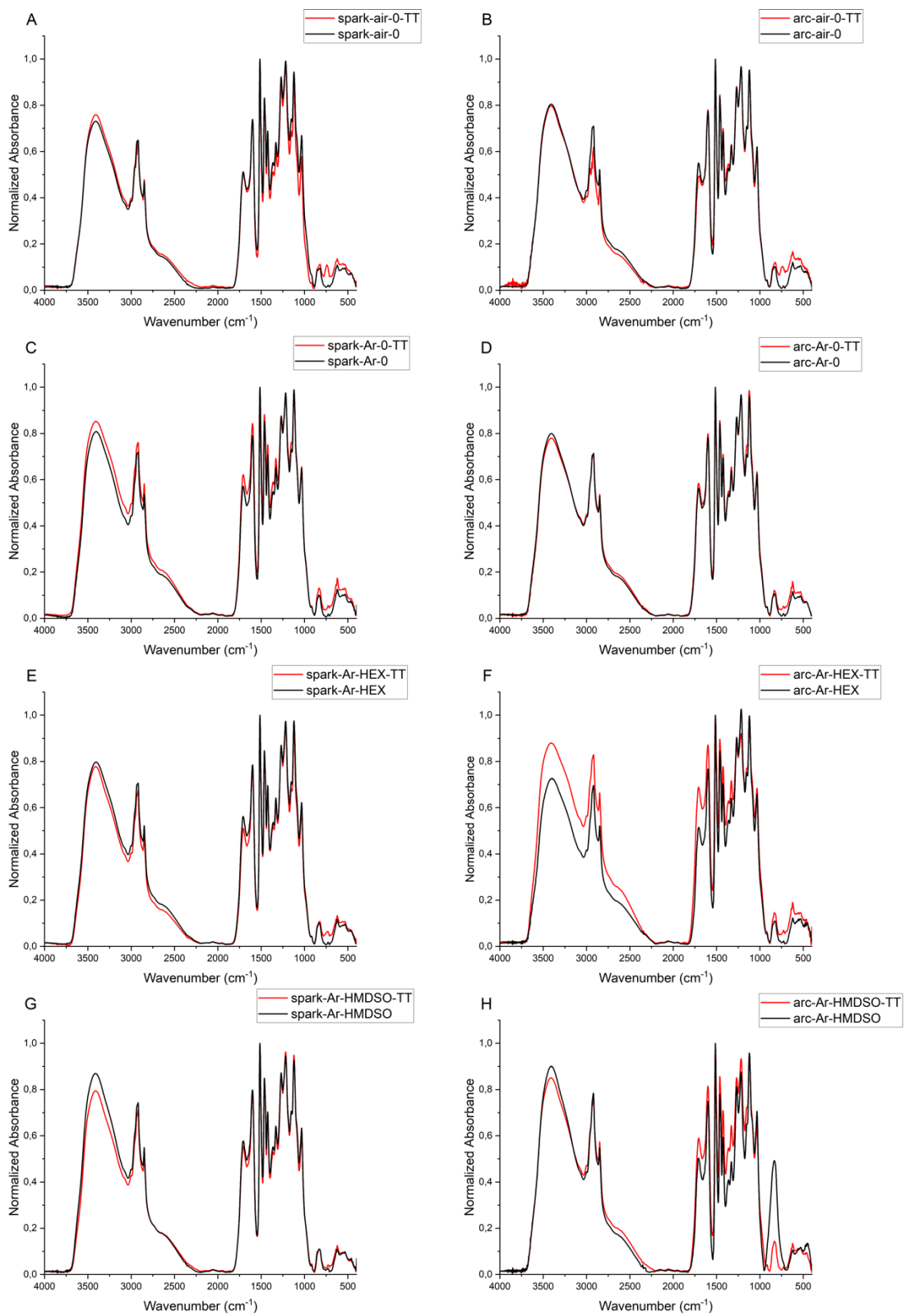
Figure 3.3 Effect of the plasma treatments on thermally treated and not thermally treated lignin.

No relevant differences are detected between the pre-treated and non-pre-treated samples. It seems that the result of the plasma treatment is slightly affected by the thermal treatment on lignin only when a functionalizing gas is employed (graphs E, F, G, H), especially in graphs F and G. In graph H there is a notable difference in the peak at ~ 835 cm^{-1}, being the intensity in the non-pre-treated sample much higher. The peak could refer to the out-of-plane bending of the aromatic C–H, which should not be affected by the plasma treatment, or to the CH$_3$ rocking vibration in Si(CH$_3$)$_3$ associated to the deposition of HMDSO. To better understand the nature of the peak, the same sample was re-tested a few months later, and the peak was still present with similar intensity. Nonetheless, other samples subjected to the same plasma treatment have been tested, and they did not show the mid-intensity peak at ~ 835 cm^{-1}. Therefore, it was established that the presence of that peak in graph H is an anomaly relative to the specific sample of lignin that was treated.

Even though the differences detected between the two groups of samples are not remarkable, it was chosen to proceed with the pre-thermally treated lignin for future analyses since it is expected to perform better in the formation of the blend with polypropylene. The presence of humidity could indeed hinder the blending process, since it is a source of polar interactions.

In Figure 3.4 the effect of the eight plasma treatments on thermally pre-treated lignin can be compared with the reference curve of pristine Protobind lignin. The two graphs show zoomed regions of the spectrum that correspond to the -OH region (graph A) and the fingerprint region (graph B).
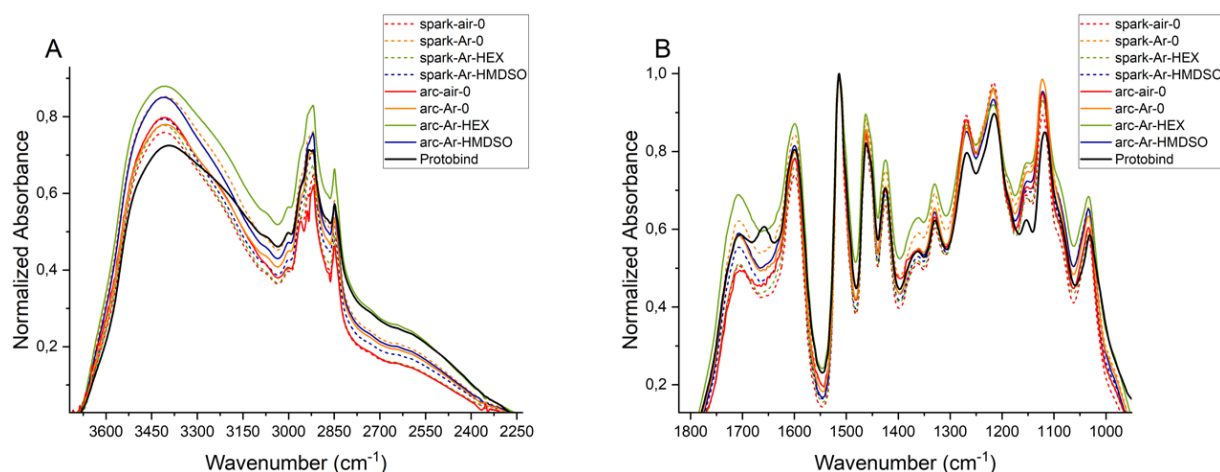
Figure 3.4 Comparison of the effect of the different plasma treatments on thermally treated lignin with pristine lignin.

As previously mentioned in section 2.3.1.1, the relevant region to evaluate the effects of the experiments is the -OH region (graph A), as the fingerprint region should not be

affected by the plasma treatment and the trend of the graph should not be subjected to great variations. This corresponds to what is shown in graph B, where all the trends are similar, except for the region 1615 - 1720 cm^{-1}, which represents C=O stretching in ketones, carbonyls and in ester groups. Particularly, the peak at ~ 1660 cm^{-1} disappears after performing the plasma treatments, which refers to conjugated carbonyl groups.

By looking at graph A, it can be noticed that all the treatments on lignin brought slight changes to the original chemistry of the material (black line). All of them show an increase in the intensity of the peak referring to the hydroxyl group stretching (3400 – 3000 cm^{-1}). In some of the treatments, especially the four performed without functionalizing gas (red lines and orange lines), while the intensity of the broad band relative to -OH stretching has increased, the height of the peaks at 3000 – 2800 cm^{-1} decreased. This phenomenon could be interpreted as de-methylation. Indeed, it might be that the treatments caused the loss of -CH$_3$ in methoxyl groups (-O-CH$_3$) with the consecutive formation of an -OH group [35].

Some other lines, particularly the ones referring to treatments with HMDSO or hexane (blue lines or green lines), show an increase in the intensity of both the -OH and C-H stretching peaks. These results suggest an increase in the amount of both functional groups. In the case of treatment performed with n-hexane, de-methylation with consequent addition of -OH functional groups could have been accompanied by intensification of the C-H stretching vibration peak at 3000 – 2800 cm^{-1} due to radicals' deposition from n-hexane.

Overall, FT-IR spectra do not highlight great differences before and after the treatments, which suggest that a different quantitative characterization method is needed to draw more objective conclusions about chemical changes in the samples.

3.2.1.2 Effects of time on plasma treatments

FR-IR spectroscopy was also used to evaluate any chemical change occurred in the samples after 50 days from the plasma functionalization, to assess the effect of time on the treatments. The resulting spectra are shown in Figure 3.5.
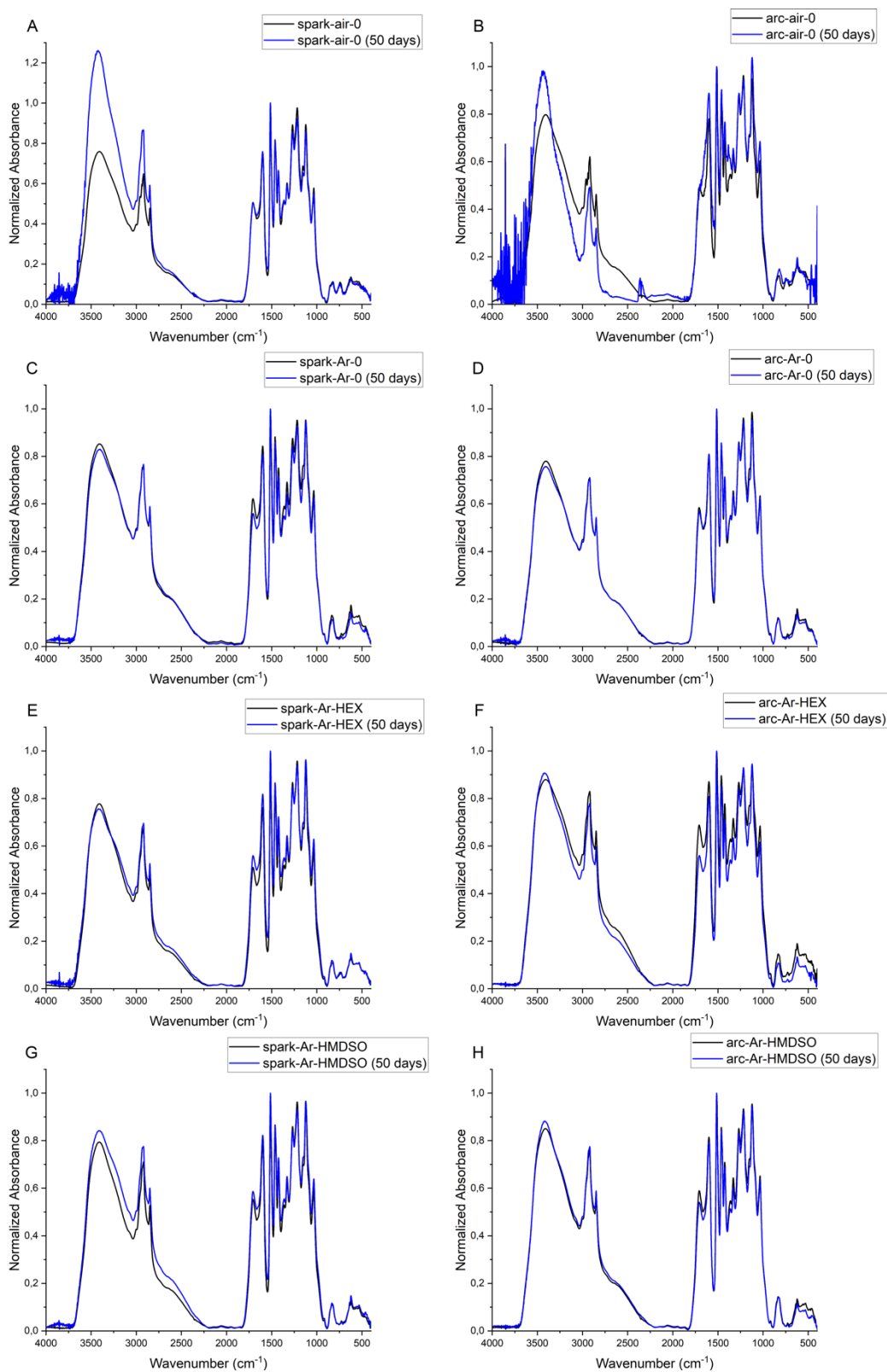
Figure 3.5 Differences on the FT-IR spectra of the plasma treated powders 1 day after the treatment was performed and 50 days after the treatment.

Almost all graphs show no or slight differences among the two curves, except for graphs A and B which correspond to the two treatments performed in air. In both cases the intensity of the peak corresponding to the -OH stretching vibration strongly intensifies. This phenomenon could be related both to aging or post-deposition reactions due to the presence of species, such as oxygen or humidity, entrapped during the plasma treatment [22], [38].

3.2.1.3 Differences between plasma-treated lignin collected from the filter and from the GAT chamber

The decision of performing distinct characterization tests on lignin extracted from the chamber and from the filter arises from the experimental evidence that chamber samples were subjected to much longer treatment times, and possible differences among the two wanted to be investigated.

Only four treatments among the eight performed were selected for these tests: two performed without functionalizing gas (Spark-Ar-0, Arc-Ar-0) and two with functionalizing gas (Spark-Ar-HMDSO, Arc-Ar-HMDSO). Results are shown in Figure 3.6.
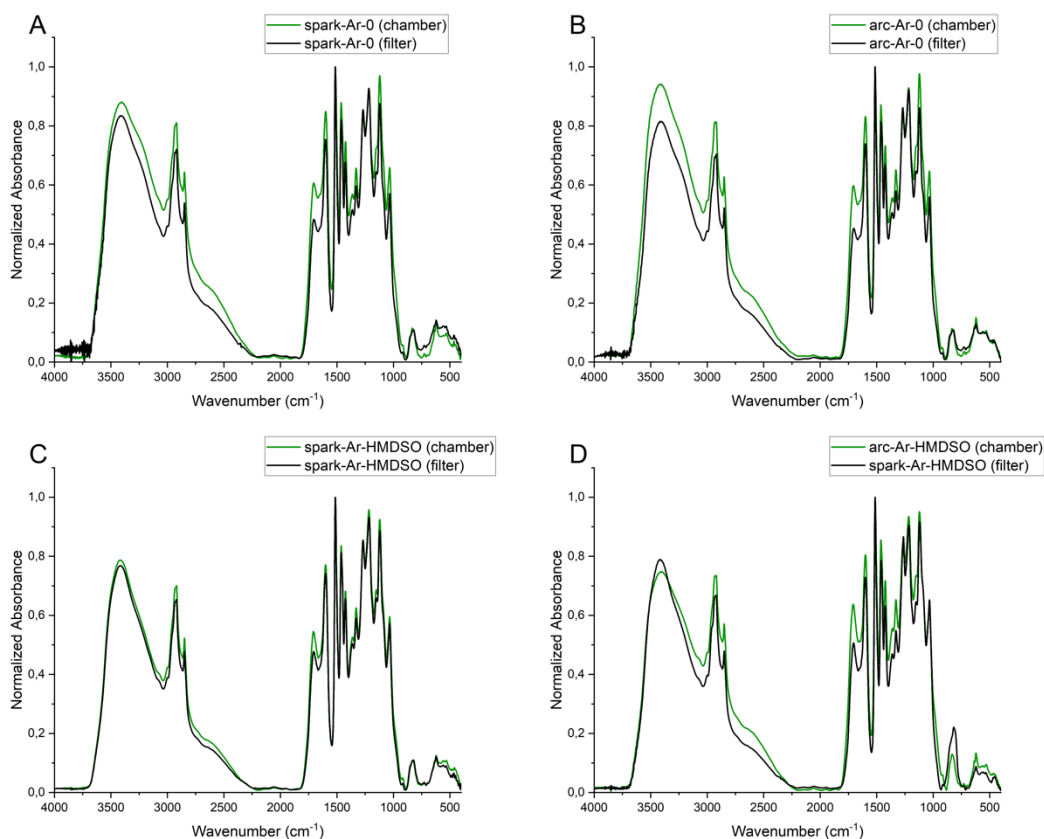
Figure 3.6 Differences on the FT-IR spectra of the plasma treated powders extracted from the collecting filter and from the GAT chamber for four different plasma treatments.

Almost no differences are detected between the two curves in graphs C and D, while in graphs A and B both the curves referring to lignin samples extracted from the chamber show a more intense peaks in the -OH region at 3400-2700 cm^{-1}. Also, peaks representing the C=O stretching vibration at 1615 – 1720 cm^{-1} in the fingerprint region appear more intense. These results suggest both increased oxidation of the sample and a slight de-methylation, as it is usually observed when treating polymers with Argon plasma [30].

3.2.2 DSC

3.2.2.1 *Influence of the different plasma treatments on lignin T_g*

The results of DSC are indicative to evaluate if a change in lignin chemistry or structure has occurred. By performing the plasma treatment on the powders, the aim is to induce reactions at the most reactive sites of the polymer (hydroxyl groups and aromatic rings) to hinder its polar behaviour. By doing this, some free radicals form where there were -OH groups, which can either react with the species in the chamber or with the

skeleton of the polymer through repolymerization, or they can also remain unreacted. These two events might have opposing results on the glass transition temperature: by substituting hydroxyl groups with radicals from hexane or HMDSO the internal interactions of the polymer are expected to decrease, as well as the T_g, while repolymerization causes an increase in the molecular weight of lignin with consequent increase in the glass transition temperature. Therefore, to reduce the polarity of the polymer, it would be desirable to achieve a glass transition temperature lower than the one of pristine lignin, but all the different factors influencing the T_g must be considered. It is indeed not straightforward to connect the variations in the T_g to chemical or structural changes in lignin. DSC must be used as a technique to evaluate the effects of different treatments, although no definitive conclusions can be drawn about the effective changes that occurred in the polymer without other characterizations results to support them.

The glass transition temperatures of all the treated samples are listed in Table 3.4 and a graphic representation of the DSC tests results is shown in Figure 3.7. The T_g value of untreated lignin is 132°C, measured in previous works.

Table 3.4 Glass transition temperatures of plasma treated lignin.

Gas source – Functionalizing gas	T_g (°C) – Spark regime	T_g (°C) – Arc regime
Air - /	133	148
Argon - /	138	138
Argon - Hexane	147	138
Argon - HMDSO	140	137
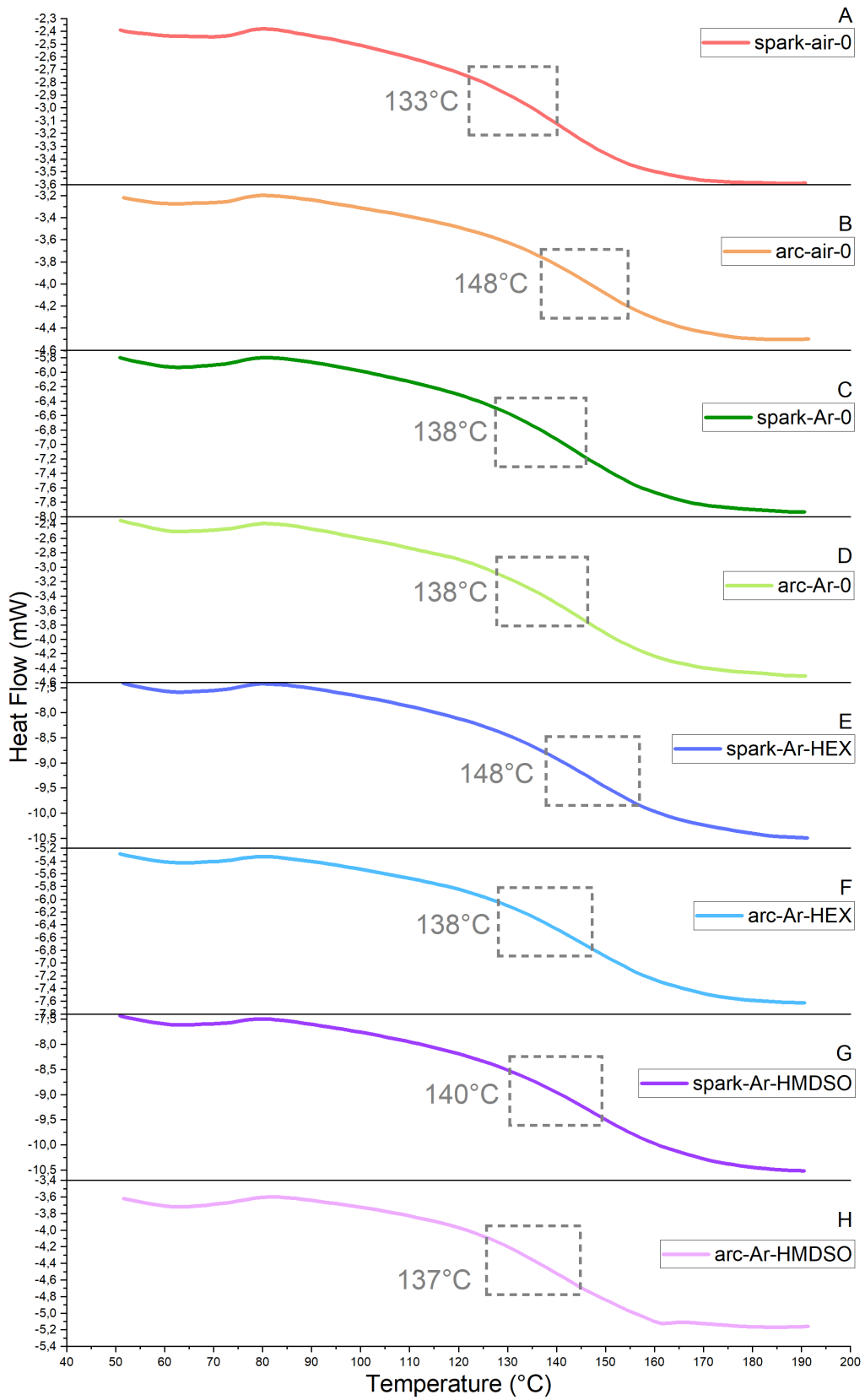
Figure 3.7 Glass transition temperatures of plasma treated lignin.

The glass transition temperatures of all treated samples are higher than the reference value of 132°C. In the four experiments performed with a functionalizing gas, the T_g of the samples treated in arc regime are higher than the spark ones. The opposite trend is observed in the couple of samples treated in air, while in the ones treated in Argon without functionalizing gas almost no difference is detected between the spark and the arc treatments. As explanation to this trend, it can be hypothesized that all the treatments induced repolymerization of lignin within itself, which increased the T_g of all samples. To interpret the difference between the treatments in spark and arc regime, we should consider that the ones performed in arc regime induce a much higher power to the powders and the gases in the reaction chamber. This might facilitate the reaction between them, bringing to more oxidized lignin in the treatment with air (and therefore stronger polarity and higher T_g with the arc regime) and more hydrophobic lignin (and lower T_g with the arc regime) in the treatments in Argon with functionalizing gases.

3.2.2.2   *Comparison between the T_g of the treated powders extracted from the collecting filter and from the chamber*

Differences were valued in the T_g of treated lignin extracted from the reaction chamber and from the filter. This was done to verify that the lignin extracted from the chamber did not undergo degradation, which would have brought to shorter chains and consequently a lower glass transition temperature. Only four treatments among the eight performed were selected for these tests, which are the same selected for the FT-IR tests in section 3.2.1.3. Results are shown in Table 3.5.

Table 3.5 Differences between the T_g of the plasma treated powders extracted from the collecting filter and from the GAT chamber for four different plasma treatments.

Sample	FILTER sample Tg (°C)	CHAMBER sample Tg (°C)
Spark-Ar-0	136	135
Arc-Ar-0	135	134
Spark-Ar-HMDSO	135	137
Arc-Ar-HMDSO	132	132

The samples extracted from the chamber and from the filter show a difference of 1°C or maximum 2°C in the case of Spark-Ar-HMDSO, which suggests that the chemical characteristics of the two samples are the same and degradation of lignin extracted from the chamber did not occur. Slightly higher glass transition temperatures are

detected in the case of treatments performed in the spark regime, consistent with what was shown in Table 3.4.

Considering both the results from DSC and from FT-IR on the treated powders extracted from the chamber or from the filter, it can be stated that no remarkable differences are detected among the two samples and there is no need to further investigate the differences among them with other characterization techniques.

3.2.3 Solubility tests

Solubility tests were performed to visually evaluate any change in the solubility behaviour of lignin after the plasma treatments. Therefore, it is expected to see an improvement of solubility in non-polar solvents if the plasma treatment has the aimed result of eliminating polar groups from the surface of the powder. It is although worth to be mentioned that several parameters can affect solubility, and it must be evaluated if a change in the powder properties can be related to those. For instance, it could happen that the plasma treatment is energetic enough to cause the break of lignin's backbone and an increase in its solubility could be related to a reduction in its molecular weight.

In this work, two non-polar solvents (cyclohexane, toluene) and two polar solvents (ethyl acetate and methylethylketone) have been chosen, and they were presented in section 2.1.3.1. The results, to be compared with the mixture containing pristine lignin, are discussed as follows.

The partial solubility of soda lignin in ethyl acetate, cited in section 2.3.2 was furtherly proven by the solubility test performed for this thesis (Figure 3.8).
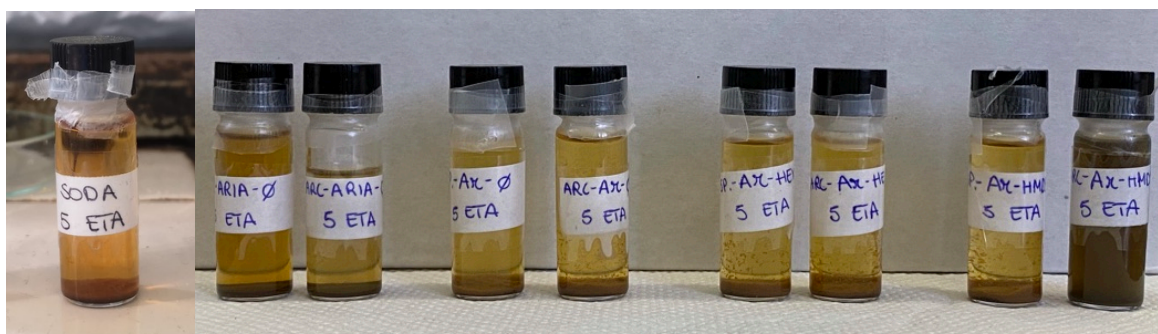
Figure 3.8 Solubility test of pristine lignin (left) and plasma treated lignin in ethyl acetate. In the picture on the right the plasma treated powders are divided in couples (spark on the left, arc on the right) and treatments are ordered as follows: air-0, Ar-0, Ar-HEX, Ar-HMDSO.

There are no great visual differences between the untreated and the treated samples, except for the plasma treated lignin on the right in the bottom picture (arc-Ar-HMDSO). The liquid in this vial appears dark brown and turbid. This could be due to partial solubility of the treated powder in ethyl acetate, which would suggest an increase in the hydrophilicity of lignin, being the solvent slightly polar. Another explanation for the change in solubility is the partial degradation of lignin due to the treatment. Indeed, during the arc regime the discharge is continuous and high power is delivered to lignin with the possibility of causing burning of the powder due to the high temperatures locally reached. Degradation of lignin would cause a reduction in the molecular weight of the polymer, increasing its solubility. But for both interpretation, higher solubility should be observed in other polar solvents as well and this, as can be seen for instance from Figure 3.10, does not happen. The dark colour of the solution could instead be explained by the change of colour experienced by the powder during the treatment (Figure 3.9).
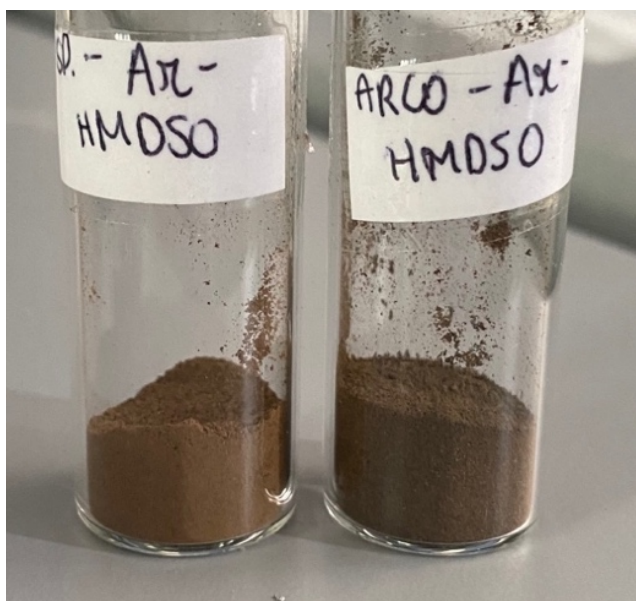
Figure 3.9 Visual difference between lignin treated in the spark regime (left) and the arc regime (right) for the Ar-HMDSO treatment.

Partial solubility of lignin is observed in methylethylketone as well (Figure 3.10).

Figure 3.10 Solubility test of pristine lignin (left) and plasma treated lignin in methylethylketone. In the picture on the right the plasma treated powders are divided in couples (spark on the left, arc on the right) and treatments are ordered as follows: air-0, Ar-0, Ar-HEX, Ar-HMDSO.

Partial solubility of lignin in methylethylketone is consistent with the theory, being the solvent polar and therefore chemically similar to lignin. For what concerns differences in the solubility behaviour of treated samples, they look almost identical with no detectable differences between treated and untreated lignin.

Results of solubility test of pristine lignin and plasma treated lignin in toluene are shown in Figure 3.11.

Figure 3.11 Solubility test of pristine lignin (two pictures on the left) and plasma treated lignin in toluene. In the picture on the right the plasma treated powders are divided in couples (spark on the left, arc on the right) and treatments are ordered as follows: air-0, Ar-0, Ar-HEX, Ar-HMDSO.

From the experiments performed in this thesis work, it seems that soda lignin has very low solubility in toluene. In all the vials the liquid appears clear, while in the mixture containing untreated lignin part of the powder got sticked to the vial walls. All the vials containing the treated samples have a similar appearance to the pristine one, which suggest similar solubility properties in toluene before and after the treatment.

Figure 3.12 shows the different solubility of pristine lignin and plasma treated lignin in cyclohexane.
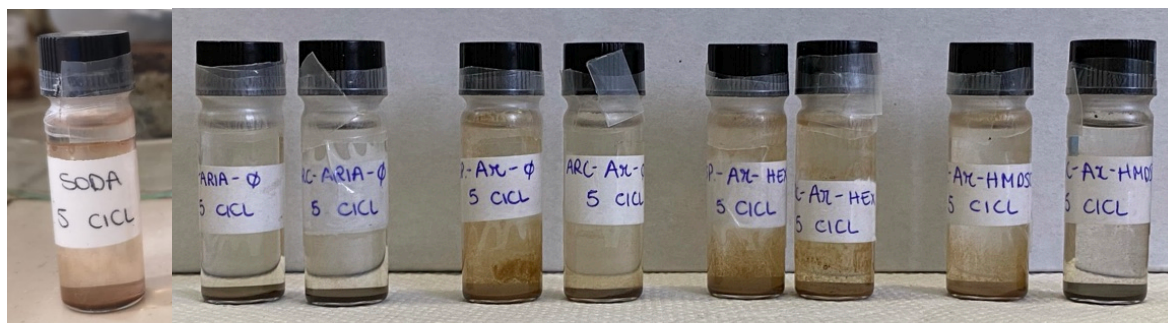
Figure 3.12 Solubility test of pristine lignin (left) and plasma treated lignin in cyclohexane. In the picture on the right the plasma treated powders are divided in couples (spark on the left, arc on the right) and treatments are ordered as follows: air-0, Ar-0, Ar-HEX, Ar-HMDSO.

The reference sample with pristine lignin shows almost no solubility of the powder in cyclohexane, as expected, being the solvent highly hydrophobic. The appearance of the vials with treated lignin is not much different. Some vials appear weakly brown, but this is just due to the lignin that has attached on the internal surface of the container.

Overall, not remarkable differences in the solubility behaviour of pristine and plasma treated lignin can be detected. This suggest that hydrophilicity of lignin was not reduced so highly that it could show different solubility in the selected solvents.

3.2.4 ^{31}P-NMR

3.2.4.1   Effects of different plasma treatments on lignin

^{31}P-NMR was used to quantitatively evaluate the change in the hydroxyl groups concentration between the treated and the untreated samples. Table 3.6 shows the concentrations of aliphatic -OH, phenolic -OH and carboxylic -COOH of both pristine and plasma treated lignin. A graphic representation of the results is also shown in Figure 3.13. Lignin treated with all the eight combinations of parameters considered in this thesis work were tested shortly after the treatments.

Table 3.6 Hydroxyl and carboxylic groups concentration in pristine lignin (SODA) and plasma treated lignin.

Sample name	Aliphatic [OH] (mmol/g)	Phenolic [OH] (mmol/g)	Total [OH] (mmol/g)	Carboxylic [COOH] (mmol/g)
SODA	2,18	3,39	5,57	1,03
Spark-air-0	2,34	4,24	6,58	1,26
Arc-air-0	2,09	4,18	6,27	0,92
Spark-Ar-0	2,02	3,64	5,66	1,07
Arc-Ar-0	2,22	3,95	6,17	0,95
Spark-Ar-HEX	2,51	4,00	6,51	1,30
Arc-Ar-HEX	2,42	3,99	6,41	1,28
Spark-Ar-HMDSO	1,43	2,51	3,94	0,73
Arc-Ar-HMDSO	1,29	2,40	3,69	0,69
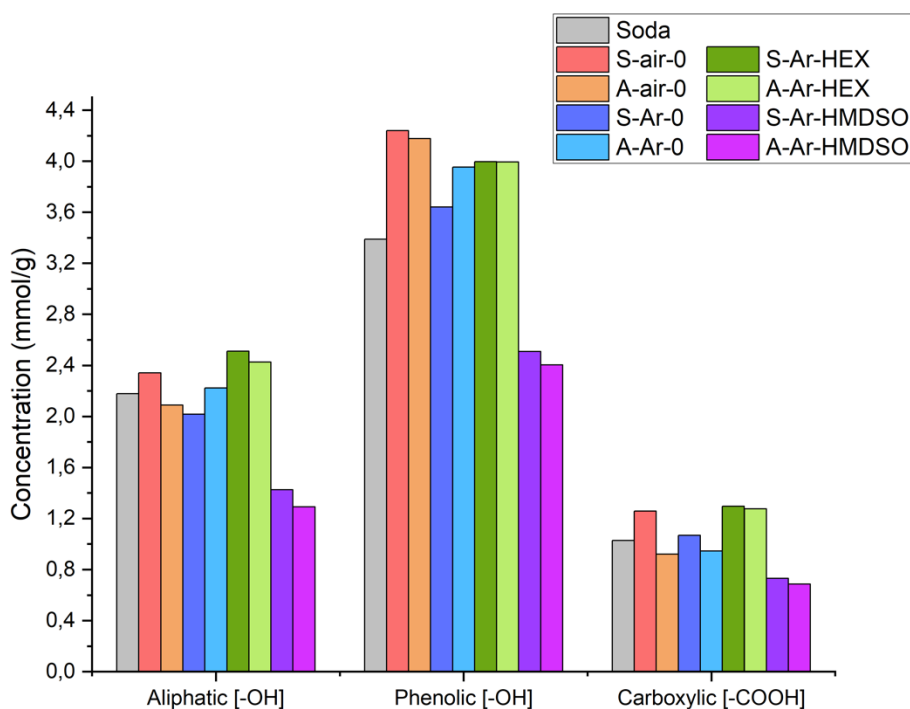
Figure 3.13 Comparison between the hydroxyl and carboxylic groups concentration in pristine lignin (SODA) and plasma treated lignin.

The only treatments that effectively reduced the overall -OH concentration in lignin samples are the ones performed with HMDSO, both in spark and arc regime. Indeed, in the Arc-Ar-HMDSO sample the aliphatic [OH] was reduced to 60% of the one in the

untreated sample, while the reductions in phenolic [OH] and carboxylic [COOH] correspond to 72% and 71%. Similar but slightly higher percentages are reached with the treatment in the spark regime.

Unexpectedly, a higher concentration of hydroxyl groups is obtained when performing the plasma treatment with hexane. Since the functionalizing chemical does not contain hydroxyl groups that could have been deposited, it might be that the reaction with lignin did not occur properly, or that the deposited species underwent further oxidation when exposed to air after the treatment causing an increase in the aliphatic [-OH]. Aging phenomena, such as this, have already been seen after performing plasma polymerization of n-hexane on a substrate [38].

Plasma treatments in compressed air and Argon alone are usually performed on polymers for surface oxidation (section 1.3.3), and this is partly observed here as well. With both plasma gases higher concentrations of phenolic -OH groups are obtained, while in some cases, with the samples Arc-Air-0 and Spark-Ar-0, the aliphatic [OH] and carboxylic [COOH] is reduced. It might have happened that the plasma treatment favoured internal reaction of lignin between itself reducing therefore the hydroxyl groups concentration. Another possible explanation is that new active sites formed during the treatment took the place of some -OH and they were still unreacted at the time of the measurement.

^{31}P-NMR revealed itself to be a determining technique to evaluate the effectiveness of the different plasma treatments and to interpret results from other characterization methods. Because of this, results from ^{31}P-NMR were used to select the interesting treatments to proceed with for the lignin-polypropylene blend production. Overall, only the treatments performed with HMDSO seem to reduce the degree of hydrophilicity of lignin, and because of this, they were chosen for the compound production. Other than those, considering the results from Table 3.6, the couple of treatments performed in Argon were also chosen for the blend production.

3.2.4.2 Effects of time on plasma treatments

Effects of time on plasma treatments were investigated on the 4 treatments selected for the blend production, therefore the two performed in Argon alone and the two in HMDSO. Results of the ^{31}P-NMR tests done 60 days after the treatment was performed are shown in Table 3.7, together with the respective results previously presented in Table 3.6.

Table 3.7 Comparison between the hydroxyl groups concentrations 1 day after the plasma treatment was performed and 60 days from the treatment for four selected samples.

Sample name	Functional group	1 day after the treatment (mmol/g)	60 days after the treatment (mmol/g)
Spark-Ar-0	Aliphatic [OH]	2,02	3,21
	Phenolic [OH]	3,64	5,11
	Carboxylic [COOH]	1,07	1,24
Arc-Ar-0	Aliphatic [OH]	2,22	2,65
	Phenolic [OH]	3,95	4,55
	Carboxylic [COOH]	0,95	1,23
Spark-Ar-HMDSO	Aliphatic [OH]	1,43	2,47
	Phenolic [OH]	2,51	3,81
	Carboxylic [COOH]	0,73	1,23
Arc-Ar-HMDSO	Aliphatic [OH]	1,29	2,57
	Phenolic [OH]	2,40	4,01
	Carboxylic [COOH]	0,69	1,35

The tests on the plasma treated powders not only confirmed that the plasma treatment is not stable over time, but they also showed that the concentration of hydroxyl and carboxylic groups dramatically increased after 60 days to even higher values than the ones of pristine lignin. This is relatable to the weakly-hydrophilic nature of lignin, which attracts humidity from the environment. The plasma treatment probably increased the reactivity of the powder which favoured the reaction with water molecules, bringing to an increase in the polar groups concentration to a value even higher than the one of the untreated sample.

To further evaluate how time affected the results of the plasma treatment, the sample Arc-Ar-HMDSO was tested with ^{31}P-NMR also 30 days after the treatment was performed. The trend over time of the sum of aliphatic and phenolic hydroxyl groups is shown in Figure 3.14.
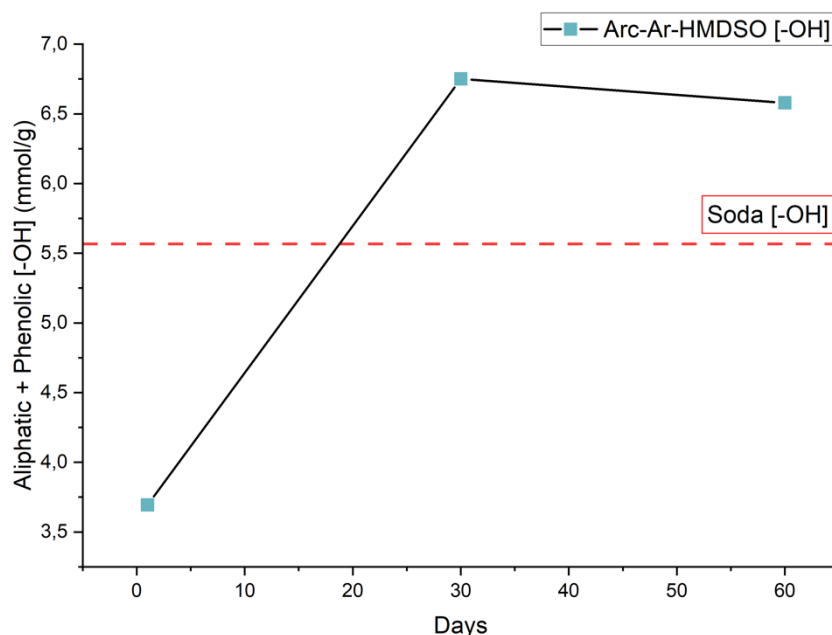
Figure 3.14 Total (aliphatic + phenolic) hydroxyl groups concentrations in Arc-Ar-HMDSO at 1, 30 and 60 days from when the treatment was performed. The reference concentration of the same groups in pristine lignin is also displayed.

The values of aliphatic [OH], phenolic [OH] and carboxylic [COOH] at 30 days are 2,24 mmol/g, 4,51 mmol/g and 0,87 mmol/g respectively. At 30 days after the treatment there already is a relevant increase in the hydroxyl groups concentrations in the sample. The aliphatic plus phenolic -OH concentration even appears higher at 30 days from the treatment than at 60. This might be due to the low reproducibility of the plasma treatment, being the tested samples at 30 and 60 days coming from two different batches. Otherwise, it might be that after one month from the treatment the powder can still undergo internal repolymerization, which might decrease the value of hydroxyl groups concentration.

Overall, it was observed that the results of the plasma treatments on lignin powders disappeared after one month.

3.3   Characterization of PP-lignin blends

Five sets of blends were produced to characterize the properties of lignin-propylene compounds and to compare the results with data of pure polypropylene (PP). As mentioned in section 2.2.2, four of the sets were obtained by blending PP with lignin plasma-treated in four different conditions, while the last one was made with untreated soda lignin. Each of these sets include three blends with different lignin content, which contain 5%, 10% and 20% lignin in mass. All the blends were analysed

through tensile tests and rheology tests, while for DSC measurements only samples with 10% and 20% lignin content were considered, and for TGA only the ones at 10% lignin content.

3.3.1 Tensile tests

Tensile tests were performed to evaluate the effects of the plasma treatments on lignin on the mechanical properties of the blends. The influence of the lignin content in the compounds was also studied. Specifically, the parameters considered to analyse the mechanical performance of PP-lignin materials are the elastic modulus (Young's modulus), the ultimate tensile stress and the elongation at break. All the five types of blends both with 5%, 10% and 20% lignin content have been tested through tensile tests. Five tests were run for each specific type of sample, in order to have a distribution of results characterized by a standard deviation.

At low deformations polymers show an elastic behaviour, which makes possible the definition of an elastic modulus (E_t). A graphic representation of the Young's modulus of blends containing treated and untreated lignin with different content is displayed in Figure 3.15. A table showing the values of elastic modulus of all samples is also present, with the correspondent standard variations (Table 3.8).
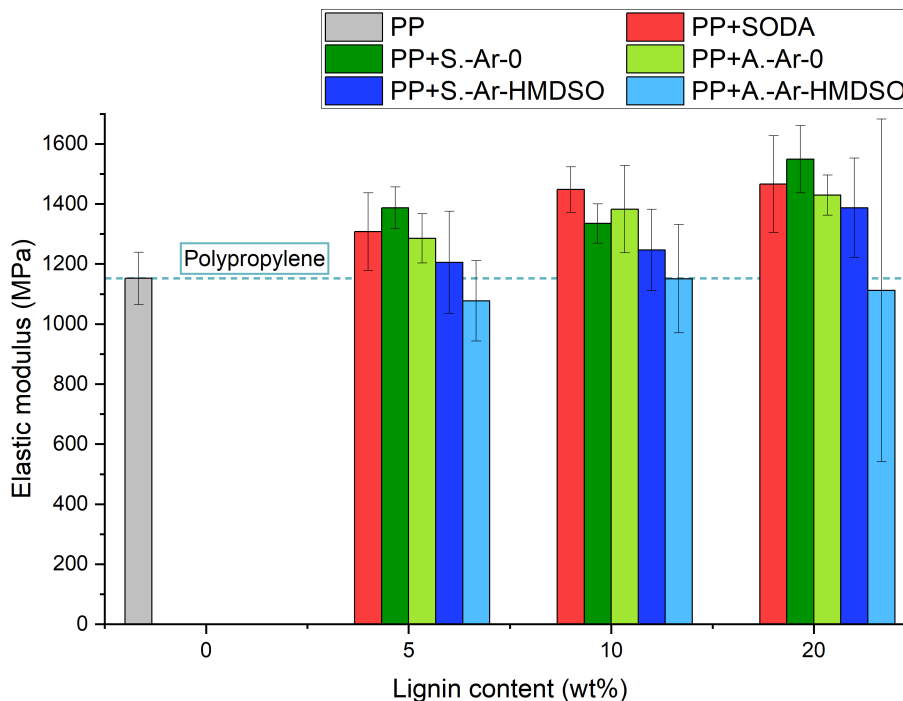
Figure 3.15 Elastic modulus of pure polypropylene and of the blends produced in this thesis work.

Table 3.8 Elastic modulus of pure polypropylene and of the blends produced in this thesis work.

Sample name	wt% Lignin	Elastic modulus (MPa)	Standard deviation
Polypropylene (PP)	0	1152	87
PP + SODA	5	1307	129
	10	1448	76
	20	1466	161
PP + Spark-Ar-0	5	1387	69
	10	1335	66
	20	1549	112
PP + Arc-Ar-0	5	1285	82
	10	1383	145
	20	1430	67
PP + Spark-Ar-HMDSO	5	1205	170
	10	1247	135
	20	1387	165
PP + Arc-Ar-HMDSO	5	1077	134
	10	1151	180
	20	1112	571

Higher values of elastic modulus are observed for almost all lignin-containing samples, compared to pure polypropylene. The elastic modulus is a measure of the material's stiffness, which represents the extent to which an object resists deformation in response to an applied force. High values of modulus are proper of those materials that exercise high resistance to deformation, while low values characterize flexible materials. Therefore, the blends are generally more rigid than pure polypropylene.

It can be observed that for all the blends an increase in the elastic modulus is occurred, compared to the one of pure polypropylene. This is reasonable, being lignin a component that generally provides stiffness when blended with other polymers [40].

There are although some exception where plasticization of PP probably occurred, lowering its modulus. In this work, an increase in the elastic modulus by increasing the lignin content is generally observed, with values of E_t closer to the one of polypropylene for 5% lignin content.

The ultimate tensile stress (σ_u) represents the maximum value of stress that the stress-strain curve reaches during the test, and it is a measure of the material's strength. It is the maximum stress that the material can withstand. The results of the tensile tests are shown in Figure 3.16 and listed in Table 3.9.
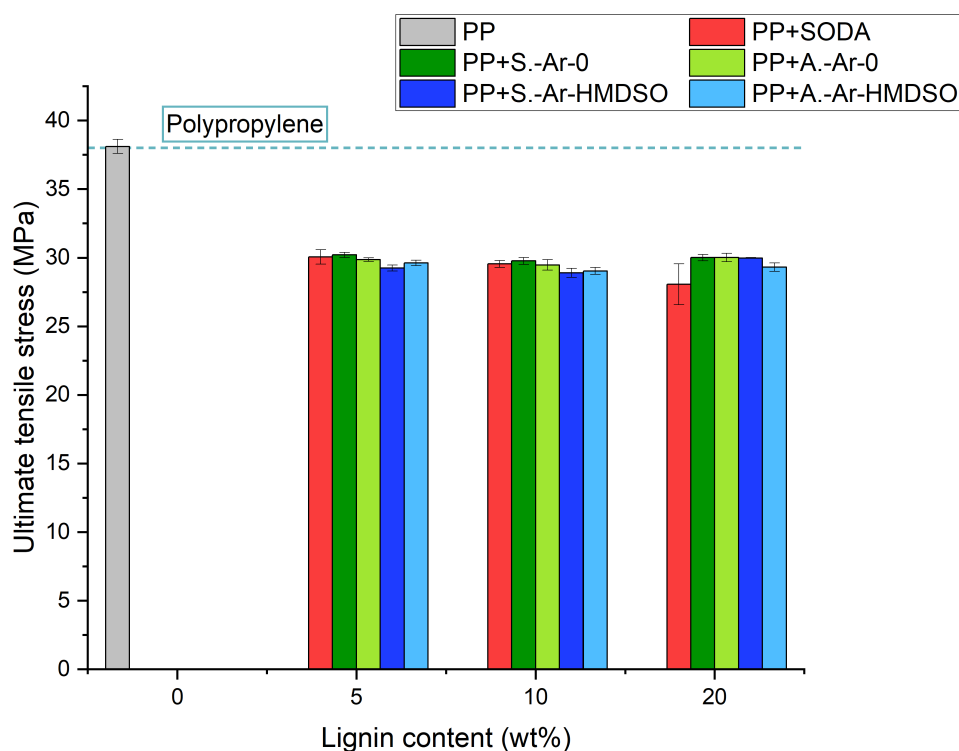
Figure 3.16 Ultimate tensile stress of pure polypropylene and of the blends produced in this thesis work.

Table 3.9 Ultimate tensile stress of pure polypropylene and of the blends produced in this thesis work.

Sample name	wt% Lignin	Ultimate stress (MPa)	Standard deviation
Polypropylene (PP)	0	38	0,5
PP + SODA	5	30	0,5
	10	30	0,2

	20	28	1,5
PP + Spark-Ar-0	5	30	0,2
	10	30	0,3
	20	30	0,2
PP + Arc-Ar-0	5	30	0,1
	10	29	0,4
	20	30	0,3
PP + Spark-Ar-HMDSO	5	29	0,2
	10	29	0,3
	20	30	0,04
PP + Arc-Ar-HMDSO	5	30	0,2
	10	29	0,3
	20	29	0,3

All the blends containing plasma-treated lignin are characterized by a slightly lower ultimate strength than pure polypropylene, but almost no differences are detected among them in terms of σ_u. In general, all the lignin-PP compounds display a strength that is 21% lower than the one of PP. This is related to incompatibility between polypropylene and lignin, which causes a lack of cohesion between the lignin particles and the PP matrix [19]. No trends can be observed in the ultimate strength values depending on the plasma treatment or on the lignin content.

The elongation at break corresponds to the value of deformation at which the tested specimen breaks. The lignin-PP blends showed, as mentioned in section 2.3.5, a peculiar behaviour during deformation. Indeed, it is different from the one of pure polypropylene, which, after a plateau in the curve, shows an increase of the stress for high deformation. This happens because once a neck is formed in a polymer, further deformation is not restricted to the necked region. In fact, the higher stress in the neck area accelerates the molecular alignment, which is accompanied by strengthening of the material in the neck [41]. In the case of blends, at the end of the plateau, the specimen was highly damaged, and the values of stress drastically decreased for high elongations. For this reason, the elongation at break for the blends was set at the end of the plateau (Figure 3.17).
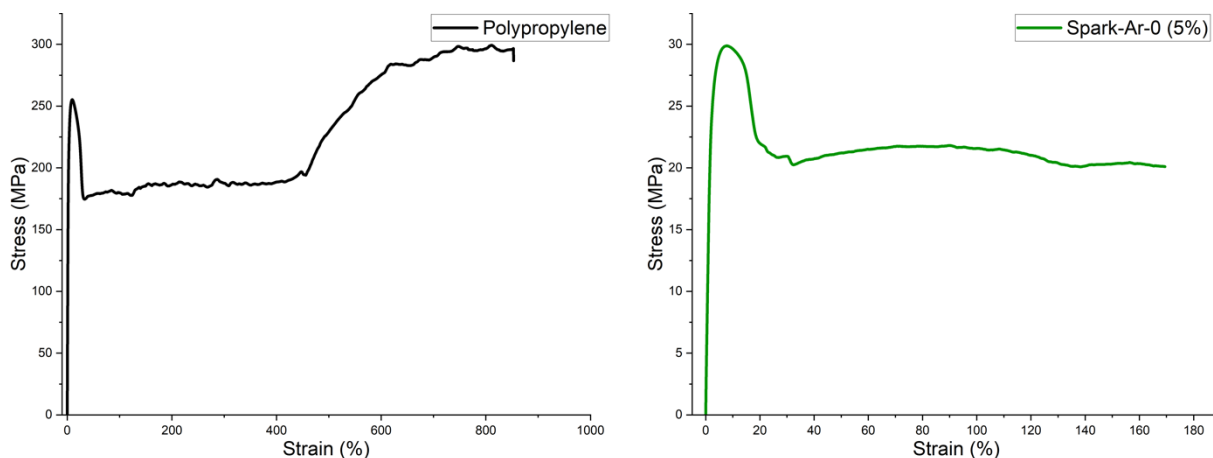
Figure 3.17 Stress-strain curve of polypropylene and of a lignin-PP compound. *Note: The curve of the compound stops at the point that was set as elongation at break, the decrease in the stress for higher deformations is not displayed.*

When commenting curves like the ones in Figure 3.17, it must be underlined that after that necking occurs, the displayed stress is apparent. Indeed, the value of the cross section of the material is considered fixed by the machine while it actually decreases during necking.

Elongation at break of pure polypropylene and of the lignin-propylene compounds produced are shown in Table 3.10 and Figure 3.18. The value of the elongation at break of pure polypropylene corresponds to 853%, significantly higher than the ones of the lignin-PP compounds. In order to make readable the differences in the ε_B of the blends, the value of pure PP was not included in the graph.
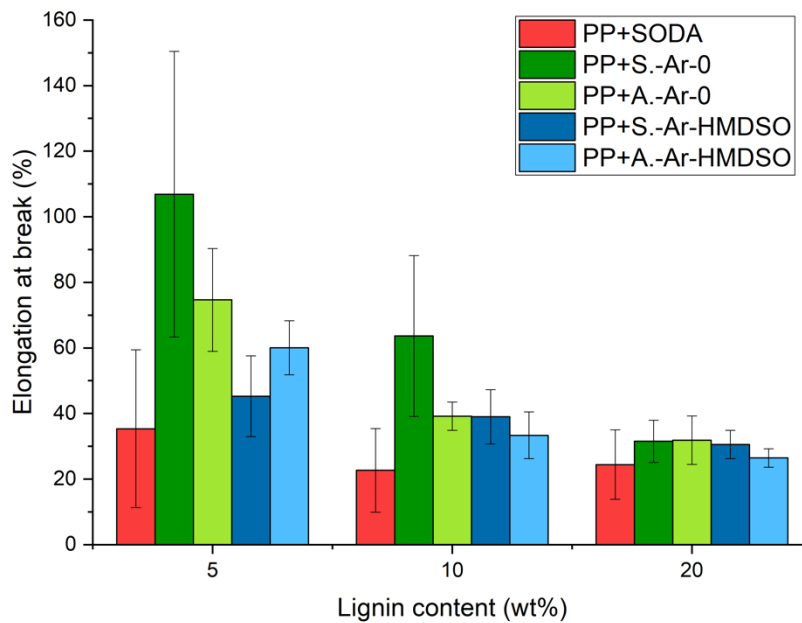
Figure 3.18 Elongation at break of the blends produced in this thesis work.

Table 3.10 Elongation at break of the blends produced in this thesis work.

Sample name	wt% Lignin	Elongation at break (%)	Standard deviation
Polypropylene	0	853	12,7
PP + SODA	5	35	24,1
	10	23	12,7
	20	24	10,6
PP + Spark-Ar-0	5	107	43,6
	10	64	24,5
	20	32	6,4
PP + Arc-Ar-0	5	75	15,6
	10	39	4,3
	20	32	7,4
PP + Spark-Ar-HMDSO	5	45	12,3
	10	39	8,3
	20	31	4,3

	5	60	8,2
PP + Arc-Ar-HMDSO	10	33	7,1
	20	26	2,8

All the blends containing plasma-treated lignin experienced breaking at higher deformations than the ones containing untreated lignin. Great increase in the elongation at break can be observed for low values of lignin content, while in the case of 20% lignin content the value of ε_B becomes quite similar for all the five samples. Generally, higher deformations could be achieved with the samples containing lignin treated in Argon without a functionalizing gas, where the best results were obtained with the treatment performed in the spark regime. This result can be related to the formation of new active sites on lignin during the plasma treatment, which reacted with polypropylene during the blending process, improving compatibility among the two polymers more than the -OH groups decrease with HMDSO. A visual comparison of the elongation at break of the PP + Spark-Ar-0 blends and the soda lignin compounds are shown in Figure 3.19.
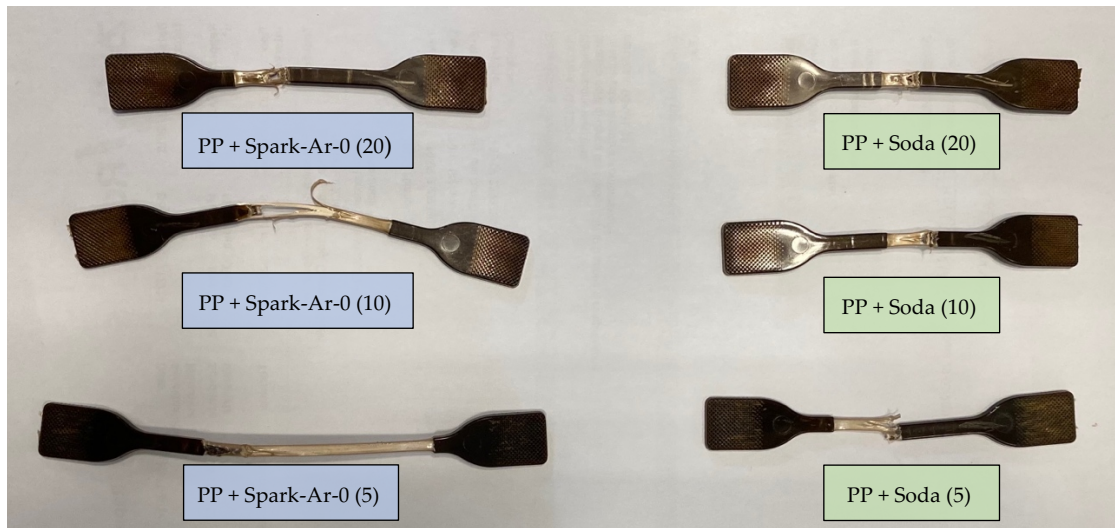
Figure 3.19 Tested samples of PP + Spark-Ar-0 (left) and PP + SODA (right) with the corresponding lignin contents.

Overall, the blends containing plasma-treated lignin show significantly improved elongation at break compared to the ones of pristine lignin-polypropylene compounds. The blends containing the plasma-treated lignin in Argon are the ones that show the greatest improvement, considering for instance that the elongation at

break of PP + Spark-Ar-0 can be three times the one of PP + SODA at 5% lignin content. The blends with lignin treated in Argon and HMDSO show satisfying results for elongation at break as well, but for what concerns the elastic modulus only the treatment in arc regime shows an improvement.

3.3.2 Rheology tests

All the five types of blends both with 5%, 10% and 20% lignin content have been tested with the rheometer to evaluate their rheological behaviour.

A strain sweep test on all the tested samples was performed to assess a value of strain that lied in the linear viscoelastic region (LVR) of the material and that could be set as maximum deformation for the frequency sweep tests. The strain sweep tests revealed that all the samples show a linear viscoelastic behaviour until deformations of 5%, which means that G'' is constant in that range. A reference graph is shown in Figure 3.20.
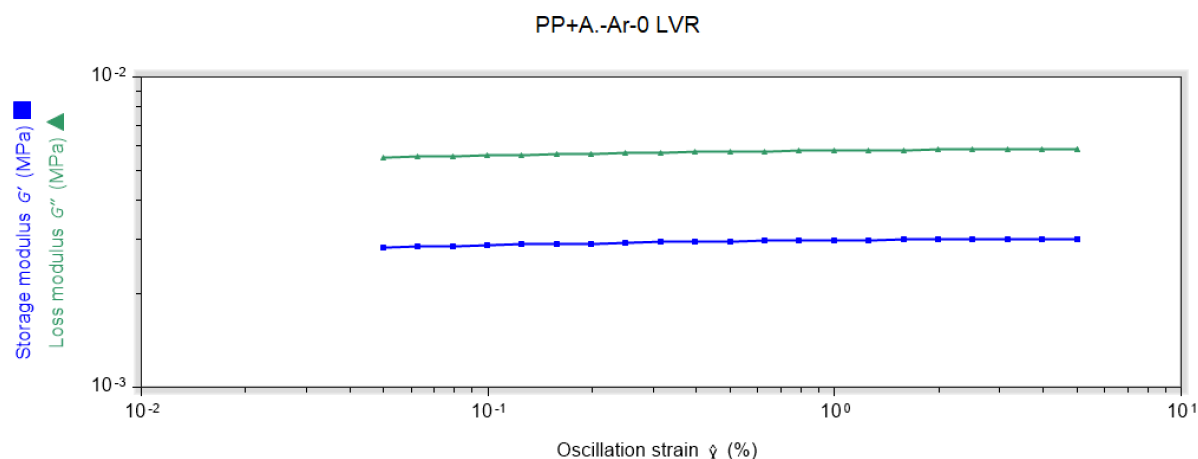
Figure 3.20 Result of the strain sweep test performed on the blend PP + Arc-Ar-0 (10% lignin content).

Because of the outcome of the strain sweep tests, the maximum deformation for the frequency sweep tests was set at 1%.

Frequency sweep tests were performed to evaluate the effects of the plasma treatments and of the lignin content on the PP relaxation time. Results from the frequency sweep tests for both lignin-PP compounds and pure polypropylene are shown in Table 3.11. The effects of the lignin content on the crossover frequency are shown in Figure 3.21 for each type of blend.

Table 3.11 Results of the frequency sweep tests performed on the lignin-polypropylene blends and on pure polypropylene.

Sample name	wt% Lignin	Crossover frequency (Hz)	Relaxation time (ms)
Polypropylene (PP)	0	16	64
PP + SODA	5	15	65
	10	16	62
	20	21	47
PP + Spark-Ar-0	5	16	64
	10	16	64
	20	23	43
PP + Arc-Ar-0	5	15	65
	10	16	63
	20	21	47
PP + Spark-Ar-HMDSO	5	15	65
	10	15	65
	20	21	47
PP + Arc-Ar-HMDSO	5	16	64
	10	16	63
	20	20	51

PP + SODA

PP + Spark-Ar-0

PP + Arc-Ar-0
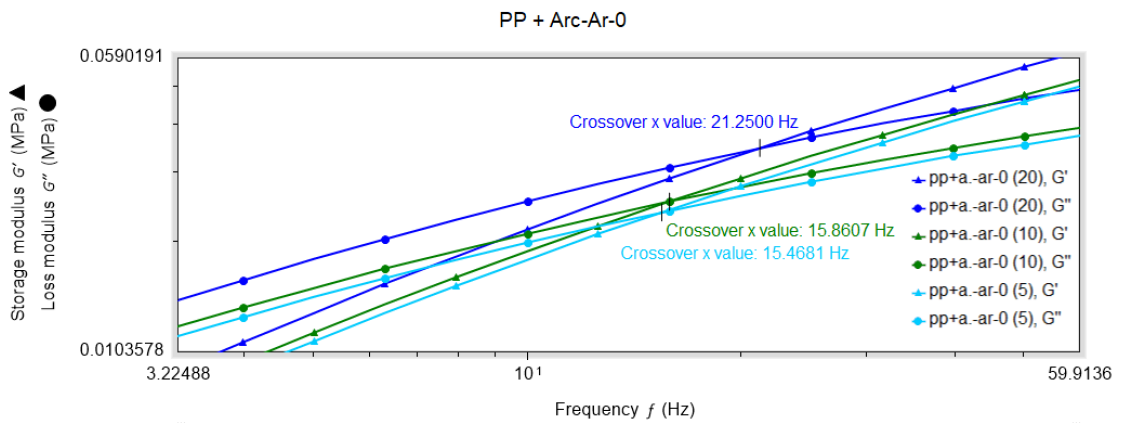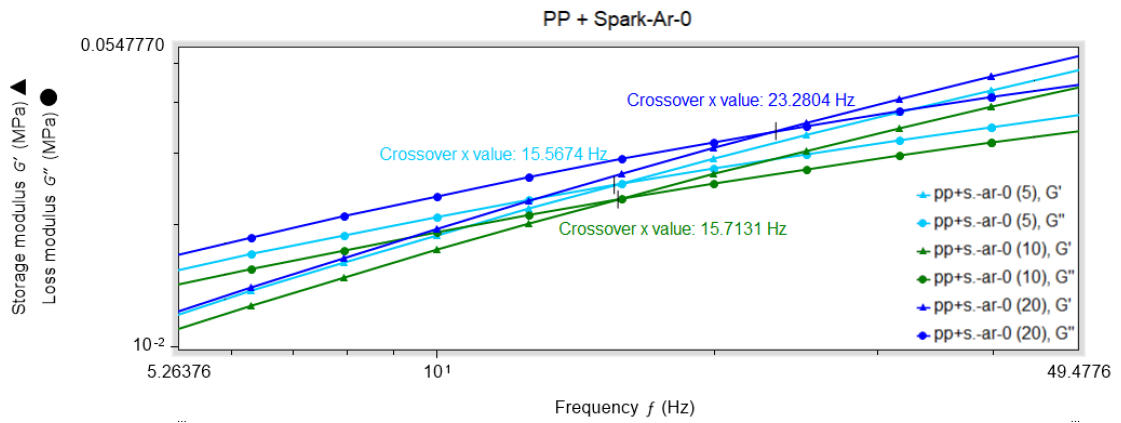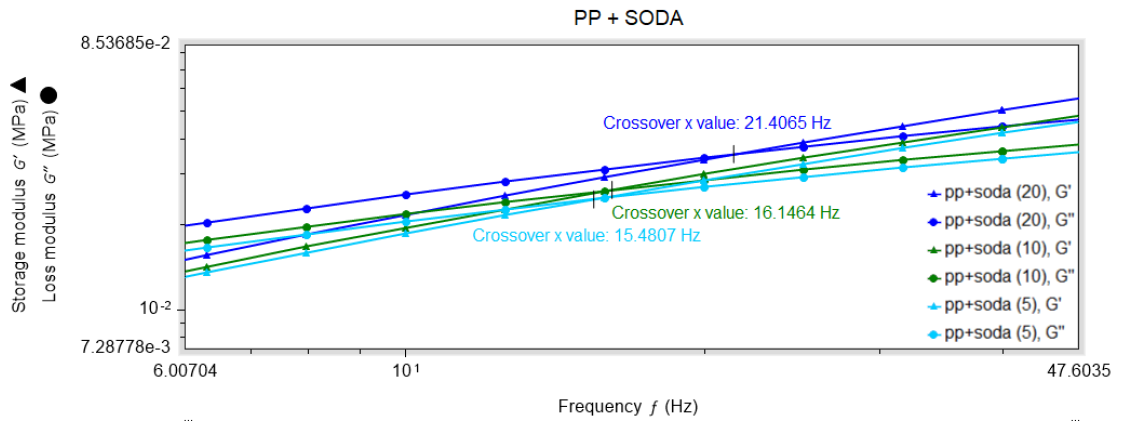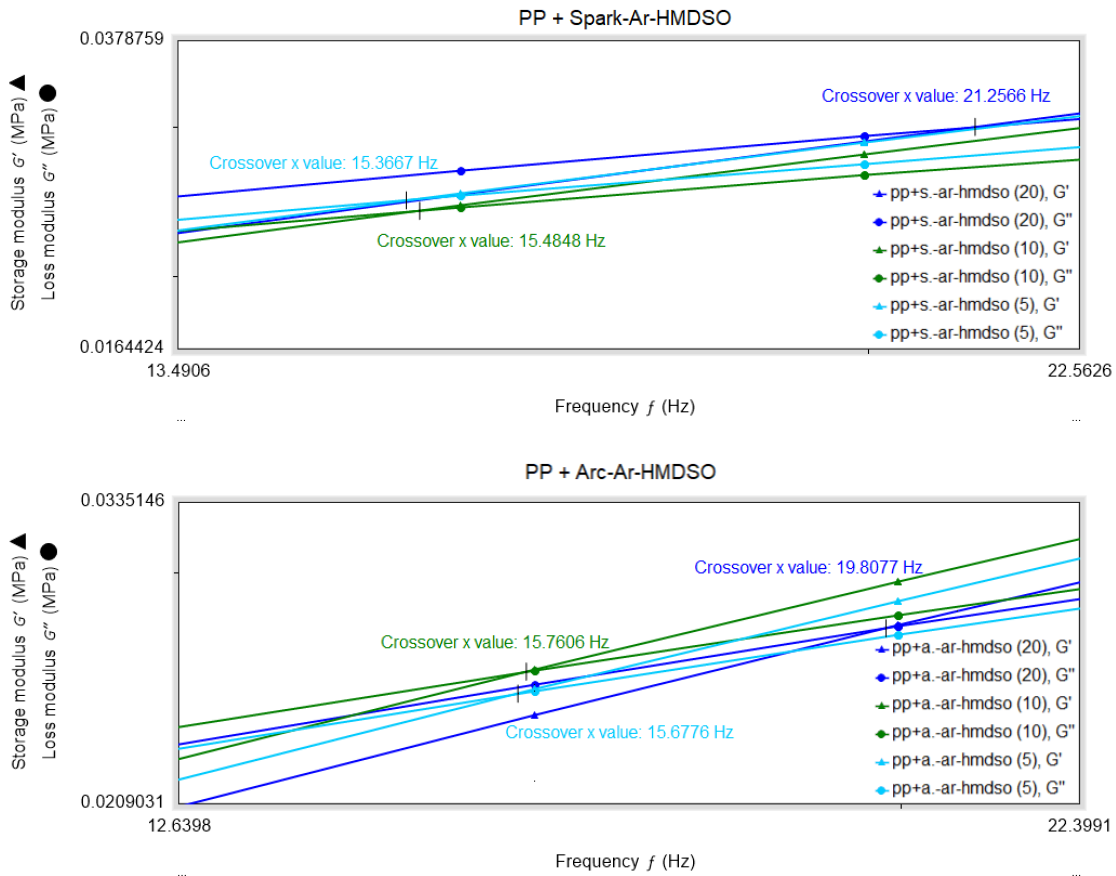
Figure 3.21 Effect of the lignin content on the crossover frequency for each lignin-polypropylene blend.

It is possible to state that the crossover frequency increases for high lignin content (20%), while almost no differences between the samples at 5% and 10% and pure polypropylene are detectable. Also, the type of treatment performed on lignin seems not to affect the position of the crossover point. It is notable that the relaxation time of blends at 20% is approximately 15 ms lower than the ones at 5% and 10%.

The relaxation time represents the point beyond which the elastic response of the material overcomes the viscous one. During the frequency sweep test, below the crossover frequency, the material is partially viscous and has a fluid-like behaviour, which means that it flows when subjected to a deformation. At higher frequency, instead, the material does not flow anymore, it becomes rigid and starts to behave like a solid.

There could be two possible explanations for the reduction in the relaxation time with 20% lignin content. One could be that lignin, when its content in the blend is sufficiently high, facilitated the degradation of polypropylene at the process

temperature of extrusion and injection moulding, causing a reduction in the molecular weight of the PP chains. To verify that this first hypothesis is true, results of the thermogravimetric analysis must be taken in consideration. A second possible explanation to this phenomenon is related to the incompatibility between lignin and polypropylene. Indeed, it is likely that perfect miscibility between the two polymers did not occur, bringing to the formation of aggregations and voids inside the compounds. The presence of voids allows the PP's chains to flow more easily, causing a decrease in the relaxation time of the material.

Overall, the rheological properties of all compounds at 5% and 10% lignin content are very similar to the ones of pure polypropylene. With 20% content, the presence of lignin becomes enough to affect the rheological behaviour of the blend bringing to lower relaxation times, allowing the polymeric chains of polypropylene to flow more easily.

3.3.3 TGA

Thermogravimetric analysis were performed on pure polypropylene and on blends with 10% lignin content to study how the degradation behaviour of PP is influenced by the presence of lignin.

The analysis focused on evaluating the differences in the following parameters: the temperatures at which the highest weight loss of the samples is observed (T_{max1}, T_{max2}), the temperatures at which 5%, 10% and 50% of weight loss occurs ($T_{5\%}$, $T_{10\%}$, $T_{50\%}$), and the residual mass in percentage that remains at the end of the thermal cycle (R_{800}). Results are shown in Table 3.12.

Table 3.12 Results of the thermogravimetric analysis on polypropylene and on the compounds with 10% lignin content.

Sample name	T_{max1} (°C)	T_{max2} (°C)	$T_{5\%}$ (°C)	$T_{10\%}$ (°C)	$T_{50\%}$ (°C)	R_{800} (%)
PP	405	-	304	322	382	0,06
PP+SODA	424	490	317	337	401	0,23
PP+Spark-Ar-0	426	495	315	336	403	0,10
PP+Arc+Ar-0	409	490	307	326	390	0,06
PP+Spark-Ar-HMDSO	425	495	320	339	402	0,17
PP+Arc-Ar-HMDSO	406	493	309	327	388	0,31

T_{max1} and T_{max2} are the temperatures at which most of the mass loss of the samples occurs, and they correspond to the peaks of the DTG curves. In case of pure polypropylene, only one peak is observed (T_{max1}), since the second one (T_{max2}) corresponds to lignin degradation. Nonetheless, the most relevant peak to analyse the degradation behaviour of the material is T_{max1}, which corresponds to more than 95% mass loss for all the tested samples. Also, it is useful to evaluate if the presence of lignin stabilizes polypropylene, bringing T_{max1} to higher values, which is what is actually observed in these experiments. This can be easily observed in Figure 3.22, where the results of the thermogravimetric analysis of pure polypropylene and of the PP-Soda blend are displayed. The curve of the compound containing pristine lignin was chosen as reference for the other blends with plasma-treated lignin that showed similar results in the analysis.
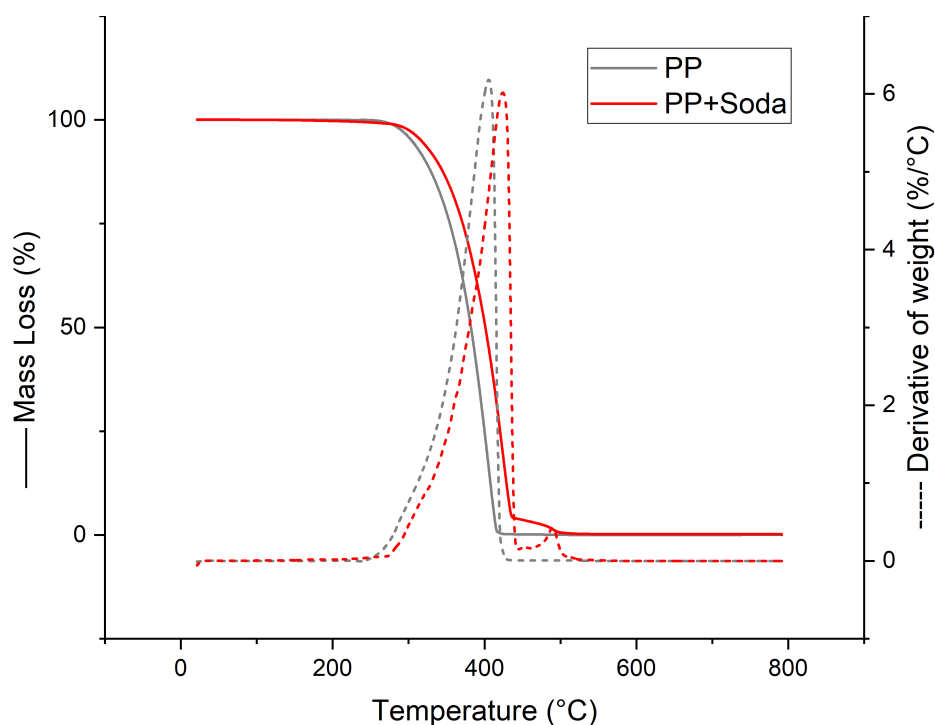
Figure 3.22 TGA curves of pure polypropylene and of the lignin-PP blend with 10% of pristine lignin.

Indeed, the presence of lignin shifts the peak of PP degradation to higher temperatures, especially in the case of pristine lignin and plasma-treated lignin in the spark regime, where an increase of approximately 20°C, i.e. +5%, can be observed.

The plasma treatments seem not to affect significantly the position of the peaks corresponding to lignin's degradation (T_{max2}), but it still provides improved stability to the blend, compared to the one of pure polypropylene. A graphic comparison of T_{max1} and T_{max2} is shown in Figure 3.23.
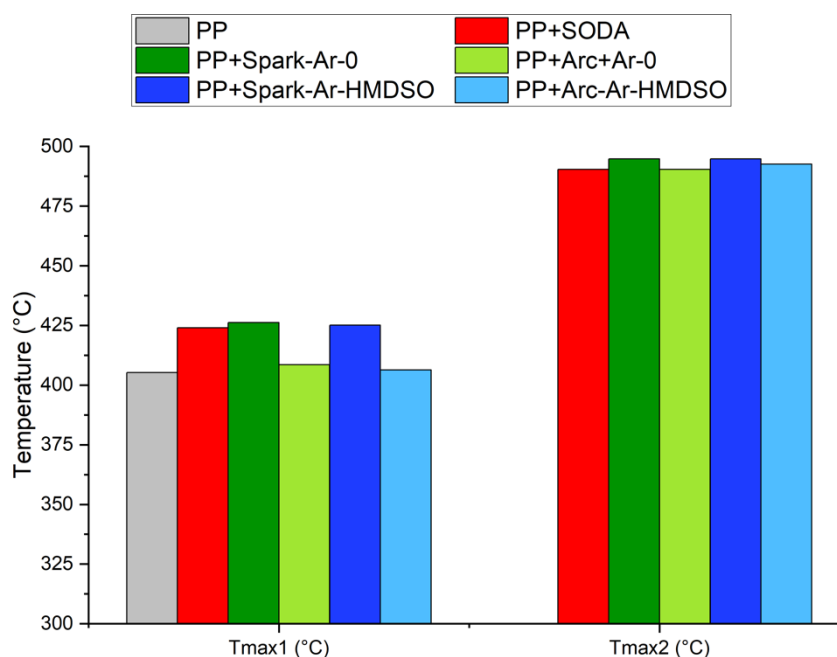
Figure 3.23 Temperatures at which the highest samples' weight loss is observed.

A similar behaviour to the one observed with T_{max1} is observed when considering the temperatures at which 5%, 10% and 50% mass loss of the samples is detected (Figure 3.24). In all the three sets of data an increase in the degradation temperature is observed with pristine and plasma-treated lignin in the spark regime, compared to pure polypropylene. The temperature increase is higher at higher values of mass loss, being +4% for 5% and 10% mass loss, and +5% for 50% mass loss.
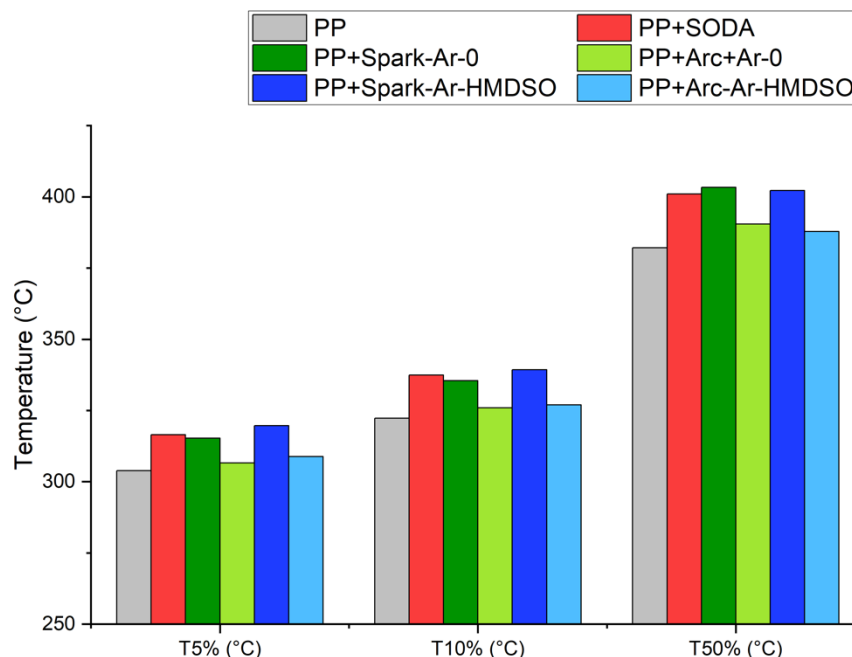
Figure 3.24 Temperatures at which 5%, 10% and 50% mass loss of the samples is observed.

For what concerns the residual mass at the end of the thermal cycle at 800°C, it is evident that lignin has higher thermal stability than pure propylene, except in the case where it was treated in Argon in the arc regime. Indeed, with PP and PP+Arc-Ar-0 only 0,06% of the initial mass of the sample is detected at the end of the experiment, while with the lignin-PP compounds the residual mass ranges from 0,10% to 0,31%.

Overall, it can be stated that lignin stabilizes polypropylene at high temperature, especially when it is untreated or plasma-treated in the spark regime. This conclusion is also useful to explain the reduction in the relaxation time that is obtained when increasing the lignin content in the blends. Indeed, since degradation of polypropylene does not happen, the reduction must be related to the non-perfect compatibility between lignin and the polymeric matrix.

3.3.4 DSC

DSC was used to study the influence of lignin on the melting behaviour of polypropylene, occurring during the third thermal cycle of the measurement (-50°C → 250°C). Specifically, this was done by investigating how the presence of the biopolymer affected the melting temperature of the blend and its normalized fusion enthalpy, compared to the ones of pure polypropylene and of the blend containing pristine lignin. Only compounds with 10% and 20% lignin content have been tested. Results of the DSC measurements are shown in Table 3.14.

Table 3.13 Melting temperature and normalized fusion enthalpy of pure polypropylene and of the lignin-polypropylene blends (10% and 20% lignin content).

Sample name	wt% Lignin	$T_{melting}$ (°C)	Normalized ΔH_{fusion} (J/g)
Polypropylene (PP)	0	166	104
PP + Soda	10	164	109
	20	167	98
PP + Spark-Ar-0	10	165	102
	20	163	99
PP + Arc-Ar-0	10	164	103
	20	165	97
PP + Spark-Ar-HMDSO	10	164	104
	20	168	93
PP + Arc-Ar-HMDSO	10	166	99
	20	168	96

The presence of lignin in the compounds seems not to affect the position of the melting temperature of pure polypropylene, independently on its content in the blend. The endothermic fusion peaks of the materials are shown in Figure 3.25. Indeed, only variations of ± 3°C are observed, without a specific trend depending either on the type of plasma treatment lignin underwent or on the lignin content.
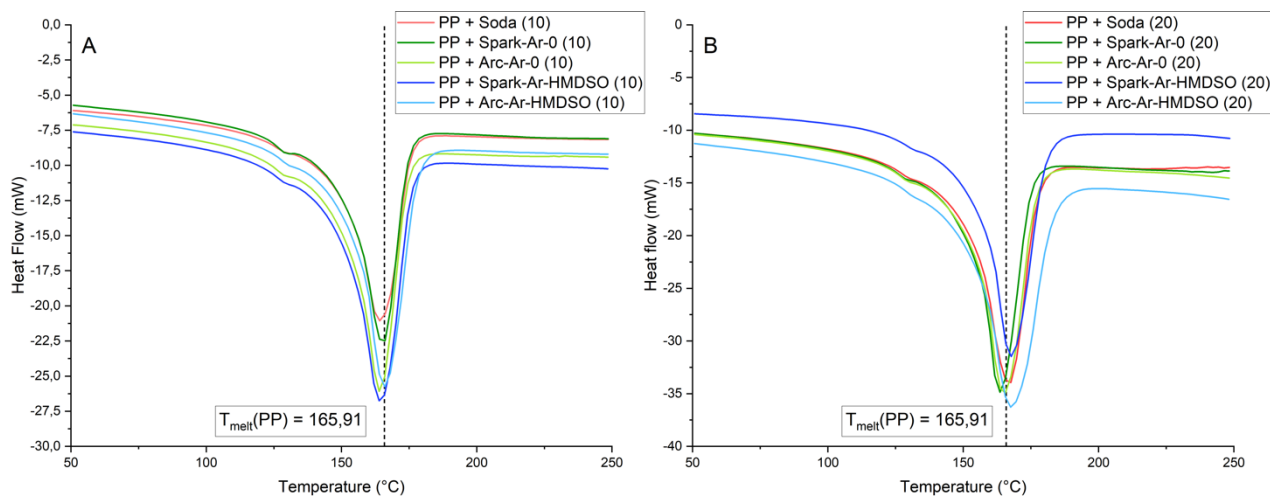
Figure 3.25 DSC fusion peaks of lignin-polypropylene blends with 10% (graph A) and 20% lignin content (graph B) with a comparison of their melting temperature with the one of pure polypropylene.

Different considerations can be made for what concerns the normalized enthalpy of fusion of the blends, compared to the one of pure polypropylene. A histogram to compare the results of the tests is shown in Figure 3.26.
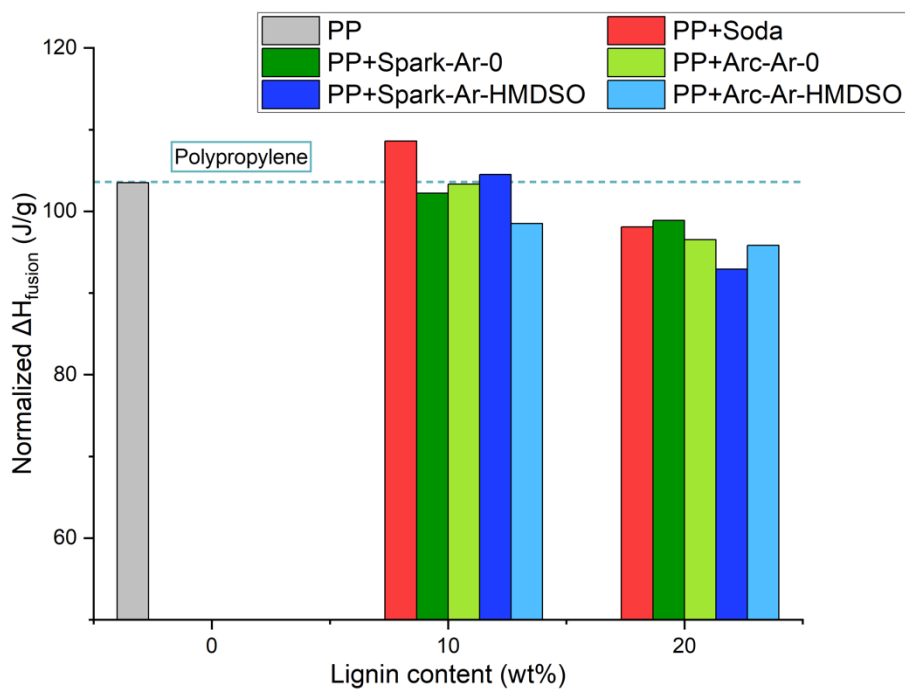
Figure 3.26 Normalized fusion enthalpy of pure polypropylene and of the lignin-polypropylene blends with 10% and 20% lignin content.

The normalized fusion enthalpy represents the amount of heat, i.e. thermal energy, that one gram of material requires to melt. When PP is blended with lignin, the fraction of crystallized material is lower, since lignin does not crystallize, and consequently the normalized enthalpy of fusion is lower than the one of pure polypropylene.

By blending polypropylene with 10% of lignin, either pristine or plasma-treated, the material generally requires a similar amount of energy per gram to melt, compared to pure PP. This is an unexpected result, being the fraction of crystalline material lower. As interpretation to this phenomenon, it might be that lignin acted as nucleating site for the formation of the new phase (liquid), balancing therefore the effect of the reduction in the fraction of crystalline material [42].

At 20% lignin content it is observed that all the compounds require a lower amount of energy per gram to melt. In this case, the effect of the decrease in the fraction of crystalline material is evident and it seems that for higher values of lignin content (20%) the biopolymer does not act as nucleating site during the phase transition.

4. Conclusions

This thesis work is aimed at finding alternative ways to re-design plastic production, to make it more sustainable and to reduce the problems of resource depletion, greenhouse gases emissions and plastic pollution. The implementation of biopolymers in plastic production is today the most attractive and promising way to reduce the environmental impact of plastic. However, products composed of biopolymers alone are not able to provide satisfying mechanical performances. Because of this, compounds made both of biopolymers and fuel-derived polymers are being studied for bulk applications. Lignin is a plant-derived resource that is highly attractive for the formation of this type of compounds, having many attractive properties for high-value applications, including high carbon content, high thermal stability, and favourable stiffness. Its implementation also lies in a perspective of circular economy, being a sub-product of paper production. Moreover, being lignin bio-degradable, its use in polymeric products would tackle the problem of plastic waste disposal.

Lignin is although a weakly-hydrophilic material that does not blend properly with highly non-polar polymers, such as polyolefins, bringing to compatibility problems and consequent unsatisfactory mechanical behaviour. Nonetheless, blending lignin with polyolefins is extremely attractive both from an environmental and economical point of view since they belong to the class of the commodities and have a huge market. Implementing a renewable and highly available resource like lignin would bring to consistent reduction of resource depletion and greenhouse gases emissions, but also an economical gain. During this thesis work, effects of plasma-treatments on the hydrophobicity of lignin and on mechanical properties of lignin-polypropylene blends have been investigated. Plasma-treatments were expected to graft the surface of lignin particles both by substituting hydroxyl functional groups with non-polar groups and by generating new active sites.

FT-IR spectroscopy on the plasma-treated powders did not reveal substantial variation in the chemistry of the material. Indeed, FT-IR is a characterization technique that only allows the study of the functional groups present in the samples, without providing

precise information when their concentration changes. Solubility tests as well did not provide results that could have allowed the detection of a switch in the solubility behaviour of the treated powders from a weakly-hydrophilic to a hydrophobic one. Indeed, solubility of plasma-treated and untreated lignin appeared to be approximately the same for all the employed solvents. DSC measurements, instead, detected some differences in the glass transition temperature of pristine lignin and plasma-treated lignin, also depending on the type of treatment performed. All the eight plasma treatments investigated in this work increased the glass transition temperature of pristine lignin, probably inducing repolymerization of the material within itself. Relatively to the 6 treatments performed either with compressed air as plasma gas or in the presence of a functionalizing gas, the arc regime probably promoted the reaction with gases in the GAT chamber more than in the spark regime. Indeed, a higher T_g is observed in Arc-Air-0 rather than in Spark-Air-0 likely due to higher oxidation of the powder and therefore increased polar interactions inside the material. On the other hand, when a functionalizing gas was employed, the arc regime caused lower glass transition temperatures than the spark regime, probably because of the implantation of non-polar groups at the place of hydroxyl groups. Overall, FT-IR, DSC and solubility tests could not provide useful results to determine the chemical changes that occurred in the plasma-treated lignins. FT-IR and DSC were also employed to study samples of treated lignin extracted from the GAT chamber and from the collecting filter for treated powders, being the two subjected to different treatment times. No detectable differences were observed with these characterization methods, which is why it was decided to investigate distinctions among the two sets of treated powders no further.

Eventually, ^{31}P-NMR was used to quantify any variations in the hydroxyl and carboxylic functional groups concentration in the plasma-treated samples compared to pristine lignin. Only the treatments performed by using HMDSO efficiently decreased the -OH concentration of lignin, lowering aliphatic -OH, phenolic -OH and carboxylic -COOH to respectively ~60%, ~72% and ~71% of their original values, with almost no differences between the treatment in spark and arc regime. Experiments performed with n-hexane surprisingly brought to an increase in the hydroxyl groups concentrations more than any other treatment, probably due to fast ageing of the treated samples. A slight decrease in the aliphatic hydroxyl and carboxylic groups concentrations was also observed with some of the treatments performed in compressed air or Argon as plasma gases. These results are surprising as well, being those types of treatments generally performed for the surface oxidation of polymers to increase their hydrophilicity. It might have happened that internal repolymerization was favoured over oxidation, as well as the grafting of new active sites that were still unreacted at the time of the testing. ^{31}P-NMR revealed itself to be a crucial

characterization method to select the plasma treatments to proceed with for the formation of the lignin-polypropylene compounds, considering those that overall caused the largest decrease in the hydrophilicity of the material.

Tensile tests on the selected lignin-PP blends revealed that improved mechanical performances can be achieved with plasma-treated lignin, compared to the ones with pristine lignin. Specifically, the blends containing lignin treated in Argon provided better results for elongation at break than the ones treated in Argon plus HMDSO. The results from tensile tests could seem to be inconsistent with the ones of ^{31}P-NMR, since the samples treated in HMDSO are more hydrophobic than the ones treated in only Argon, and they are expected to provide better compatibility between polypropylene and lignin. The improved mechanical performances of the lignin treated in Argon could be related to the grafting of new active sites on the particles, which reacted with polypropylene during the blending process, improving compatibility among the two polymers more than the -OH groups decrease with HMDSO. Considering that the aim of the thesis was to improve lignin-polypropylene compatibility, aiming at improved mechanical performances, it can be stated that the achieved results during the tensile tests are satisfying, especially for what concerns the elongation at break of the material, but they could still be improved.

Through thermogravimetric analysis it was proved that the presence of pristine or plasma treated lignin in the spark regime stabilizes polypropylene by increasing the temperature at which maximum degradation of the sample is observed. Moreover, also the residual mass at the end of the thermal cycle is increased. This result is useful to interpretate the reason behind the decrease of 25% in the relaxation time experienced by the samples with high (20%) lignin content. Indeed, since the decrease cannot be related to degradation of the sample, since lignin appears to stabilize polypropylene at high temperatures, it is likely that incompatibility between the two polymers generates voids in the material favouring the flow of the polymeric chains. Lastly, the samples were subjected to DSC measurements to detect how the presence of lignin affected the melting temperature of pure polypropylene. Fusion of all the samples happened in a range of ± 2°C from the one of pure polypropylene, and therefore, no great variations were observed. For what concerns the normalized fusion enthalpy required by the samples to melt, very small variations were observed at 5% lignin content, even though the decrease in the crystallinity fraction of the samples should have brought to a decrease in the values. It might have happened that lignin acted as nucleating site for the formation of the new phase during the phase transition, cancelling the effect of the crystallinity reduction.

Plasma-treatment on lignin was found to be an effective technique to improve interactions, and therefore compatibility, with the polypropylene matrix. This was

specifically observed with treatments that did not involve the use of n-hexane or HMDSO. Performing plasma treatments on lignin without functionalizing gases makes the treatment even more environmentally friendly.

5. Future developments

For possible future developments of this thesis work, some points should undergo further investigation. One of the main complications that was met in the evaluation of the results of the tests was related to the low reproducibility of the plasma treatment. It would be interesting to study possible chemical differences between different batches of lignin treated with the same experimental conditions and to study how to improve reproducibility. Another issue that was encountered during the project was the stability of the plasma treatment over time. Indeed, it should be investigated at shorter times than the ones considered in this work to evaluate in detail the range of stability of the samples.

An important conclusion that was drawn from the experiments was that the plasma treatments in Argon improved lignin-PP compatibility more than the ones performed with Argon and HMDSO, even though they presented a higher hydroxyl groups concentration according to ^{31}P-NMR. It is likely that grafting of unreacted active sites on the surface of lignin particles is more effective than grafting of non-polar functional groups on the miscibility between the two polymers. It would be interesting to further investigate the plasma treatment on lignin using inert gases as plasma gas, maybe also shortening the time between the treatment and the blending process with polypropylene. Another possibility for future developments of plasma treatments on lignin would be to study the effect of grafting lignin with different functionalizing chemicals than the ones used in this thesis work. A study proved that enhanced hydrophobicity of cellulose can be achieved with plasma-induced polymerization of butyl acrylate and 2-ethylhexyl acrylate on its surface (Figure 5.1) [43]. The two chemicals could be employed to try to reduce lignin's hydrophilicity with the GAT device.
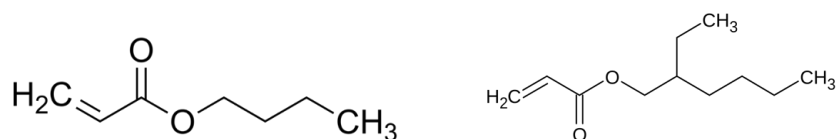
Figure 5.1 Butyl acrylate (left) and 2-ethylhexyl acrylate's (right) chemical structures.

Bibliography

[1]   WMO, *State of the Global Climate 2020*, no. 1264. 2021.

[2]   "Intergovernmental Panel on Climate Change | 2021 Report." https://www.ipcc.ch/2021/08/09/ar6-wg1-20210809-pr/.

[3]   J. Woetzel *et al.*, "Climate risk and response," *McKinsey*, no. January, p. 164, 2020, [Online]. Available: https://www.mckinsey.com/business-functions/sustainability/our-insights/climate-risk-and-response-physical-hazards-and-socioeconomic-impacts.

[4]   "United Nations | Climate Action | Paris Agreement." https://www.un.org/en/climatechange/paris-agreement (accessed Sep. 22, 2021).

[5]   O. Anastasia, "Developing Mid-Century Long-Term Low Emission Development Strategies (LT-LEDS)," *Global Green Growth Institute (GGGI)*, 2019.

[6]   "United Nations | Climate Action | Net-zero Emissions." https://www.un.org/en/climatechange/net-zero-coalition (accessed Sep. 25, 2021).

[7]   "United Nations | Sustainable Development Goals." https://www.un.org/sustainabledevelopment/development-agenda/ (accessed Sep. 23, 2021).

[8]   "United Nations | Sustainable Development Goals | Oceans." https://www.un.org/en/conferences/ocean2022 (accessed Sep. 23, 2021).

[9]   "United Nations | Sustainable Development Goals | World Oceans Day." https://www.un.org/sustainabledevelopment/blog/2018/06/world-oceans-day-2018-to-focus-on-cleaning-up-plastic-in-oceans/.

[10]   L. Copello de Souza, "Civil Society Report," 2019.

[11]   T. R. Walker, "(Micro)plastics and the UN Sustainable Development Goals," *Curr. Opin. Green Sustain. Chem.*, vol. 30, p. 100497, 2021, doi: 10.1016/j.cogsc.2021.100497.

[12]   C. J. Rhodes, "Plastic pollution and potential solutions," *Sci. Prog.*, vol. 101, no. 3, pp. 207–260, 2018, doi: 10.3184/003685018X15294876706211.

[13] S. B. Borrelle, J. Ringma, C. C. Monnahan, and K. Lavender Law, "Predicted growth in plastic waste exceeds efforts to mitigate plastic pollution," *Science*, vol. 369, no. 6510, pp. 1515–1518, 2020.

[14] M. Kedzierski, D. Frère, G. Le Maguer, and S. Bruzaud, "Why is there plastic packaging in the natural environment? Understanding the roots of our individual plastic waste management behaviours," *Sci. Total Environ.*, vol. 740, p. 139985, 2020, doi: 10.1016/j.scitotenv.2020.139985.

[15] S. Rajendran, A. Hodzic, C. Soutis, and M. A. Al-Maadeed, "Review of life cycle assessment on polyolefins and related materials," *Plast. Rubber Compos.*, vol. 41, no. 4–5, pp. 159–168, 2012, doi: 10.1179/1743289811Y.0000000051.

[16] B. M. Upton and A. M. Kasko, "Strategies for the conversion of lignin to high-value polymeric materials: Review and perspective," *Chem. Rev.*, vol. 116, no. 4, pp. 2275–2306, 2016, doi: 10.1021/acs.chemrev.5b00345.

[17] D. Kai, M. J. Tan, P. L. Chee, Y. K. Chua, Y. L. Yap, and X. J. Loh, "Towards lignin-based functional materials in a sustainable world," *Green Chem.*, vol. 18, no. 5, pp. 1175–1200, 2016, doi: 10.1039/c5gc02616d.

[18] S. Bertella and J. S. Luterbacher, "Lignin Functionalization for the Production of Novel Materials," *Trends Chem.*, vol. 2, no. 5, pp. 440–453, 2020, doi: 10.1016/j.trechm.2020.03.001.

[19] D. Kun and B. Pukánszky, "Polymer/lignin blends: Interactions, properties, applications," *Eur. Polym. J.*, vol. 93, pp. 618–641, 2017, doi: 10.1016/j.eurpolymj.2017.04.035.

[20] T. Saito *et al.*, "Turning renewable resources into value-added polymer: Development of lignin-based thermoplastic," *Green Chem.*, vol. 14, no. 12, pp. 3295–3303, 2012, doi: 10.1039/c2gc35933b.

[21] P. Alexy, B. Košíková, and G. Podstránska, "The effect of blending lignin with polyethylene and polypropylene on physical properties," *Polymer (Guildf).*, vol. 41, no. 13, pp. 4901–4908, 2000, doi: 10.1016/S0032-3861(99)00714-4.

[22] T. R. Gengenbach, Z. R. Vasic, R. C. Chatelier, and H. J. Griesser, "Concurrent restructuring and oxidation of the surface of N-hexane plasma polymers during aging in air," *Plasmas Polym.*, vol. 1, no. 3, pp. 207–228, 1996, doi: 10.1007/BF02532817.

[23] D. S. Wavhal, J. Zhang, M. L. Steen, and E. R. Fisher, "Investigation of gas phase species and deposition of SiO2 films from HMDSO/O2 plasmas," *Plasma Process. Polym.*, vol. 3, no. 3, pp. 276–287, 2006, doi: 10.1002/ppap.200500140.

[24] P. M. Ossi, *Plasmi per Superfici*, First Edit. Milano, 2006.

[25] A. A. Kobelev, N. A. Andrianov, A. S. Smirnov, and Y. Vladimirovich Barsukov, "Boron Trichloride Dry Etching," *Res. Gate*, 2016.

[26] K. T. A. L. Burm, "Calculation of the townsend discharge coefficients and the Paschen curve coefficients," *Contrib. to Plasma Phys.*, vol. 47, no. 3, pp. 177–182, 2007, doi: 10.1002/ctpp.200710025.

[27] C. F. Gallo, "Coronas and Gas Discharges in Electrophotography: a Review," *IEEE Trans. Ind. Appl.*, vol. IA-11, no. 6, pp. 739–748, 1975.

[28] E. Hontañón *et al.*, "The transition from spark to arc discharge and its implications with respect to nanoparticle production," *J. Nanoparticle Res.*, vol. 15, no. 9, 2013, doi: 10.1007/s11051-013-1957-y.

[29] R. Barni *et al.*, "Characterization of the electrical and optical properties of a gliding arc tornado device," *Eur. Phys. J. D*, vol. 75, no. 5, pp. 1–6, 2021, doi: 10.1140/epjd/s10053-021-00121-8.

[30] B. Keun, T. Lee, J. M. Goddard, and J. H. Hotchkiss, "Plasma Modification of Polyolefin Surfaces," *Packag. Technol. Sci.*, vol. 22, no. 3, 2008, pp. 139–150, 2009, doi: 10.1002/pts.829

[31] J. M. Grace and L. J. Gerenser, Plasma treatment of polymers, *Journal of dispersion science and technology*, vol. 24, no. 3–4, pp-205-341, 2003, doi: 10.1081/DIS-120021793.

[32] E. M. Liston, L. Martinu, and M. R. Wertheimer, "Plasma surface modification of polymers for improved adhesion: A critical review," *J. Adhes. Sci. Technol.*, vol. 7, no. 10, pp. 1091–1127, 1993, doi: 10.1163/156856193X00600.

[33] T. Atz Dick, J. Couve, O. Gimello, A. Mas, and J. J. Robin, "Chemical modification and plasma-induced grafting of pyrolitic lignin. Evaluation of the reinforcing effect on lignin/poly(L-lactide) composites," *Polymer (Guildf).*, vol. 118, pp. 280–296, 2017, doi: 10.1016/j.polymer.2017.04.036.

[34] G. Toriz, J. Ramos, and R. A. Young, "Lignin-polypropylene composites. II. Plasma modification of kraft lignin and particulate polypropylene," *J. Appl. Polym. Sci.*, vol. 91, no. 3, pp. 1920–1926, 2004, doi: 10.1002/app.13412.

[35] I. Bykov, "Characterization of Natural and Technical Lignins using FTIR Spectroscopy," *Master thesis in chemical technology*, 2008.

[36] N. Kumar *et al.*, "Optimal extraction, sequential fractionation and structural characterization of soda lignin," *Res. Chem. Intermed.*, vol. 44, no. 9, pp. 5403–

5417, 2018, doi: 10.1007/s11164-018-3430-0.

[37] M. . Mohamad Ibrahim, S. . Chuah, and W. D. Wan Rosli, "Characterization of Lignin Precipitated From The Soda Black Liquor of Oil Palm Empty Fruit Bunch Fibers by Various Mineral Acids," *ASEAN J. Sci. Technol. Dev.*, vol. 21, no. 1, p. 57, 2017, doi: 10.29037/ajstd.92.

[38] T. R. Gengenbach, Z. R. Vasic, R. C. Chatelier, and H. J. Griesser, "A multi-technique study of the spontaneous oxidation of N-hexane plasma polymers," *J. Polym. Sci. Part A Polym. Chem.*, vol. 32, no. 8, pp. 1399–1414, 1994, doi: 10.1002/pola.1994.080320801.

[39] J. Sameni, S. Krigstin, and M. Sain, "Solubility of Lignin and Acetylated Lignin in Organic Solvents," *BioResources*, vol. 12, no. 1, pp. 1548–1565, 2017, doi: 10.15376/biores.12.1.1548-1565.

[40] F. Chen, H. Dai, X. Dong, J. Yang, and M. Zhong, "Physical Properties of Lignin-Based Polypropylene Blends," Polym. Compos., vol. 32, no. 7, pp. 1019–1025, 2011, doi: 10.1002/pc.21087.

[41] R. Pinto, "Necking: a comparative study of deformation in polymers and metals," 2016. https://mse.engin.umich.edu/internal/demos/necking-a-comparative-study-of-deformation-in-polymers-and-metals (accessed Nov. 28, 2021).

[42] S. Sahoo, M. Misra, and A. K. Mohanty, "Enhanced properties of lignin-based biodegradable polymer composites using injection moulding process," *Compos. Part A Appl. Sci. Manuf.*, vol. 42, no. 11, pp. 1710–1718, 2011, doi: 10.1016/j.compositesa.2011.07.025.

[43] Z. Song, J. Tang, J. Li, and H. Xiao, "Plasma-induced polymerization for enhancing paper hydrophobicity," *Carbohydr. Polym.*, vol. 92, no. 1, pp. 928–933, 2013, doi: 10.1016/j.carbpol.2012.09.089.

List of Figures

List of Tables